Institut für Technische Chemie
der Technischen Universität München
Lehrstuhl II

Active Acid Sites in Zeolite Catalyzed Iso-butane/cis-2-Butene Alkylation

Alexander Guzmán Monsalve

Vollständiger Abdruck der von der Fakultät für Chemie der Technischen Universität München zur Erlangung des akademischen Grades eines

Doktors der Naturwissenschaften

genehmigten Dissertation.

Vorsitzender: Univ. –Prof. Dr. Klaus Köhler

Prüfer der Dissertation:

1. Univ. –Prof. Dr. Johannes A. Lercher
2. Priv.-Doz. Dr. Peter Härter

Die Dissertation wurde am 04.11.04 bei der Technischen Universität München eingereicht und durch die Fakultät für Chemie am 09.12.04 angenommen.

Acknowledgements

First, I would like to thank Johannes (Prof. J.A. Lercher) for giving me the opportunity to work in his group. During this period of time I have learnt with him that not only the academic part is important for our future career but also the personal character plays an important role. His permanent input on this point is especially thanked. The experience of working in the chair for chemical technology leaded by an important personality in the catalysis field like Johannes was for me an honor.

I would also like to express my gratitude to Roberta, who helped me to improve the quality of my thesis and spent many hours discussing data and interpretations with me. Her help encouraged me to go on with the difficult task of writing and interpreting data. Thanks also for "teaching" me how to cook asparagus.

Thanks to Iker, my project partner, for all the nice days that we spent particularly in the short time that we were "single" men. Walking around the wonderful city of Munich, Englisher Garten, Marienplatz, etc., with a beer in the hand was a nice experience. Of course, the laboratory work with him was also good.

Thanks to Andreas Feller, who gave me a warm welcome and introduced me into the alkylation world.

Thanks to Frau Hermann and Frau Schüler for helping me especially with the difficult task to find a place to live.

Thanks to Carsten Sievers for his help and for giving me the opportunity to improve my German.

Thanks to Florencia. You're really a special person. Thanks to Oriol for his permanent update of Colombia.

I am grateful for the funding help by Süd-Chemie AG and also for preparing and supplying of catalyst samples. Thanks Manfred for your help and for the nice moments that I spent with you, especially, by the "Metzger".

Thanks to all my colleges. It has been a great experience to meet people from all over the world. Thanks to Xaver, Andreas M. and Martin for their technical support.

Thanks to Xuebing (for drinking with me Jägermeister), Ayumu (for your Japanese chewing gums), Chintan (for your company in Holland), Philipp (for protecting my Rücken), thanks to everybody!

Thanks to family. I love you. Alex

November 2004

Chapter 1

1.1. General introduction
1.1.1. Structures of zeolites
1.1.2. Location of exchange sites in zeolites
1.1.2.1. Lanthanum X zeolite
1.1.2.2. Protonated form of Y zeolite
1.2. Scope of the thesis
1.3. References

Chapter 2

2.1 Introduction
2.2 Experimental
2.2.1 Material preparation
2.2.2 Material characterization
2.2.3 Catalytic experiments
2.3 Results
2.3.1 Hydroxyl groups formation on lanthanum exchanged Na-X zeolites
2.3.2 Acidic properties of the lanthanum exchanged Na-X zeolites at different preparation steps
2.3.3 Catalytic activity over lanthanum exchanged Na-X zeolites at different preparation steps
2.4 Discussion
2.4.1 Hydroxyl groups formation on lanthanum exchanged X zeolites
2.4.2 Acidic properties of the lanthanum exchange X zeolites with different ion exchange degrees
2.5 Conclusions
2.6 Acknowledgments
2.7 References

Chapter 3

3.1 Introduction
3.2 Experimental
3.2.1 Material preparation
3.2.2 Material characterization
3.2.3 Catalytic experiments
3.3 Results
3.3.1 ^{29}Si NMR and IR spectroscopy of La-X zeolites
3.3.2 IR spectroscopy of La-Y zeolite
3.3.3 IR spectroscopy of H-Y zeolite
3.3.4 IR spectroscopy of H-La-Y zeolite
3.3.5 IR spectroscopy of H-La-USY zeolite
3.3.6 SEM images and IR spectroscopy of H-EMT zeolite
3.3.7 IR spectroscopy of H-BEA zeolite
3.3.8 Isobutane/cis-2-butene adsorption monitored by IR spectroscopy
3.3.9 Physicochemical characterization and alkylation activity of the different materials
3.4 Discussion
3.4.1 Acidity in La-X zeolites with different Si/Al ratios
3.4.2 Acidity in La-Y type zeolite. Comparison with La-X
3.4.3 Acidity in H-Y zeolite
3.4.4 Acidity in H-La-Y zeolite
3.4.5 Acidity in H-La-USY zeolite
3.4.6 Acidity in H-EMT
3.4.7 Acidity of H-BEA
3.4.8 Isobutane/cis-2-butene adsorption on zeolites and correlation with acidic properties
3.4.9 Alkylation activity of the different zeolites
3.5 Conclusions
3.6 Acknowledgments
3.7 References

Chapter 4

4.1 Introduction

4.2 Experimental

4.2.1 Material preparation

4.2.2 Material characterization

4.2.3 Catalytic experiments

4.3 Results

4.3.1 Influence of the activation temperature on the physicochemical properties of La-X samples

4.3.1.1 Surface area

4.3.1.2 IR spectra

4.3.1.3 TPD profiles

4.3.1.4 NMR spectra

4.3.1.5 Acidity measurement by Pyridine-IR spectroscopy

4.3.2 Effect of the activation temperature on isobutane/cis-2-butene adsorption on La-X samples

4.3.3 Effect of activation temperature on catalytic activity of La-X samples in isobutane/cis-2-butene alkylation

4.4 Discussion

4.4.1 Effect of the activation temperature on the physicochemical properties of La-X zeolite

4.4.2 Effect of the activation temperature on isobutane/cis-2-butene adsorption on La-X samples

4.4.3 Catalytic activity of La-X zeolite activated at temperatures between 120 and 280°C in isobutane/cis-2-butene alkylation

4.5 Conclusions

4.6 Acknowledgments

4.7 References

Chapter 1

1.1. General introduction

Alkylation of isobutane with C_3-C_5 olefins catalyzed by strong acid sites is an important refining process in which high octane gasoline is produced [1]. The gasoline from alkylation consists basically of a mixture of branched saturated hydrocarbons with desired physicochemical properties like low octane sensitivity (difference between research and motor octane numbers), low Reid vapor pressure, lack of aromatics and alkenes and nearly lack of sulfur. Industrially two catalysts are widely employed in this process: sulfuric and anhydrous hydrofluoric acids. Both acids suffer from several drawbacks concerning specially corrosiveness and toxicity. Alternative catalysts based mainly on solid zeolites have received interest in the last decades. However, due to their rapid deactivation, they have been not implemented in industry [2].

Among large-pore zeolites, FAU and BEA-type materials have been especially studied as potential alkylation catalysts. Their pore dimensions are required to minimize diffusion limitation of the highly branched hydrocarbons formed during alkylation. Details on the alkylation mechanism have been recently investigated [3]. FAU-type zeolites are also attractive for their content of aluminum because acidity in zeolites is closely related to this parameter. Thus, large-pore structures combined with high concentration of acid sites make such materials potential good alkylation catalyst [4]. Because most of the work presented in this thesis focuses on material properties, a brief description of the structure and acidity of the investigated zeolites is presented in the next sections.

1.1.1. Structures of zeolites

The elementary building units of zeolites are SiO_4 and AlO_4 tetrahedra [5,6]. The tetrahedra form a three-dimensional framework sharing one oxygen atom between each two tetrahedra. The framework of a zeolite contains channels, channel intersections and/or cages with dimensions from ca. 2 to 10 Å. The zeolitic framework loses electroneutrality when lattice Si^{4+} cations are replaced by lattice Al^{3+} cations.

The excess lattice negative charge has to be compensated by positively charged ions. After synthesis the most common cations are the alkali Na^+ and K^+, which find a location in the microporous zeolite channel system. Acid sites can be introduced by ion exchange with NH_4^+ or other cations like rare earth elements. After heating the NH_4^+ cations are decomposed into NH_3 and H^+. The ammonia molecule desorbs, and the proton is left bonded to a bridging lattice oxygen atom, which connects a tetrahedron with a four valent Si^{4+} atom and one that contains a three valent Al^{3+}

$$C_{y/m}^{m+}[(SiO_2)_x \cdot (AlO_2^-)_y] \cdot zH_2O \qquad (1)$$

atom. The chemical composition of a zeolite can hence be represented by a formula of the type:

where C is a cation with the charge m, (x + y) is the number of tetrahedra per crystallographic unit cell (UC) and x/y is the so-called framework silicon/aluminum ratio (Si/Al).

In the case of rare earth ion exchanged zeolites the acidity is generated when the polyvalent cations are hydrolyzed according to the following mechanism (referred as Hirschler-Plank scheme):

$$[La(H_2O)_n]^{3+}(Z^-)_3 \xrightarrow[-(n-2)\,H_2O]{\approx 573K} [(LaOH)(H_2O)]^{2+}H^+(Z^-)_3 \longrightarrow [(La(OH)_2]^+(H^+)_2(Z^-)_3 \qquad (2)$$

where Z^- represents the negatively charged zeolite.

According to this mechanism, from the water molecules solvating the rare earth cation a proton is produced and transferred to the oxygen of the associated tetrahedra upon thermal treatment of the sample. If the temperature is further increased a second proton can be transferred [7].

In FAU-type zeolites are found 192 (silicon + aluminum) tetrahedra per UC with Si/Al ratio values between ca. 1 and 5. FAU zeolites with Si/Al ratios between 1 and 1.5 belong to the group X zeolites while FAU-type zeolites with higher Si/Al ratios than 1.5 are classified as Y zeolites. The schematic representation of the FAU structure is presented in Fig. 1.1. In FAU-type zeolites when 24 silicon and aluminum primary building blocks of zeolites are linked, they form a cubo-octahedra or so-called sodalite cage unit. Molecules can penetrate into this secondary building block through the six-membered oxygen rings, which have a free diameter of 2.6 Å. Since

the pore diameter is so small, only very small molecules, e.g. water can enter the sodalite cage. If sodalite units are connected via their hexagonal faces as shown in Fig. 1.1, the structure of the mineral faujasite results. Its pore system is relatively spacious and consists of spherical cages, referred as supercages or large cavities, which are sufficiently large for an inscribed sphere with a diameter of approximately 13 Å. The opening into this large cavity is bounded by sodalite units, resulting in a 12-membered oxygen ring with a 7.4 Å free diameter. Each cavity is connected to four other cavities, which in turn are themselves connected to three-dimensional cavities to form a highly porous framework structure.

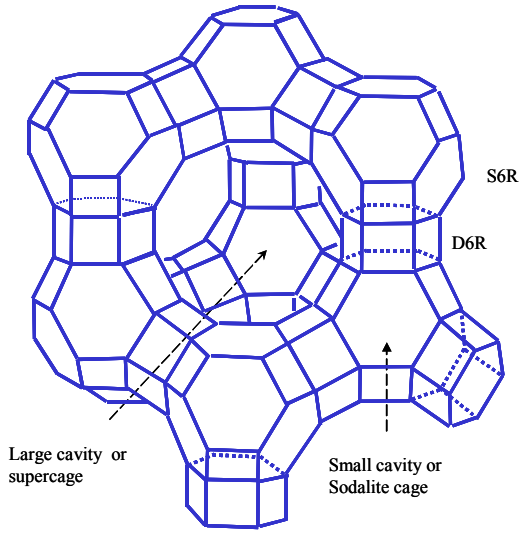

Figure 1.1: Schematic representation of the faujasite structure. The corners denote the positions of the T atoms (T = Si or Al) and the lines represent the bridging oxygens atoms.

1.1.2. Location of exchange sites in zeolites

1.1.2.1. Lanthanum X zeolite

The distribution of the location of acid sites in the framework structure of a zeolite is of great importance in catalysis. Based on the description above all the charge compensating cations can be exchanged by NH_4^+ or rare earth cations and after activation the acidic form of the zeolite can be produced. However, the two network of cavities, sodalite and supercage, have openings of markedly different size and

therefore the ion exchange at low temperatures is restricted only to cations with hydrated radius smaller than the opening of the cavities [8]. For the Na-X type of synthetic faujasite, 16 of the 88 sodium ions in the UC are located in the network of sodalite cages; the other 72 are in the network of supercages. Thus, an ingoing ion must penetrate both networks if all the Na^+ ions are to be replaced. In the case of the hydrated rare earth lanthanum cation with a hydrated ion radius of 3.96 Å only Na^+ ions in the supercages can be replaced by these cations. In order to achieve higher degrees of ion exchange water molecules in the hydration sphere of the rare earth cation must be removed. This can be done by calcination of the exchanged zeolite (Eq. 2). This process leads to the hydrolysis of the hydrated rare earth cations and therefore to the migration to the sodalite cages. Although in most of the cases a temperature of approximately 573K has been proposed as the maximal temperature required to induce the migration of the lanthanum ions into the small cavities, Lee *et al*. [9], studying the effect of calcination temperature on the migration of the lanthanum ions from the supercages to the small cages, found that migration starts at a temperature ≥ 333K and that the amount of lanthanum in the small cages becomes constant at temperatures ≥ 573K. A linear relationship between number of lanthanum ions that migrate in the small cages and water molecules desorbed was also found.

Although until now it has been distinguished between positions in the small or large cavities, protons or cations present in the FAU-type zeolites occupy several locations in both cavities [10-12]. Olson [12] studying a fully exchanged La-X zeolite found the following site location: Site I (SI) at the center of the hexagonal prism D6R, Site II (SII) located in the sodalite cage and just outside the plane of D6R, Site III (SIII) located in the sodalite cage just outside the plane of the supercage 6MR, Site IV (SIV) located in the supercage just inside the plane of the supercage 6MR, and Site V (SV) located in the center of the 12MR of the supercage (Fig. 1.2). In the uncalcined La-X zeolite 12 and 21 lanthanum cations were found in the sodalite cages and supercages, respectively. All 12 lanthanum cations were located at positions SII in the small cavities while from the 21 in the supercages, 17 and 4 lanthanum cations, were located at positions SIV and SV, respectively. When the zeolite was dehydrated, all lanthanum ions moved into the sodalite cage cavity. 30 lanthanum cations were located at SII sites.

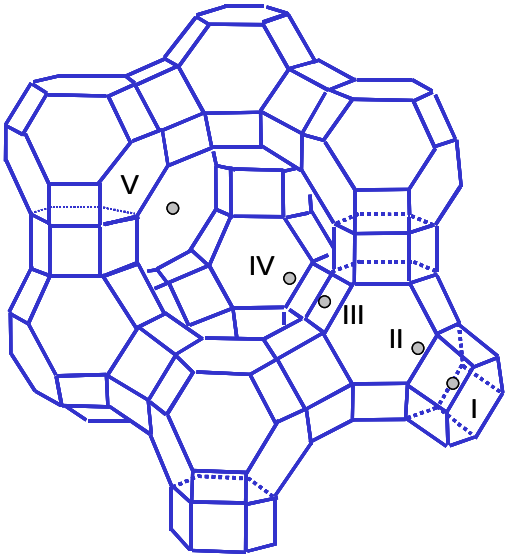

Figure 1.2: Schematic representation of the faujasite structure. Extraframework lanthanum positions in a fully exchanged La-X zeolite.

It is important to note that in the uncalcined La-X of Olson 12 lanthanum cations were found in the small cavities of the zeolite. As discussed above, thermal treatment of the rare earth exchanged FAU-type zeolites is required to induce the migration of the lanthanum hydrated cations to the small cavities. However, as it was also discussed by Sherry [8], an increase of the temperature during the ion exchange leads to a removal of water molecules from the hydration sphere of the cation and to a partially replacement of sodium ions in the small cages by lanthanum. Olson exchanged the Na-X zeolite at 373K.

1.1.2.2. Protonated form of Y zeolite

Location of the extraframework cations in zeolites can be also described from the point of view of the framework oxygens to which the cations or protons are bonded. In the protonic form of the Y zeolite 4 types of framework oxygens can be distinguished [13]; they are normally labeled as O_1, O_2, O_3 and O_4 (Fig. 1.3). Protons bonded to these oxygens originate the hydroxyl groups that are responsible for the Brønsted acidity of this type of zeolite [14]. Three hydroxyl groups are observed in the IR spectrum of decationated Y zeolite: at ca. 3750 cm^{-1} a band due to terminal silanol groups, at ca. 3650 and 3550 cm^{-1} the so-called high- and low frequency bands. The high-frequency protons (HF) have been identified with the O_1 site, which

is the oxygen that connects the six rings in the double ring unit. O_2 has been found to be partially occupied.

Whereas the O_1 site has been identified with the HF band, the O_3 site has been identified with the low-frequency band (LF). The O_3 site lies direct inwards toward the center of the six ring structure, inaccessible to molecules with diameters larger than the openings of the sodalite cages. Therefore the most likely proton sites in the protonic form of Y zeolite are the O_1 and O_3. Direct observation by high-resolution neutron powder diffraction and computer simulation of protonated Y zeolites [14, 15] supported this assignment.

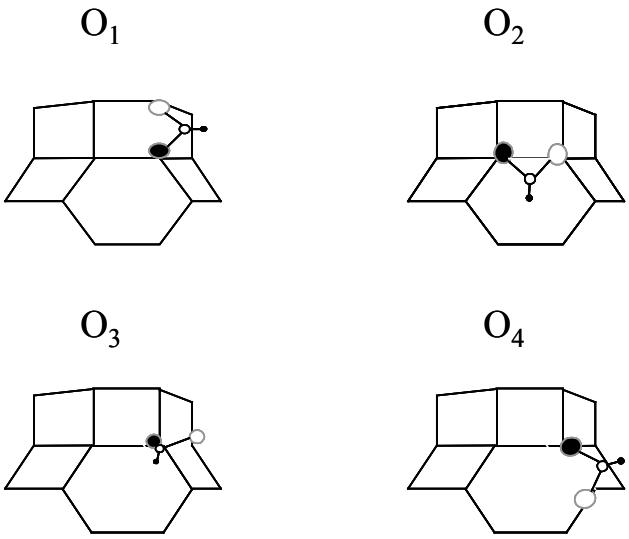

Figure 1.3: The four different positions of the protons that are bonded to the framework oxygen atoms around an aluminum atom.

While the assignment of the HF and LF bands in the protonic form of the Y zeolite based on crystallographic data seems to be unequivocal, IR data of adsorbed molecules on this zeolite are still controversial. Ward [14] found that addition of excess of pyridine (no adsorption pressure was mentioned) resulted in a considerably decrease of the LF band. If the O_3 involved in the hydroxyl group responsible of the LF bands are in inaccessible positions to molecules like pyridine (kinetic diameter 5.4 Å) the intensity of this band would remain unaltered during pyridine adsorption. Two alternative explanations were suggested, one based on the strength of these Brønsted acid sites and the other considering the LF band as composed not only of protons attached to O_3 type oxygens but also to O_2 and O_4.

Van Santen *et al*. [5] explained the lower reactivity of the LF band on the basis that the O_3 proton can form a weak hydrogen bond to another oxygen atom of the tetrahedral six ring in which it participates. This additional hydrogen bond will weaken the OH bond.

Jacobs *et al*. [16] using a deconvolution method showed that the LF band is the superposition of different components. The multiplicity of the components can be explained if all the oxygens O_2, O_3 and O_4 are considered as possible proton location sites.

1.2. Scope of the thesis

Sulfuric and anhydrous hydrofluoric acids employed industrially in the alkylation of isobutane with C_3-C_5 olefins as catalysts are toxic and corrosive. That has stimulated that many research groups devote a lot effort to the development of a more friendly environmental and safer alternative process. Numerous alternative processes, most of them base on solid acid catalysts, have been examined.

A development of such alternative process can be only achieved by identifying the physicochemical properties of the catalyst and the reaction parameters that determine the catalytic performance. A profound knowledge of the properties of the catalyst, especially its acidic properties, is mandatory.

In this thesis special attention has been dedicated to understand the nature of the acid sites. In chapter 2 the acid catalyst properties at different preparation steps are discussed. Various physicochemical methods have been implied to investigate the formation of the acid sites in La-X zeolites. Especially the influence of water on the formation of the acid sites was studied in detail. Chapter 3 focuses on preparation and characterization of the most attractive zeolites used in isobutane/butene alkylation: FAU-type zeolites, especially X and Y zeolites, and BEA-type zeolites. Acid sites responsible for the catalytic activity were studied thoroughly by IR spectroscopy. Chapter 4 deals with the effect of activation temperature on the catalytic performance of the catalyst based on La-X zeolite. Activation temperatures between 393-723K were investigated. The role of remaining physisorbed water, depending on the activation temperature, was studied in detail.

1.3. References

[1] J. Weitkamp, Y. Traa, Catal. Today, 49 (1999) 193.

[2] A. Corma, A. Martinez, Catal. Rev.-Sci. Eng. 35 (1993) 483.

[3] A. Feller, A. Guzman, I. Zuazo, J.A. Lercher, J. Catal. 224 (2204) 80.

[4] J. Weitkamp, Y. Traa, in: G. Ertl, H. Knözinger, J. Weitkamp (Eds), Handbook of Heterogeneous Catalysis, Vol. 4, 1997, p. 2039.

[5] R.A. Van Santen, G.J. Kramer, Chem. Rev. 95 (1995) 637.

[6] J. Weitkamp, Y. Traa, Solid State Ionics, 131 (2000) 175.

[7] P.B. Venuto, L.A. Hamilton, P.S. Landis, J. Catal. 5 (1966) 484.

[8] H.S. Sherry, J. Colloid Interf. Sci. 28 (1968) 288.

[9] E.F.T. Lee, L.V.C. Rees, Zeolites. 7 (1987) 143.

[10] L. Zhu, K. Seff, J. Phys. Chem. B. 103 (1999) 9512.

[11] D.H. Olson, Zeolites. 15 (1995) 439.

[12] D.H. Olson, G.T. Kokotailo, J.F. Charnell, J. Colloid Interf. Sci. 28 (1968) 305.

[13] M. Czjzek, H. Jobic, A.N. Fitch, T. Vogt, J. Phys. Chem. 96 (1992) 1535.

[14] J.W. Ward, J. Catal. 9 (1967) 225.

[15] M. Leslie, C.R.A. Catlow, J.M. Thomas, Chem. Phys. Lett. 188 (1992) 320.

[16] P.A. Jacobs, J.B. Uytterhoeven, J. Chem. Soc., Faraday Trans. I. 69 (1973) 373.

Chapter 2

On the formation of the acid sites of lanthanum X zeolites for isobutane/cis-2-butene alkylation

Abstract

The acid sites generated at different steps during the preparation of La-H-X zeolites were characterized by physicochemical methods. The resulting materials were tested in isobutane/cis-2-butene alkylation in a continuously operated stirred tank reactor, under industrially relevant conditions.

The rehydration of materials calcined only one time changes the distribution of hydroxyl groups, the Brønsted acidic bridging hydroxyl groups being strongly affected (IR band at 3640 cm^{-1}). Rehydration leads to dealumination and, as consequence, the concentration of silanol groups (IR band at 3740 cm^{-1}) and of Lewis acid sites increases. This in turn results in an enhanced thermal stability of the rare earth zeolite for the next steps of the catalyst preparation.

A correlation between catalytic activity in isobutane/cis-2-butene alkylation and the fraction of strong Brønsted to total Brønsted acid sites was observed. Catalysts with similar concentration of strong Brønsted acid sites and higher concentration of weak Brønsted sites showed shorter lifetime. The strength of the Brønsted acid sites was shown to be a function of the hydrolysis of hydrated lanthanum cations and removal of sodium cations.

Keywords: IR spectroscopy, ion exchange degree (IExD), zeolitic hydroxyl groups, alkylation

2.1. Introduction

Isobutane/butene alkylation is an important refining process in which the C_4 byproducts from fluid catalytic cracking units are converted into a complex mixture of branched alkanes (alkylate), which are an excellent blending component in the gasoline pool [1]. The catalysts normally used in commercial processes are sulfuric and hydrofluoric acids [2]. In line with general trends, the development of new alkylation technologies based on non-toxic, non-corrosive and environmentally friendly catalysts has a high incentive. In this context, highly Brønsted acidic zeolites and especially large pore zeolites are a potential alternative able to overcome the problems related to liquid acids. However, the industrial application of zeolites is constrained by rapid deactivation.

The overall cycle in the alkylation reaction comprises the addition of n-butene to an isobutyl carbenium ion to form an octyl carbenium ion, which in turn is removed from the acid site by hydride transfer from isobutane leading to trimethylpentanes as primary products and to another isobutyl carbenium ion [3] (Scheme 1). Competition between hydride transfer and oligomerization of butene as secondary reaction determines the lifetime of the catalyst. The higher is the ratio of hydride transfer *vs.* the rate of oligomerization, the more the primary products trimethylpentanes will be produced and the more the catalyst deactivation will be slowed down (Scheme 1) [4].

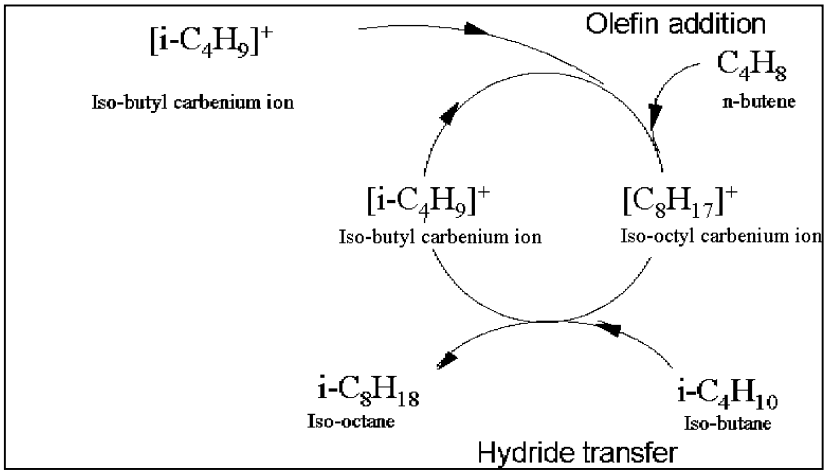

Scheme 2.1: Simplified alkylation mechanism.

Among the large pore zeolites, rare earth exchanged faujasites have shown to have a good ability to catalyze hydride transfer in alkylation reaction because of their high concentration of strong Brønsted acid sites, an essential factor to overcome the higher energy barrier required for the hydride transfer in solid catalysts compared to liquid acids [5-7].

The nature of the acid sites in the rare earth exchanged FAU zeolites has been extensively studied. It has been proposed that the rare earth ions exchanged in X or Y zeolites are hydrolyzed upon calcination according to the Scheme 2. The resulting protons are attached to the framework oxygens and generate the Brønsted acidy [8-10].

$$[La(H_2O)_n]^{3+} \rightleftharpoons [La(OH)(H_2O)_{n-1}]^{2+} + H^+$$

Scheme 2.2: Hydrolysis of hydrated lanthanum ions.

Direct evidence for hydrolysis comes from IR spectra showing O-H stretching bands that can be ascribed to OH groups attached to the exchanged metal cation and to the aluminosilicate framework [11]. Similarly, inelastic neutron diffraction has provided direct evidence for metal cation hydrolysis [12].

The effect of calcination temperature on the migration of lanthanum ions from the supercages to the sodalite cages has been likewise investigated [13]. It has been reported that at temperatures higher than 333 K the hydrated La^{3+} cations begin hydrolyzing water and migrating to the small cages. During calcination, the hydrolysis of the rare earth cations produces not only Brønsted acid sites, but also Lewis acid sites [8]. Potential processes involving the framework at these relatively low temperatures have not been characterized well. Especially it is unclear under which conditions water may lead to the partial or full hydrolysis of framework aluminum atoms and what role the rare earth metal cations play in this process.

Here, IR spectroscopy is used to provide information about the formation of the acid sites in the lanthanum exchanged X zeolites and to investigate the influence of water on the structural OH groups of the calcined materials. A series of lanthanum exchanged X zeolites was examined to establish how the acidic properties, the concentration and the strength of the modified materials varied with the lanthanum

exchange degree. These findings have been correlated with the catalytic activity in alkylation.

2.2. Experimental

2.2.1. Material preparation

The samples in this study were prepared from a Na-X zeolite obtained from Chemische Werke Bad Köstritz (Si/Al = 1.2). The Na-X material was gradually brought into the acidic form by ion exchange with 0.2 M lanthanum nitrate solution using a liquid-to-solid ratio between 5 and 10 mL/g. The pH of the freshly prepared lanthanum nitrate solution was about 3. The ion exchange was carried out at 353K for 2 h. This step was done 1 or 2 times. After washing and drying, the resulting materials were calcined in 100 mL/min flowing air for 1 h at 723 K ("*first calcination*"). To achieve a higher lanthanum ion exchange degree the materials were further exchanged between 1 and 3 times following the same procedure above described including a second calcination at 723 K ("*second calcination*").

2.2.2. Material characterization

The ion-exchanged materials were characterized by XRD (determination of the unit cell size UCS by ASTM D-3942-85 [17]) and ^{1}H NMR. The ion exchange degree (IExD) [IExD = (1-Na/Al)*100] was determined by AAS.

The effect of the calcination steps ("*first and second calcinations*") during the catalyst preparation was monitored by mass spectrometry and IR spectroscopy. Two different calcination procedures were employed: calcination directly in the IR flow cell ("*in situ calcination*") and calcination in a shallow bed type oven ("*ex situ calcination*" with respect to the IR cell). The temperature program and the air flow used during these calcinations were identical.

The effect of IExD on the acidity of the materials at different preparation steps was studied by IR spectroscopy. The samples were pressed into a self-supporting wafer (with a density between 5 and 10 mg/cm^2) and activated in vacuum at 723 K for 1h. After cooling down to 423 K, a spectrum was recorded ("*spectrum of activated sample*"). Pyridine with a partial pressure of 1 Pa was introduced into the cell. After

saturation, the cell was evacuated at 423 and 723 K for 1h, and IR spectra recorded at 423 K. The concentrations of Brønsted and Lewis acid sites were estimated from the bands at 1540 and 1454 cm^{-1} corresponding to the pyridinium ion and coordinatively bound pyridine to aluminum extraframework (EFAL) species, respectively. The extinction coefficients were taken from Emeis [18]. The Brønsted and Lewis acid site concentrations measured after outgassing at 423 K are referred as BAS_{423} ("*total Brønsted acidity*") and LAS_{423} ("*total Lewis acidity*"), and after outgassing at 723 K as BAS_{723} ("*strong Brønsted acidity*") and LAS_{723} ("*strong Lewis acidity*"), respectively.

2.2.3. Catalytic experiments

The alkylation of isobutane with 2-cis-butene was performed in a stirred tank reactor operated in continuous mode. The liquefied gases were received from Messer with a purity of 99.95% (isobutane) and 99.5% (cis-2-butene). The catalyst (typically 1-3g) was activated *in situ* within the alkylation reactor at 443 K for 16 h in 100mL/min flowing hydrogen. After cooling down to reaction temperature (348 K) the reactor was pressurized to $2x10^3$ KPa and filled with isobutane. The stirring speed was about 1600 rpm. The reaction started by feeding a mixture of isobutane/cis-2-butene (10/1 ratio). The catalyst lifetime was defined as the time on stream at which the conversion was lower than 99%. Details on the reaction conditions are described elsewhere [4].

2.3. Results

2.3.1. Hydroxyl group formation on lanthanum exchanged Na-X zeolites

The acidity of La-X zeolites has been attributed to the protons that are generated when water of the hydrated lanthanum cations is hydrolyzed by calcination at temperatures between 343 and ca. 573 K [8-10].

In this study, the calcination of a Na-X zeolite exchanged two times with lanthanum cations was monitored by mass spectrometry (MS) analysis of the outlet of the calcination oven and by IR spectroscopy.

Fig. 2.1 shows the MS signal for m/e 18 recorded during the calcination. The signal showed two sharp and intense maxima at 393 and 573 K and a peak of low intensity at about 423 K. During heating, three possibilities for producing water from the sample exist, i.e., release of physisorbed water, dehydration of the lanthanum cations and dehydroxylation of the zeolite. The peak at 393 K is attributed to molecularly adsorbed water, that at 423 K to the combined release of molecularly adsorbed water and to the recombination of the lanthanum OH groups and the proton at a bridging hydroxyl group and the peak at 573 K is attributed to the dehydroxylation of the zeolite.

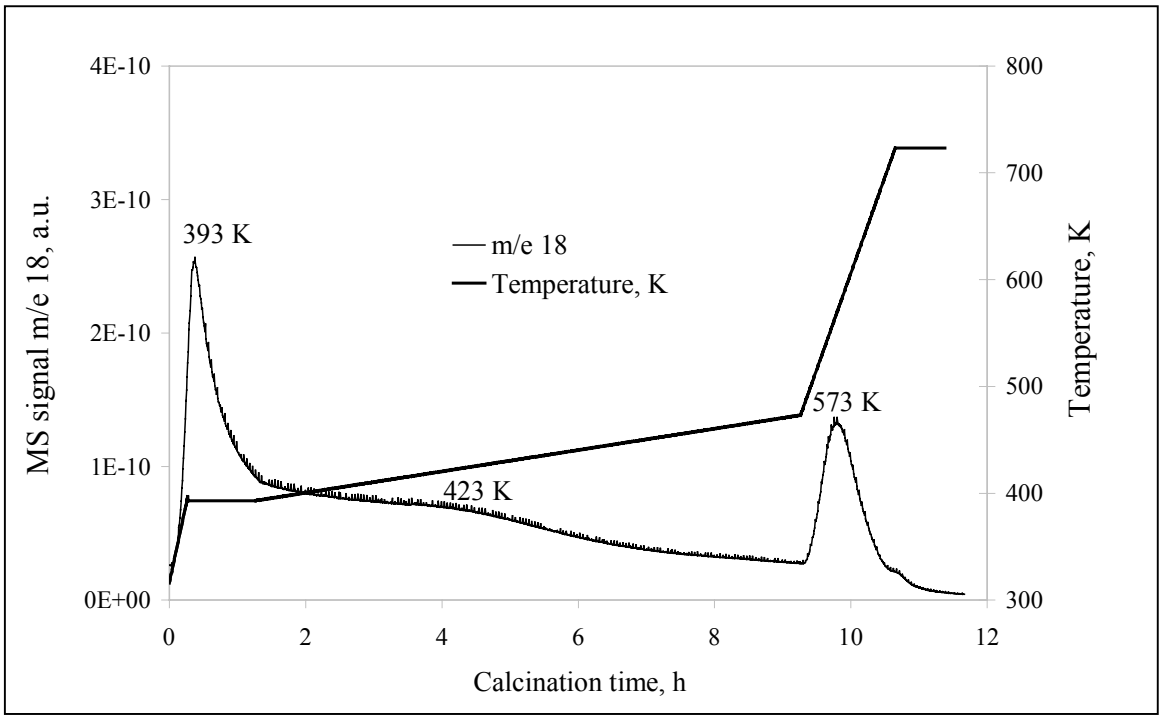

Figure 2.1: MS signal for m/e 18 recorded during the *in situ first calcination* of a two times lanthanum exchanged Na-X zeolite.

Fig. 2.2 shows the IR spectra recorded during calcination in the IR flow cell ("*in situ calcination*") of the same sample. At temperatures below 393 K it was not possible to distinguish well-defined bands in the hydroxyl region. After calcination at 393 K five bands were observed corresponding to terminal silanol groups (3743 cm^{-1}), to the bridging hydroxyl groups of the zeolite (3640 and 3600 cm^{-1}), to physisorbed water (3570 cm^{-1} [19]), and to lanthanum hydroxyl groups (3520 cm^{-1}). When the calcination temperature reached 573 K, the bands at 3570 cm^{-1} and the deformation band of water at 1630 cm^{-1} disappeared completely. For calcination temperatures

above 573 K, the intensities of the bands corresponding to hydroxyl groups at 3600 cm^{-1} and to lanthanum hydroxyl groups at 3520 cm^{-1} decreased progressively. The intensity of the band at 3640 cm^{-1} decreased slightly until approximately 593 K and then increased for higher temperatures. In the whole temperature range studied the silanol band at 3743 cm^{-1} was very weak.

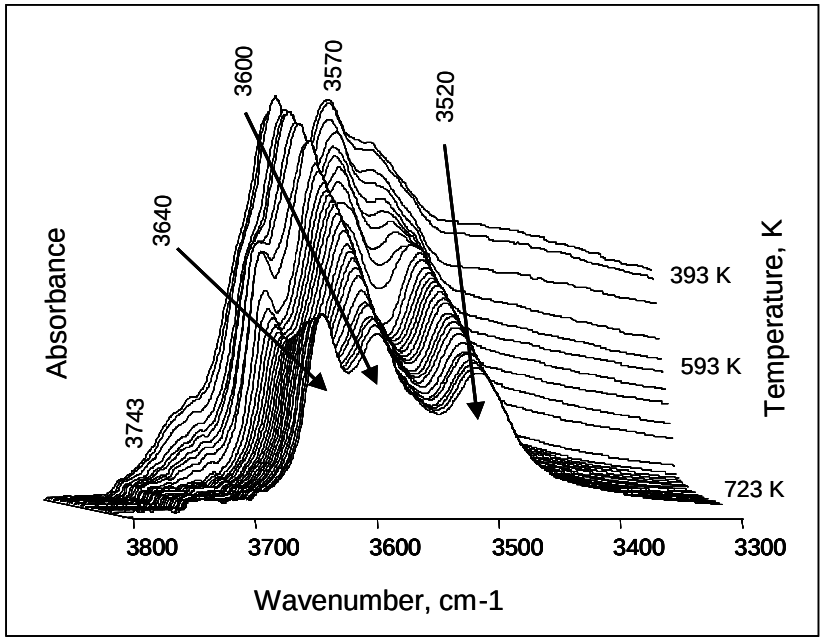

Figure 2.2: IR spectra recorded during the *in situ first calcination* of a two times lanthanum exchanged Na-X zeolite.

The activation of the "*ex situ*" calcined zeolite (stored in air) was followed by IR during increasing of the temperature up to 723 K in flowing air. The relative intensities of the IR bands differed markedly from those of the sample calcined *in situ.* With the latter the intensity of the hydroxyl groups at 3640 cm^{-1} was higher than the intensities of the $La[OH]^{2+}$ groups at 3520 cm^{-1} and of the hydroxyl groups at 3600 cm^{-1}. The band of the silanol groups at 3743 cm^{-1} was less intense. An example of the IR spectra of the two samples recorded at the same temperature is shown in Fig. 2.3.

These results were confirmed by ^{1}H MAS NMR measurements. In the sample calcined *in situ* the intensity of the protons associated to bridging hydroxyl groups at ca. 4 ppm [20] was higher than that of the protons associated with the $La[OH]^{2+}$ groups at ca. 6.6 ppm, while the intensity of the protons corresponding to silanol groups at ca.1.8 ppm was lower. In addition, the total Brønsted acidity of the *in situ* and *ex situ* calcined samples was 0.77 and 0.50 mmol/g, respectively, while the total Lewis acidity was 0.06 and 0.13 mmol/g.

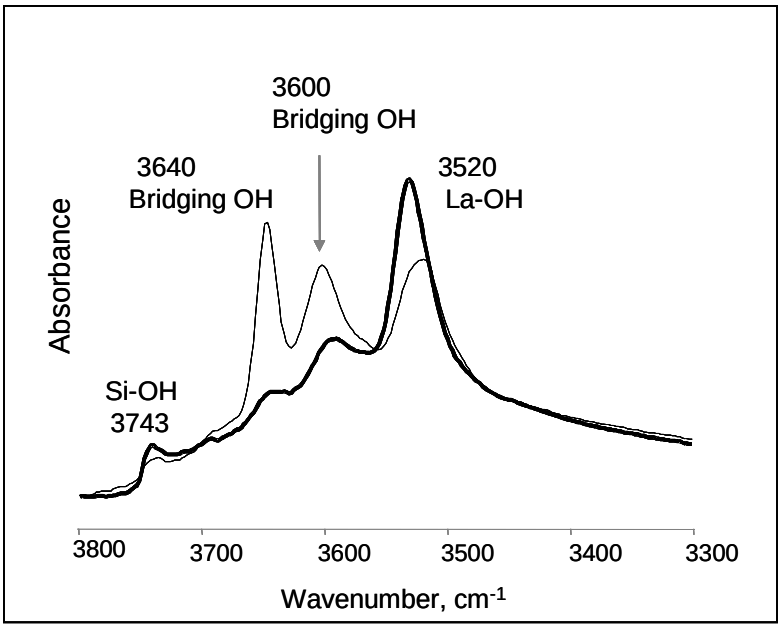

Figure 2.3: Comparison between IR spectra (recorded at 303 K) of a two times lanthanum exchanged Na-X zeolite calcined at 723 K (*first calcinations*) *in situ* (gray line) and *ex situ* (black line) with respect to the IR cell.

After calcination in the IR flow cell (*in situ calcination*), the sample was cooled down to 303 K and approximately 0.01mmol water/min were dosed for 10 minutes using air as carrier gas. Then, the sample was heated up to 723 K. When the temperature reached ca. 393 K (temperature at which the hydroxyl groups in the zeolite can be distinguished from the very broad and intense water hydroxyl vibrations in this region) the IR spectra were similar to those obtained from the sample calcined *ex situ* (Fig. 2.4), i.e., the band at 3640 cm^{-1} was much weaker than those at 3600 and at 3520 cm^{-1}, while the band at 3743 cm^{-1} was more intense.

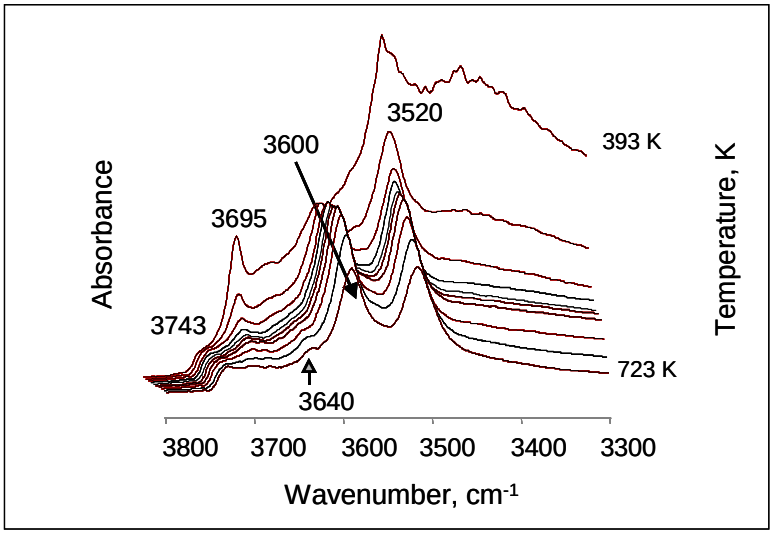

Figure 2.4: IR spectra recorded during *in situ* re-calcination after water adsorption on the two times lanthanum exchanged Na-X zeolite calcined *in situ* (*first calcination*).

In order to investigate, if also the adsorption of water after the "*second calcination*" can modify the relative intensity of the hydroxyl groups, the same hydration-calcination experiment was performed with a sample further exchanged with lanthanum (three times) after the "*first calcination*" and finally undergone to the "*second calcination*". As shown in Fig. 2.5 significant changes in the IR spectra between the sample calcined *in situ* and *ex situ* ("*second calcination*") were not

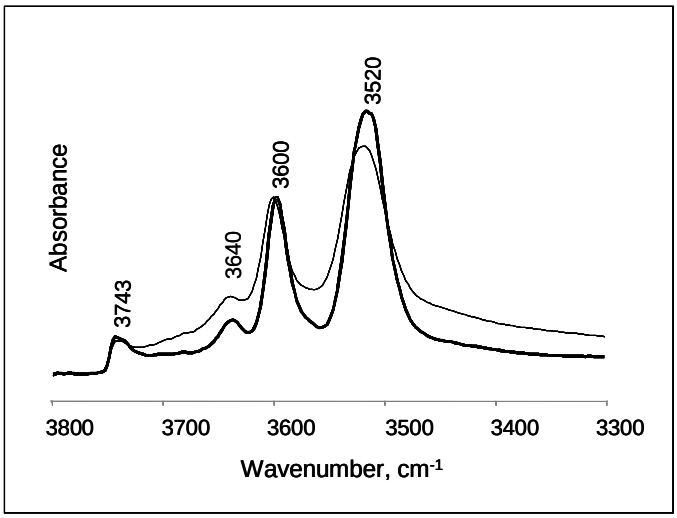

observed.

Figure 2.5: Comparison between IR spectra (recorded at 303 K) of a La-X zeolite calcined at 723 K (*second calcinations*) *in situ* (gray line) and *ex situ* (black line) with respect to the IR cell.

2.3.2 Acidic properties of the lanthanum exchanged Na-X zeolites at different preparation steps

The normal procedure followed for the preparation of the lanthanum exchanged Na-X zeolites implies 1 or 2 exchanges with lanthanum salt solutions followed by a first calcination and a maximum of 3 further exchange steps followed by a second calcination. Samples at different steps of this preparation procedure were systematically collected. Their properties (ion exchange degree, unit cell size, acidity and catalyst lifetime in alkylation reaction) are compiled in Table 1. The fraction of strong Brønsted acid sites (BAS_{723}/BAS_{423}) increased with IExD. Additionally, the two samples with the highest concentration of total Lewis acid sites LAS_{423} (2LaC and 2LaC+3LaC) showed also the lowest values for the UCS. This suggests a relation between the content of lanthanum, which increases with increasing IExD, and the formation of Lewis acid sites.

Sample identification	Preparation	IExD	UCS	BAS		LAS		BAS_{723}/BAS_{423}	Cat. Lifetime
				BAS_{423}	BAS_{723}	LAS_{423}	LAS_{723}		
		(1-Na/Al)*100	Å	(mmol/g)	(mmol/g)	(mmol/g)	(mmol/g)		h
Parent material	calc.	0.0	24.983	0.01	0.00	0.00	0.00	0.00	-
1LaC	$1La^{3+}$ + calc.	37.3	25.035	0.17	0.02	0.01	0.00	0.13	-
2LaC	$2La^{3+}$ + calc.	82.2	25.015	0.49	0.18	0.13	0.09	0.37	-
1LaC+1LaC	$1La^{3+}$ + calc. + $1La^{3+}$ + calc.	90.8	25.019	0.51	0.17	0.06	0.03	0.34	3.0
1LaC+2LaC	$1La^{3+}$ + calc. + $2La^{3+}$ + calc.	95.5	25.022	0.59	0.24	0.03	0.02	0.40	4.0
1LaC+3LaC	$1La^{3+}$ + calc. + $3La^{3+}$ + calc.	97.7	25.019	0.52	0.26	0.09	0.04	0.50	13.5
2LaC+3LaC	$2La^{3+}$ + calc. + $3La^{3+}$ + calc.	99.6	25.009	0.44	0.24	0.11	0.06	0.56	12.0

Table 2.1: Physicochemical properties of different lanthanum exchanged Na-X zeolites: ion exchange degree (IExD), unit cell size (UCS), acidity (concentration of Brønsted and Lewis acid sites determined by pyridine adsorption and outgassing at 423 and 723 K) and catalyst lifetime in alkylation.

Fig. 2.6 (a) shows the IR spectra recorded at 423 K after activation in vacuum at 723 K for 1h of samples with different IExD (gray line) and the corresponding spectra after pyridine adsorption and outgassing at 423 K (black line). In Fig. 2.6 (b) the profile obtained by subtraction of the spectra recorded after and before pyridine adsorption are also shown. In the spectra of activated materials the band characteristic

of the lanthanum hydroxyl groups was progressively shifted to lower wavenumbers, from 3533 to 3514 cm^{-1}, as the ion exchange degree increased. Simultaneously, the intensity of this band increased exponentially. The bridging hydroxyl band at approximately 3600 cm^{-1} increased with the IExD, though not exponentially, while the intensity of the second bridging hydroxyl band at 3640 cm^{-1} was almost constant.

After adsorption of pyridine, the intensity of the lanthanum hydroxyl band of the sample with 37.3% IExD was higher compared to that of the activated sample. At 82.2% IExD pyridine was not adsorbed on the $La[OH]^{2+}$ groups, while it reacted in the samples with higher IExD, the extent of the interaction being higher for the samples with higher IExD (90.8-97.7%). However, in the fully La^{3+} exchanged zeolite (99.6% IExD) the interaction between lanthanum hydroxyl band and pyridine was practically not observed. This result suggests that in this sample all lanthanum hydroxyl groups are located in the sodalite cages and, therefore, they are not accessible to pyridine.

The reactivity of the band at 3600 cm^{-1} increased with IExD and only for low IExD this band did not disappear completely after pyridine adsorption. Additionally, the non reactive part of this band at low IExD appeared slightly shifted to 3584 cm^{-1}. These findings are in agreement with the lower strength of the acid sites due to the remaining sodium cations [21].

For all the samples the bridging hydroxyl groups at 3640 cm^{-1} reacted completely with pyridine.

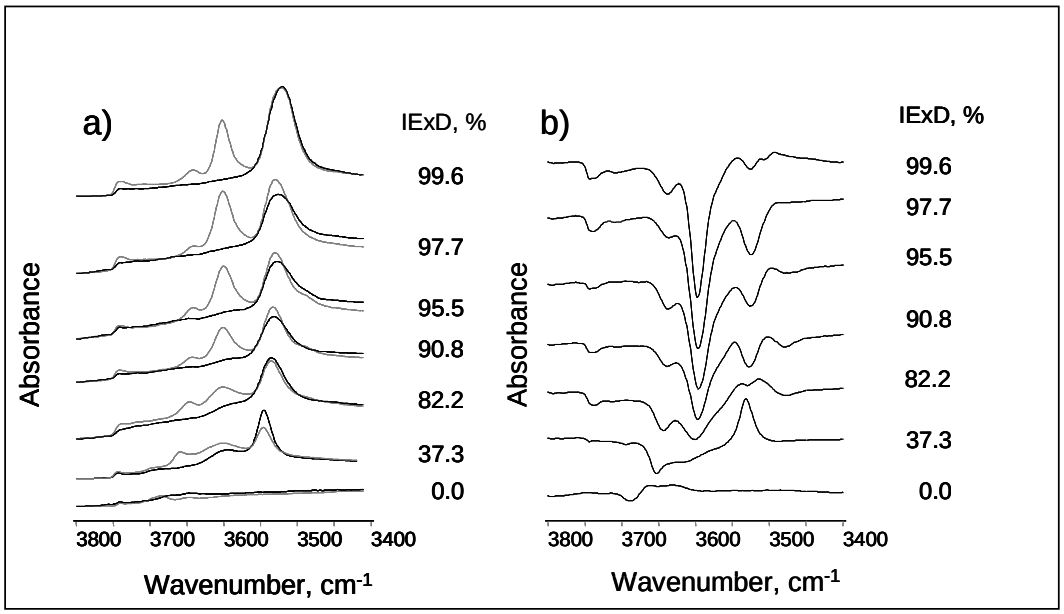

Figure 2.6: a) IR spectra of activated samples (gray line) and after pyridine adsorption (black lines) at different preparation steps. b) Profile obtained by subtraction of the spectra recorded after and before pyridine adsorption.

The effect of the IExD on the Brønsted and Lewis acidity was studied by IR spectroscopy with pyridine as probe molecule. The Brønsted acid sites were identified by the band at 1543 cm^{-1} (pyridinium ion), while the Lewis acid sites by the band at 1454 cm^{-1} attributed to pyridine coordinatively bound to cationic extraframework aluminum species [22]. Fig. 2.7 shows that the total concentration of the Brønsted acid sites (BAS_{423}) passed through a maximum at 95.5 % IExD, while the concentration of the strong Brønsted acid sites (BAS_{723}) increased continuously up to about 99.6 % IExD (0.25 mmol/g). Thus, fraction of strong Brønsted acid sites (BAS_{723}/ BAS_{423}) increased exponentially with IExD. It is interesting to note that a linear correlation between the intensity of the $[La(OH)]^{2+}$ band at ca. 3520 cm^{-1} and the fraction of strong Brønsted acid sites (BAS_{723}/ BAS_{423}) exists (see Fig. 2.8).

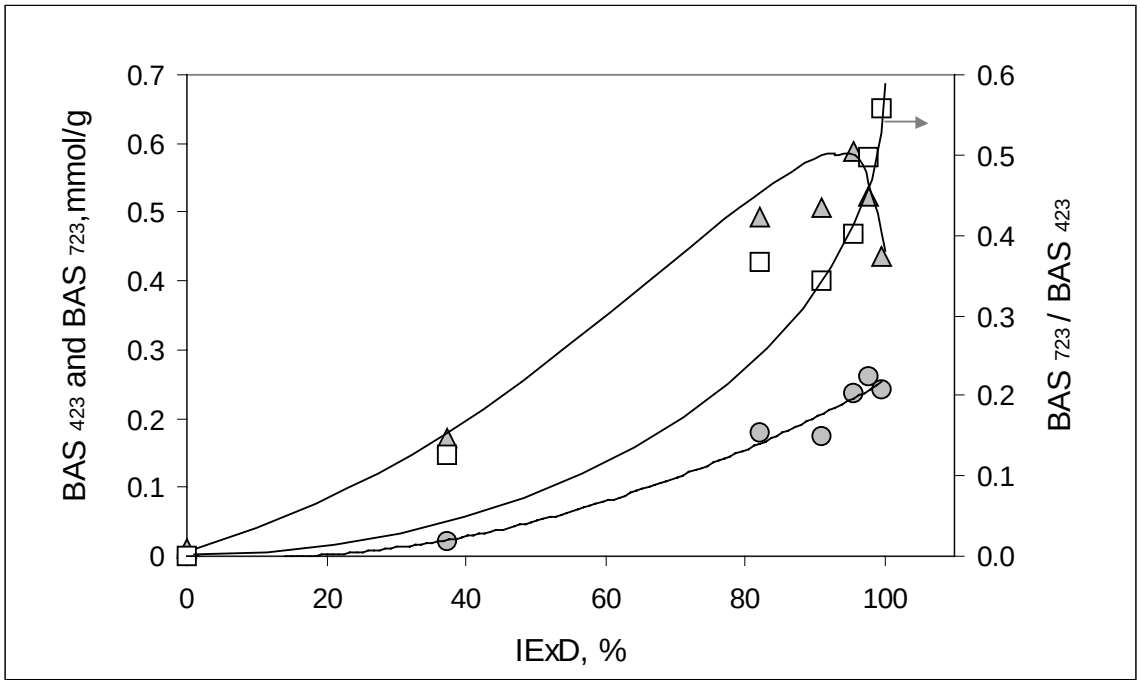

Figure 2.7: Effect of the IExD on the concentration of total (△ BAS_{423}) and strong Brønsted acid sites (○ BAS_{723}) and on the fraction of strong Brønsted acid sites (□BAS_{723}/BAS_{423}).

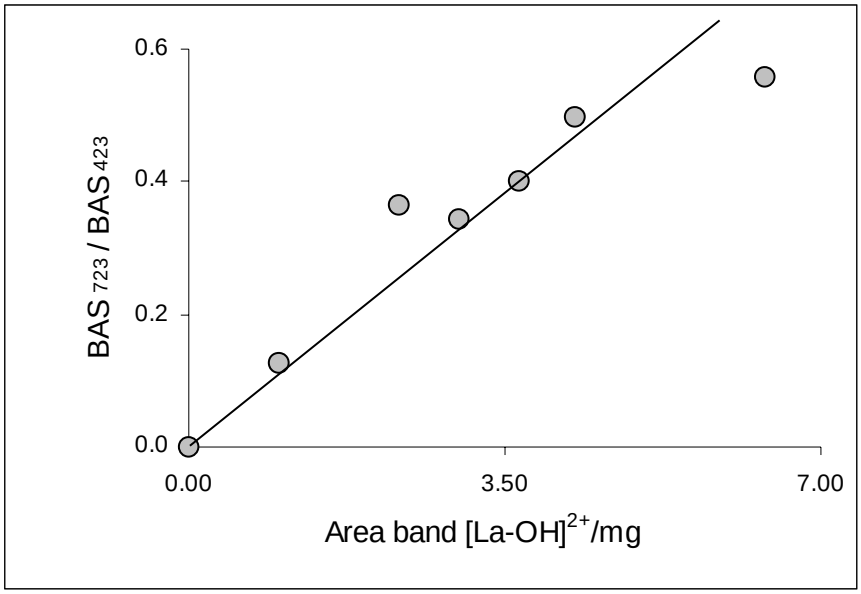

Figure 2.8: Correlation between the fraction of strong Brønsted acid sites (BAS_{723}/BAS_{423}) and the normalized area of the hydroxyl groups band at 3520 cm^{-1}.

Fig. 2.9 shows the effect of the IExD on the total concentration of Lewis acid sites (LAS_{423}). A minimum (0.03 mmol/g) was observed for 95.5% IExD. The sample twice exchanged before the first calcination (82.2% IExD) showed the highest concentration of total Lewis acid sites (0.13 mmol/g). For the sample with 37.3% IExD strong Lewis acid sites were not observed.

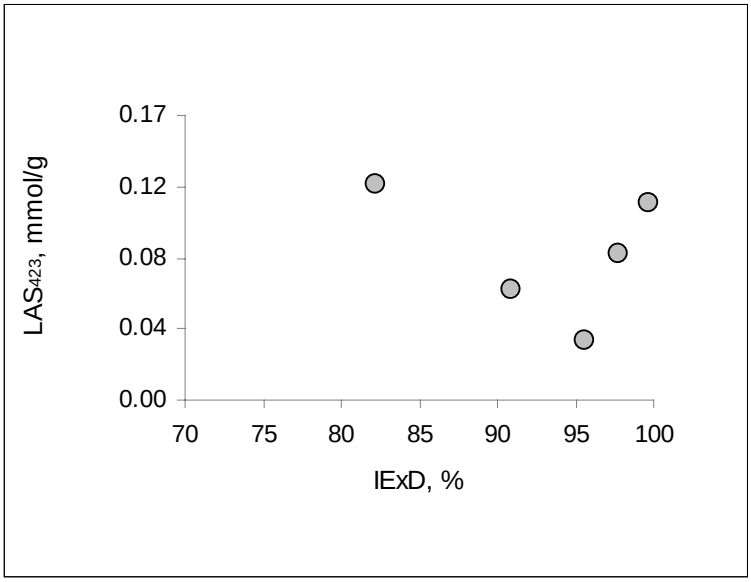

Figure 2.9: Effect of the IExD on the concentration of total Lewis acid sites (LAS_{423}).

Another typical band observed in the spectra of adsorbed pyridine on this series of samples appeared at ca. 1444 cm^{-1}. The assignment of the IR band at 1444 cm^{-1} has been discussed by several authors. It has been associated to pyridine interacting with aluminum extraframework species [22], with cations, whose wavenumber depends on the type of cation compensating the zeolite negative charge [23], and with hydroxyl groups [24]. Lercher *et al*. [24] assigned a band at 1440 cm^{-1} to pyridine adsorbed on OH groups and a band at 1448 cm^{-1} to pyridine adsorbed on Na^+ cations. The thermal stability was used as the most important criterion to distinguish between pyridine adsorbed on OH groups (low thermal stability) and on accessible cations (high thermal stability). However, the temperatures used in the present study to distinguish between strong and weak acid sites, 423 and 723 K, were higher compared to the temperatures used in ref. [24]. As a consequence pyridine adsorbed on Na^+ or hydrogen bonded to OH groups was drastically reduced after heating to 723 K. It is very likely that after this thermal treatment only pyridine interacting with aluminum extraframework species was still adsorbed.

Although the extinction coefficients for the bands at ca. 1444 cm^{-1} have not been quantitatively measured, the weighted normalized area obtained after pyridine adsorption/desorption at 423K was used to follow its behavior with IExD. As shown in Fig. 2.10 the band at 1444 cm^{-1} had a minimum intensity between 90.8 and 95.5 % IExD. At higher IExD the intensity of this band increased. This is interpreted as follows: at low IExD, i.e. at high concentration of Na^+, the contribution of the pyridine coordinatively bound to these cations predominated at this adsorption temperature, while at high IExD (>95.5%) pyridine hydrogen bonded to OH and aluminum extraframework dominated. As a consequence a minimum is observed.

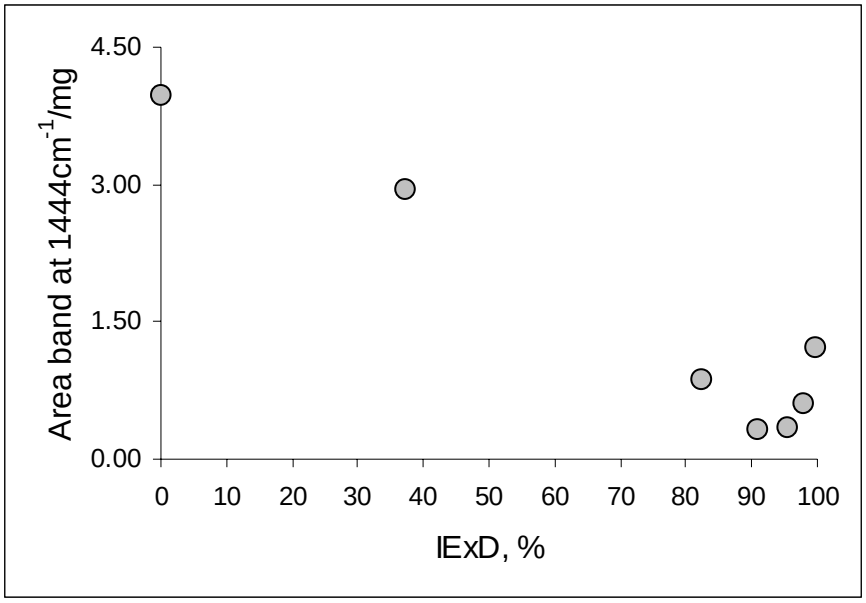

Figure 2.10: Effect of the IExD on the normalized area of the IR band at 1444 cm^{-1}.

2.3.3 Catalytic activity over lanthanum exchanged Na-X zeolites at different preparation steps

In order to investigate, how the acidic properties of the samples at different preparation steps are related to the catalytic activity, the samples with IExD ≥ 90.8% (Table 1) were tested for isobutane/cis-2-butene alkylation in a CSTR type reactor. The lifetime of these catalysts increased with IExD from 3.0 to 13.5 h. In Fig. 2.11 (a) the dependence of the integral selectivities (until the end of the catalyst lifetime) upon the catalyst lifetime is shown. The C_8 fraction dominated in the alkylate. The integral selectivity to n-butane increased slightly with lifetime.

In the C_8 fraction the selectivities to 2,2,4-TMP and to 2,2,3-TMP + 2,5-DMH increased, while the selectivities to 2,3,4-TMP and 2,3,3-TMP decreased (Fig. 2.11 (b)).

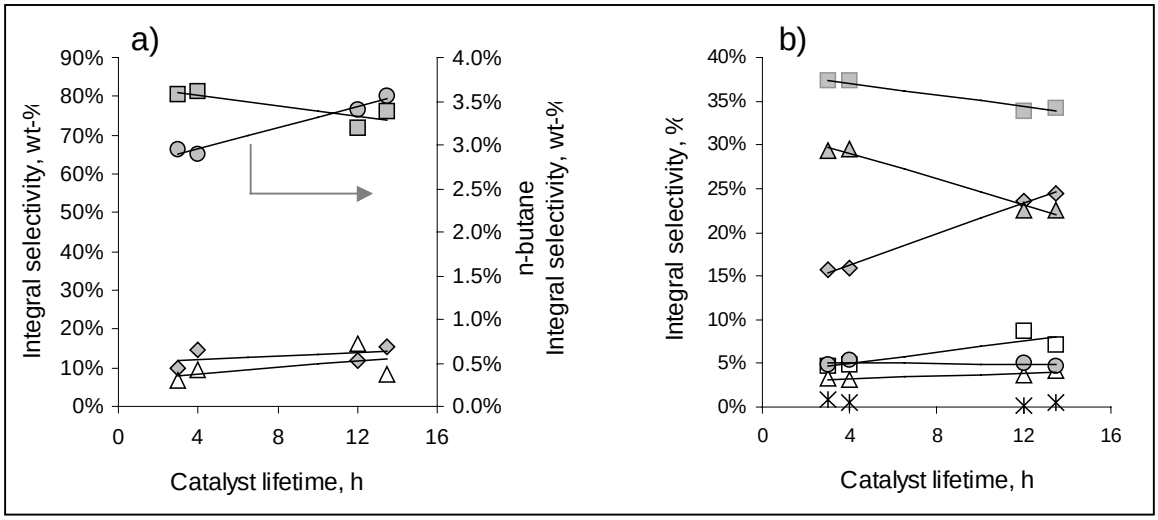

Figure 2.11: Variation in selectivities with catalyst lifetime of the lanthanum exchanged Na-X zeolites with IExD ≥90.8%. a) Integral selectivities to the different product groups as a function of catalyst lifetime (○ n-butane, □ C_8 products, ◇ C_5-C_7 products, △ C_{9+}); b) Integral selectivities to the individuals C_8 products as a function of catalyst lifetime (—□— 2,3,3-TMP, —△— 2,3,4-TMP, —◇— 2,4,4-TMP, —□— 2,2,3-TMP + 2,5-DMH, —○— 2,3-DMH, —△— 2,4-DMH, ✳ octenes).

As shown in Fig. 2.12, the catalyst lifetime and the fraction of strong Brønsted acid sites (BAS_{723}/BAS_{423}) are directly correlated. A high fraction of strong Brønsted acid sites has been demonstrated to be mandatory for long catalyst life in isobutane/cis-2-butene alkylation on zeolite based catalysts [4].

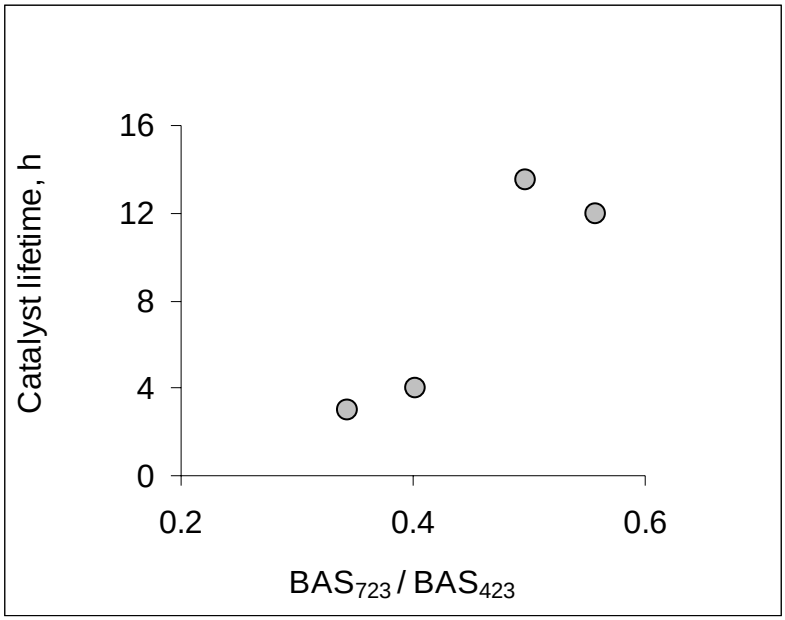

Figure 2.12: Catalyst lifetime in alkylation reaction as a function of the fraction of strong Brønsted acid sites (BAS_{723}/BAS_{423}).

2.4. Discussion

2.4.1. Hydroxyl groups formation on lanthanum exchanged X zeolites

The presence of bridging hydroxyl groups (IR bands at 3600 and 3640 cm^{-1}) and of lanthanum hydroxyl groups (IR band at 3520 cm^{-1}) on lanthanum exchanged Na-X after the calcination at 393 K indicates that the hydrolysis of hydrated lanthanum cations starts at such low temperatures. Upon further increase of the calcination temperature, physisorbed water is removed (decrease of the IR bands at 3570 cm^{-1}) and the intensity of hydroxyl groups, bridging and associated with lanthanum, decreases up to approximately 593 K. From this temperature the band of the bridging hydroxyl group at 3640 cm^{-1} increases, while the lanthanum hydroxyl band $[LaOH]^{2+}$ (3520 cm^{-1}) and the band of the bridging hydroxyl group at 3600 cm^{-1} decrease. This suggests a gradual dehydroxylation of the zeolite as the calcination temperature increases. The decrease of the intensity of the IR bands is not due to an effect of the temperature (see e.g. ref. [25]), as confirmed by comparison of the IR spectra recorded at the same temperature, before and after heating step. Thus, water evolution

monitored during calcination can be attributed to water from dehydroxylation of lanthanum hydroxyl groups and bridging hydroxyl groups at 3600 cm^{-1}. The presence of Lewis acid sites in the *in situ* calcined sample supports this interpretation. However, the increase in the hydroxyl groups at 3640 cm^{-1} suggests that hydrolysis of lanthanum cations is not complete at low calcination temperatures and that calcination temperatures above 593 K are required to exchange Na^{+} cations in the sodalite cages.

The exposure to water after the "*first calcination*" has a strong effect on the hydroxyl groups, as observed by comparison of the IR spectra recorded after "*in situ"* and "*ex situ*" calcination (Fig. 2.3). After water adsorption the band at 3640 cm^{-1} decreases in intensity, while the silanol band increases. This process is accompanied by the decrease of the total Brønsted acidity from 0.77 to 0.50 mmol/g and by a significant increase of the total Lewis acidity (from 0.06 to 0.13 mmol/g). Thus we conclude that the zeolite is significantly dealuminated, when it is contacted with humid atmosphere after the "*first calcination*".

Chemically, dealumination is the reaction between the aluminum mostly bearing hydroxyl groups in the framework with water [26]. Therefore, it is reasonable to assume that dealumination of the La-Na-X zeolite is associated with the protons produced in the dissociative adsorption of water on the La^{3+} cations. The decrease of the band of the bridging hydroxyl groups at 3640 cm^{-1} is attributed to the reaction of the associated aluminum with water. The preference of the dealumination at aluminum- oxygen tetrahedra associated with the 3640 cm^{-1} OH band in comparison to the aluminum-oxygen tetrahedra leading to the band at 3600 cm^{-1} is tentatively attributed to more accessible or labile aluminum-oxygen bonds. The acidic protons associated with the IR band at 3640 cm^{-1} are consumed considerably during the rehydration and subsequent dealumination of the zeolite and lead to new SiOH groups. After these structural changes the zeolite becomes thermal stable. In fact the water adsorbed after the "*second calcination*" did not affect the IR spectrum (Fig. 2.5). UCS measurements for these samples are in good agreement with the variations in the intensities of the OH bands, i.e., the UCS before calcination, after the "*first* and the *second calcination*" were 25.139, 25.019 and 25.035 Å, respectively indicating that dealumination is more pronounced after the first calcination.

2.4.2. Acidity of La-Na-X with different ion exchange degrees and catalytic properties

Using pyridine as probe molecule the fraction of strong Brønsted acid sites is seen to increase exponentially with IExD. It should be noted, however, that samples with IExD larger than ≥ 97.7 % have the highest concentrations of strong Brønsted acid sites, while the total concentration of Brønsted acid passes through a maximum at 95.5 % IExD.

The catalyst lifetime in isobutane/cis-2-butene alkylation is correlated with the fraction of strong Brønsted acid sites (Fig. 2.12) [27]. This is well illustrated by the sample with 95.5 % IExD: it has a concentration of strong Brønsted acids similar to that of samples with higher IExD but at the same time a higher concentration of weak Brønsted acid sites and a relatively short lifetime (4 h). This short lifetime is caused by the fact that the olefin addition to an acid site to form a carbenium ion is a much more facile reaction than hydride transfer. Thus, catalysts with high concentration of weak Brønsted acid sites catalyze mainly olefin oligomerization, leading to heavy alkylate deposits, which in turn shorten the catalyst lifetime. The catalysts with the longest lifetime showed also the highest production of n-butane (Fig. 2.11). The selectivity to n-butane was shown to be dependent solely on the hydride transfer rate relative to the alkene addition rate. With higher hydride transfer rates more n-butane will be produced [27].

In line with our previous work on the mechanism of isobutane/butane alkylation catalyzed by zeolites, the increase seen in the 2,2,3-TMP + 2,5-DMH and 2,2,4-TMP selectivities (Fig. 2.11), parallel with the n-butane selectivity, is a consequence of the higher rate of hydride transfer observed in catalysts with high concentration of strong Brønsted acid sites (catalysts with 97.7 and 99.6% IExD). This mechanism is also operative in the case of alkylation catalyzed by liquid acids [27].

It is interesting to note that among the catalysts tested, the sample with 95.5% IExD has the lowest concentration of Lewis acid sites. Although it was shown that a high concentration of Lewis acid sites is detrimental for the activity in isobutane/cis-2-butene alkylation, the present results seem to suggest that the concentration of weak Brønsted acid sites has the most negative impact on the catalyst lifetime.

The presence of weak Brønsted acid sites has been mainly related to the presence of sodium cations in the zeolites [21]. However, in the present system the sodium content is not the only factor that affects the acidic properties of the catalysts. The

lanthanum exchange degree before the *first calcination* is also important. The higher the lanthanum exchange degree the higher is the concentration of acidic hydroxyl groups formed by hydrolysis of the lanthanum ions. This leads to a higher degree of dealumination during rehydration of the calcined material in the first step. Thus, the catalyst with 97.7 % IExD (1+3 lanthanum exchanges) presented a longer lifetime (13.5 h) compared to that obtained for the catalyst with the lowest concentration of remaining sodium (2+3 lanthanum exchanges; 12 h lifetime).

The band at 1444 cm^{-1} of adsorbed pyridine is complex to interpret. In the parent material this band has to be attributed to the Na^+ cations. With increasing IExD Na^+ cations are replaced by La^{3+} cations. After *the first calcination* the hydrated lanthanum cations are converted to $[LaOH]^{2+}$ and migrate in an irreversible manner to the small cages of the zeolite. Therefore, the contribution of the La^{3+} cations to the band at 1444 cm^{-1} due to pyridine interacting with cations, must be neglecting. After this *first calcination* of the exchanged zeolite, extraframework aluminum species are formed during the rehydration process and their concentration depends on protons, specially those responsible of the band at 3640 cm^{-1}, which in turn were formed by hydrolysis of the hydrated La^{3+} cations. Zeolites exchanged at higher level before the *first calcination* generate more EFAL species. After a 3-fold exchange with La^{3+} cations in the second exchange step followed by a *second calcination*, the content of lanthanum has been the highest (IExD of 99.6%). Consequently, the sodium content of this sample is very low and cannot be responsible of the band at 1444cm^{-1}. Thus, with very low concentration of Na^+ and La^{3+} in the small cavities of the zeolite, the increase of the band at 1444 cm^{-1} can be attributed to pyridine interacting mostly with EFAL species. The two partially overlapping bands at 1444 and 1454 cm^{-1} in the IR spectra of adsorbed pyridine are generally observed in zeolites containing extraframework aluminum in the form of oxidic debris and assigned to the coordinative interaction of pyridine with accessible Al^{3+} cations [22].

As indicated by the linear correlation between the $[LaOH]^{2+}$ groups (3520 cm^{-1}) and the fraction of strong Brønsted acid sites (BAS_{723}/BAS_{423}), the strong Brønsted acid sites are generated by the dissociation of water on La^{3+}. As the IExD increases more $[LaOH^{2+}]$ and bridging hydroxyl groups are formed. While the $[LaOH]^{2+}$ groups migrate to the small cavities the bridging hydroxyl groups remain in the supercages of La-Na-X. This allows more Na^+ from the ß-cages to be exchanged. At exchange degrees above 97.7% most of the lanthanum is in the small cavities while the

concentration of Na^+ is very low. These interdependent factors are responsible for the enhanced strength of the bridging hydroxyl groups in this zeolite. Although with divalent cations, for instance Mg^{2+} or Ca^{2+}, a similar situation is observed, the strength of the formed bridging hydroxyl groups by hydrolysis of the exchanged divalent cations is lower [8]. At present it cannot be decided whether this higher effect is related to a stronger polarizing effect of the cation or whether this is related to the particular location of the Brønsted acid sites.

2.5. Conclusions

Hydrolysis of the hydrated lanthanum cations starts below 393 K as evidenced by the bands corresponding of $[LaOH]^{2+}$ (3520 cm^{-1}) and bridging hydroxyl groups (3600 and 3640 cm^{-1}). As the calcination temperature is further increased dehydroxylation of the zeolite and hydrolysis of the hydrated lanthanum cations take place. While the $[La(OH)]^{2+}$ (3520 cm^{-1}) and one type of bridging hydroxyl groups (3600 cm^{-1}) decrease in concentration, the other bridging hydroxyl groups (3640 cm^{-1}) increases.

Local changes of the structure take place during rehydration of the La-Na-X zeolites after the *first calcination*. A considerable decrease of the bridging hydroxyl band (3640 cm^{-1}) and an increase of silanol band (3740 cm^{-1}) were observed after adsorption of water. These changes are attributed to the dealumination induced by the simultaneous presence of water and acidic hydroxyl groups (3640 cm^{-1}). The higher the IExD in the first exchange step the higher the concentration of protons produced by water dissociation on La^{3+} cations and consequently more EFAL species are formed during rehydration. It should be noted that this dealumination only affects rather labile Al-O tetrahedra, as rehydration after the *second calcination* did not have a recognizable effect on the acid sites.

It is important to note that the formation of $[La(OH)]^{2+}$ groups and the removal of the Na^+ cations markedly influenced the strength of the acid sites in La-Na-X.

The activity in isobutane/cis-2-butene alkylation is mainly controlled by the fraction of strong Brønsted acid sites and the space velocity of the olefin in relation to the absolute concentration of these strong Brønsted acid sites. Catalysts with similar concentration of strong Brønsted acid sites and higher concentration of weak Brønsted sites showed shorter lifetime.

2.6. Acknowledgments

Financial support from Süd-Chemie AG is gratefully acknowledged.

The author wishes also to thank Prof. Dr. Michael Hunger of University of Stuttgart for the NMR measurements of some of our samples and for his discussions on structural properties of zeolitic materials.

2.7. References

[1] J. Weitkamp, Y. Traa, Catal. Today 49 (1999) 193.

[2] J. Weitkamp, Y. Traa, in: Handbook of Heterogeneous Catalysis (G. Ertl, H. Knözinger, and J. Weitkamp, Eds). 4 (1997) 2039.

[3] A. Corma, A. Martinez, Catal. Rev.-Sci. Eng. 35 (1993) 483.

[4] A. Feller, J-O. Barth, A. Guzman, I. Zuazo, J.A. Lercher, J. Catal. 220 (2003) 192.

[5] A. Feller, I. Zuazo, A. Guzman, J-O. Barth, J.A. Lercher, J. Catal. 216 (2003) 313.

[6] V. F. Maxim, N.S. Vitali, V.B. Kazanski, J. Chem. Soc., Faraday Trans. 93 (1997) 515.

[7] M. Boronat, P. Viruela, A. Corma, J. Phys. Chem. A. 102 (1998) 9863.

[8] J.W. Ward, J. Catal. 14 (1969) 365.

[9] P.B. Venuto, L.A. Hamilton, P.S. Landis, J. Catal. 5 (1966) 484 .

[10] M. Hunger, D. Freude,H. Pfeiffer, D. Prager, W. Reschetilowski, Chem. Phys. Lett. 163 (1989) 221.

[11] J.W. Ward, J. Catal. 13 (1969) 321.

[12] A.K. Cheetham, M.M. Eddy, J.M. Thomas, J. Chem. Soc., Chem. Commun. 1337 (1984) 508.

[13] E.F.T. Lee, L.V.C. Rees, Zeolites. 7 (1987) 143.

[14] J. Scherzer, J., Octane-Enhancing Zeolitic FCC Catalysts, Marcel Dekker, INC. New York, 1990, p. 22.

[15] R. Carvajal, P. Chu, P. J.H. Lunsford, J. Catal. 125 (1990) 123.

[16] H.G. Karge, in: Studies in Surface Science and Catalysis. Catalysis and Adsorption by Zeolites (Öhlmann, G., Pfeiffer, H., and Fricke, R.) Elsevier, Netherlands. 65 (1991) 133.

[17] ASTM D 3942-85, Determination of the Unit Cell Size Dimension of a Faujasite-Type Zeolite. American Society for Testing and Materials, 1985.

[18] C.A. Emeis, J. Catal. 141 (1993) 347.

[19] J.W. Ward, J. Phys. Chem. 72 (1968) 4211.

[20] M. Hunger, Solid State Nucl. Mag. 6 (1966) 1.

[21] P.O. Fritz, J.H. Lunsford, J. Catal. 118 (1989) 85.

[22] R.M. Mihály, H.K. Beyer, V. Mavrodinova, Ch. Minchev, Y. Neinska, Micropor. Mesopor. Mat. 24 (1998) 143.

[23] J.W. Ward, J. Colloid Interf. Sci. 28 (1968) 269.

[24] J.A. Lercher, G. Ritter, H. Vinek, J. Colloid Interf. Sci. 106 (1985) 215.

[25] R.A. Schoonheydt, J.B. Uytterhoeven, J. Catal. 19 (1970) 55.

[26] G.T. Kerr, J. Phys. Chem. 71 (1967) 4155.

[27] A. Feller, A. Guzman, I. Zuazo, J.A. Lercher, J. Cat. 224 (2004) 80.

Chapter 3

Catalytic active sites on FAU, EMT and BEA type zeolites in isobutane/cis-2-butene alkylation

Abstract

A detailed IR spectroscopic study of the Brønsted and Lewis acid sites in FAU, EMT, and BEA, using pyridine and a mixture isobutane/cis-2-butene as probe molecules, was performed. The relation of the acidic properties with the catalytic activity in isobutane/cis-2-butene alkylation was also addressed. The differences in density, location and strength of the Brønsted acid sites, characteristic for the different zeolites, led to catalyst lifetimes in isobutane/cis-2-butene alkylation varying from 1 to 13 hours. Generally, a larger concentration of strong Brønsted acid sites and a low concentration of weak Brønsted acid site were required for longer lifetimes.

Keywords: IR spectroscopy, zeolitic hydroxyl groups, alkylation.

3.1. Introduction

Isobutane alkylation with C_3-C_5 olefins is a very important refining process for producing high-octane gasoline. Currently, H_2SO_4 and HF are used as catalysts in the industrial processes. Due to environmental regulations, the implementation of alternative processes, based on more friendly solid acid catalysts, has received significant attention in the last decades [1]. Among the different solid acids, large pore zeolites (especially the faujasite type) are most attractive, either in protonic form or exchanged with di- and tri-valent cations. These large pore zeolites possess 3-dimensional 12-membered-ring pore openings. BEA and EMT type zeolites also have 12-membered-ring openings, but a higher Si/Al ratio than the faujasites, property closely related to the acidity in zeolites. Catalysts based on these materials also have been studied as potential alkylation catalysts [2, 3].

The acidity is the most important property of zeolites with respect to their use as alkylation catalysts [4]. To describe the acidity adequately, it is mandatory to clearly distinguish between (i) nature (Brønsted or Lewis), (ii) density, (iii) strength and (iv) location of the acid sites. Zeolites in cationic form can be converted into the acidic form by ion exchange with either NH_4^+ or multivalent metal cations, followed by thermal treatment. In the first case the NH_4^+ ion decomposes into NH_3 and H^+ upon heating. The resulting proton remains bound to the Al-O tetrahedra generating the Brønsted acid site in the zeolite. In the case of ion exchange with multivalent cations, these will polarize and hydrolyse water present in their hydration sphere following the Hirschler-Plank scheme to produce Brønsted acid sites [5].

Although Brønsted acid sites tend to dominate the discussion on acidity in zeolites, Lewis acidity can also play an important role. Several studies have indicated that Lewis acid sites are interacting strongly with bases and, as such, they may be directly or indirectly important for alkane conversions such as catalytic cracking. However, their role is still a topic of much debate [6] despite several decades of investigations.

Strong (classical) Lewis acid sites are formed by dehydroxylation of tetrahedral framework Al (Al_f) to octahedral Al, which occurs a zeolite is heated above approximately 673K. If the temperature is not higher than approximately 873K, the Lewis acid sites can be reconverted to Brønsted sites by rehydration.

Concerning the acid site strength of zeolites with low Si/Al ratios, it has been rationalized that the local concentration of aluminum dominates the acid base properties, which has been summarized in the concept of the "next nearest neighbors" (NNN) [7]. A completely isolated aluminum tetrahedron has zero next-nearest alumina neighbors and is called a 0-NNN site. A framework aluminum having one aluminum atom as next-nearest aluminum neighbor is called 1-NNN. It is postulated that the most isolated sites (0-NNN) are stronger than 1-NNN sites and so on. However, this model has important constraints that restrict its application. One of these constraints is that, with the exception of protons, the presence of non-framework cations is not considered. Thus, in the case of alkaline earth or rare earth forms of FAU zeolites the concept cannot be directly applied. Furthermore, the extra-framework aluminum species (EFAL) may play a role in the overall acidity and activity.

There is considerable controversy whether or not the non-framework aluminum species enhance the Brønsted acidity, poison the strongest Brønsted acid sites by playing the role of a cation, lead to increased coke production due to their Lewis acidity or only block the zeolite channels, reducing the activity but having no effect on the product selectivity. In idealized zeolites with high Si/Al ratios, all the Al_f are isolated, with no NNN Al_f atoms other than 0-NNN. The acid sites should all be of similar strength and activity should decrease as framework aluminum atoms are removed.

Thus, a simple correlation between the aluminum content in a zeolite and its catalytic activity does not exist. Additionally, the acidity cannot be measured in the same conditions used for catalytic tests [8]. Although pyridine is a much stronger base compared to the reactants involved in the catalytic reactions, this molecule is still the most widely used to characterize the acidity of solid acids [9]. The main advantage of pyridine as probe molecule in IR measurements is the possibility to clearly distinguish between Brønsted and Lewis acid sites from the two bands at ca. 1540 and 1454 cm^{-1}, respectively. Furthermore, due to its size (0.54 nm) pyridine can interact only with acidic sites present in the large cavities.

In this study an attempt to correlate the acidity of different zeolite types with their activity in isobutane/cis-2-butene alkylation was made, based on a detailed IR study using pyridine and the isobutane/cis-2.butene as probe molecules.

3.2. Experimental

3.2.1. Material preparation

The two Na-X zeolites used in this study were supplied from Chemische Werke Bad Köstritz (Si/Al = 1.14) and from Grace-Davison Sylosiv A10 (Si/Al = 1.41). Both materials were brought into the acidic form by two ion exchange steps with 0.2 M lanthanum nitrate solution, using a liquid-to-solid ratio of about 10 mL/g. The ion exchange was carried out at 353K for 2 h. After washing and drying, the resulting materials were calcined at 723K for 1 h in 100 mL/min flowing air, with a slow temperature ramp up to 723K. After re-hydration by exposition to atmospheric moisture, the calcined materials were further exchanged three times with lanthanum nitrate following the same procedure above described included a second calcination step at 723K. The resulting materials are named La-X 1.1 and La-X 1.4 corresponding to the catalysts obtained from the parent materials Na-X Köstrolith (Si/Al = 1.14) and Na-X Sylosiv A10 (Si/Al = 1.41), respectively.

The Na-Y (CBV 100) and Na-USY (CBV 400) zeolites were obtained from Zeolyst International. The NH_4-Y sample was prepared following the conditions described in reference [10]. After washing, a portion of this sample was calcined at 723K (*ex situ* calcination). Another portion was directly activated in the vacuum IR cell at 723K (*in situ* calcination). To obtain H-La-Y from Na-Y CBV 100 the parent material was first exchanged twice with a 3 molar ammonium nitrate solution at 363K for 2 h, then exchanged with a 0.5 M lanthanum nitrate solution at 363K for 2 h and finally calcined at 723K. The same procedure was followed to prepare the H-La-USY sample.

La-Y was prepared from Na-Y (CBV 100) following a procedure similar to that used for the preparation of the La-X zeolites.

The Na-EMT material was synthesized according to the procedures described by Delprato *et al.* [11], using 18-crown-6 ether as template. The organic template was decomposed by calcination in air at 813K for 16 h. The H-EMT form was obtained by ammonium ion exchange of the parent material following the conditions described in reference [12].

Finally, the BEA zeolite was obtained from Zeolyst International (CLA 27923 CP806 E-22). Details on the conversion of the parent material into its acidic form H-BEA are reported elsewhere [13].

3.2.2. Material characterization

The ion-exchanged materials were characterized by SEM, XRD, and ^{29}Si NMR.

AAS was used to determine the chemical composition of the samples.

Template decomposition (18-crown-6 ether) in the synthesized EMT zeolite was studied by temperature programmed oxidation analysis (TPO).

The surface hydroxyl groups were studied by *in situ* IR spectroscopy. Before recording the spectra, the samples were activated *in situ* at 723K. For this purpose the sample was pressed into a self-supporting wafer (with a density between 5 and 10 mg/cm^2). The acidity was studied by adsorption/desorption of pyridine monitored by IR spectroscopy. After activation in vacuum for 1 h at 723K, the sample was cooled down to 423K and pyridine at a partial pressure between 1 – 5 Pa was introduced into the IR cell. Spectra were recorded at 423K before adsorption of pyridine, and after adsorption of pyridine and outgassing at 423 and 723K. The spectra were collected on a Perkin-Elmer system 2000 spectrometer with a spectral resolution of 4 cm^{-1}. The concentration of Brønsted and Lewis acid sites was estimated from the bands at 1540 and 1454 cm^{-1}, respectively. The extinction coefficients were taken from Emeis [14]. The Brønsted and Lewis acid site concentrations measured after outgassing at 423K are referred as BAS_{423} ("*total Brønsted acidity*") and LAS_{423} ("*total Lewis acidity*"), after outgassing at 723K as BAS_{723} ("*strong Brønsted acidity*") and LAS_{723K} ("*strong Lewis acidity*"), respectively.

Isobutane/cis-2-butene adsorption/desorption experiments were also monitored by IR spectroscopy. Self-supporting wafers (density between 5 and 10 mg/cm^2) were activated in a sorption cell in vacuum for 1 h at 723K. After cooling down to 348K, a mixture isobutane/cis-2-butene (with molar ratio 7/1) was introduced into the cell. The amount of mixture was dosed by using a loop of 250 µL maintained at 299K. After adsorption (40 minutes) the cell was evacuated for 30 min and the spectra recorded with a resolution of 4 cm^{-1} on a Bruker IFS88 spectrometer.

3.2.3. Catalytic experiments

The alkylation of isobutane with cis-2-butene was performed in a stirred tank reactor operated in continuous mode. The liquefied gases were received from Messer with a purity of 99.95% (isobutane) and 99.5% (cis-2-butene). The catalyst (typically 1-3 g) was activated *in situ* at 443K for 16 h in 100 mL/min flowing hydrogen. The ammonium exchanged sample was activated *in situ* at 603K for 1h in 100 mL/min flowing air. After cooling down to reaction temperature, typically 348K, the reactor was filled with liquid isobutane at a pressure of $2x10^3$ KPa and stirred at 1600 rpm. The reaction was started by admitting an isobutane/cis-2-butene mixture with a paraffin-to-olefin (P/O) ratio of 10 and an olefin space velocity (OSV) of 0.2 (g butene)$*$(g catalyst)$^{-1}*$ h^{-1}. Both reactants were fed through syringe pumps (ISCO 100D and 500D) and mixed in a non-return valve before reaching the reactor. After expansion, the product from the reactor passed through a six-port-valve with a sample loop, the content of which was injected automatically into a HP 6890 gas chromatograph equipped with a FID-detector and a 35 m DB-1 column. During the whole time on stream the product was condensed after the six-port-valve and weighted. Its integral composition was determined by GC analysis. The results obtained were compared with the mathematical integration of the differential data points gathered during the test, the differences being less than 10%.

3.3. Results

3.3.1. ^{29}Si NMR and IR spectroscopy of La-X zeolites

The composition of the aluminosilicate framework in the La-X catalysts was determined by ^{29}Si NMR. The spectrum presented five peaks at about -89.5, -93.2, -97.4, -101.8 and -106.2 ppm, corresponding to different Si(*n*Al) building blocks with *n* from 4 to 0, respectively [15]. As shown in Fig. 3.1 the relative intensity of each signal strongly depends on the Si/Al ratio. For Si/Al ratio of 1.1 the most important signal corresponds to Si(4Al) while for Si/Al 1.4 also the peaks corresponding to Si(3Al) and Si(2Al) are important. The framework Si/Al ratio obtained from the intensity of the NMR signals was 1.15 and 1.42 for La-X 1.1 and La-X 1.4, respectively.

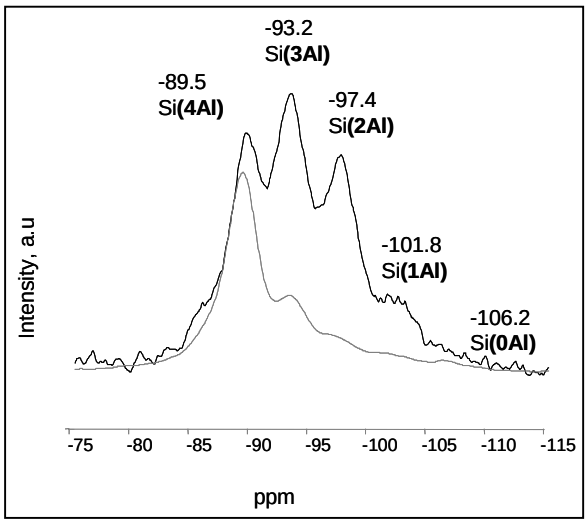

Figure 3.1: ^{29}Si NMR spectra of La-X samples with Si/Al ratio 1.4 (black line) and 1.1 (gray line).

In the region of hydroxyl stretching bands, the IR spectra of the La-X samples showed four bands corresponding to silanol groups (3740 cm^{-1}), bridging hydroxyl groups (3635-3640 and 3592-3597 cm^{-1}) and to lanthanum hydroxyl groups (3523-3512 cm^{-1}). As shown in Fig. 3.2, the IR spectra of the two La-X zeolites with different Si/Al ratio were similar, the most important difference being the intensity of the bridging hydroxyl groups at 3600 cm^{-1}. This band had a significantly higher intensity in the catalyst with lower framework Si/Al ratio (La-X 1.1), i.e., with the higher concentration of framework aluminum.

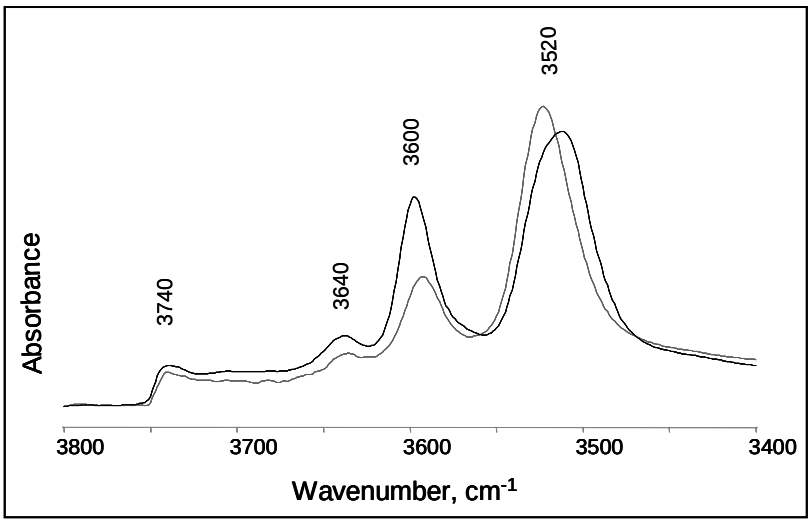

Figure 3.2: IR spectra of La-X zeolites with different Si/Al ratio 1.4 (gray line) and 1.1 (black line).

3.3.2. IR spectroscopy of La-Y zeolite

La-Y zeolite presented a different distribution of hydroxyl groups compared to the La-X material. As shown in Fig. 3.3, for La-Y zeolite a non-symmetric and broader band for lanthanum hydroxyl groups (3529 cm^{-1}) was observed. Moreover the band for bridging hydroxyl groups at ca. 3600 cm^{-1}, which is important in La-X zeolites, was not observed in the IR spectrum of La-Y. When pyridine was adsorbed on this sample, this probe molecule reacted to a significant extent with the lanthanum hydroxyl groups as evidenced by the large decrease in intensity in the corresponding bands. Simultaneously, it was possible to observe another band at ca. 3550 cm^{-1}, which has been denominated "low frequency" band. Furthermore, a small shoulder appeared at about 3570 cm^{-1}. In order to better distinguish the extent of the interaction between pyridine and the lanthanum hydroxyl groups at 3529 cm^{-1}, the profile obtained by subtraction of the spectra after pyridine adsorption is represented in Fig. 3.3 (right side). As evidenced by the negative band at 3522 cm^{-1}, the most reactive hydroxyl groups toward pyridine are the lanthanum hydroxyls at this wavenumber. Their Brønsted acid nature was shown by plotting the integrated area of the corresponding negative band versus the intensity of the pyridinium band at ca. 1542 cm^{-1}. As shown in Fig. 3.4, a linear correlation was observed.

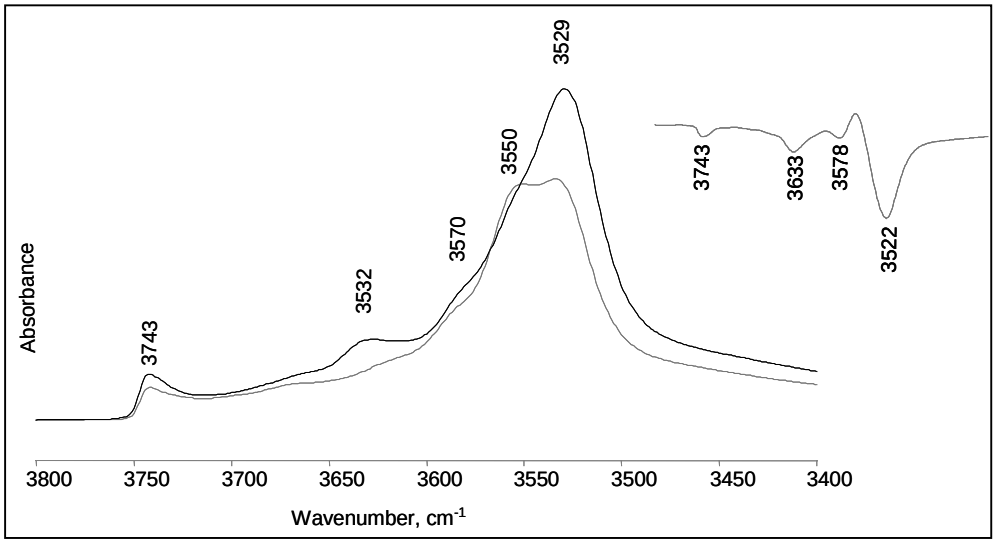

Figure 3.3: IR spectra of the La-Y zeolite after (gray line) and before (black line) pyridine adsorption. On the right the profile obtained by subtraction of the IR spectra after and before pyridine adsorption.

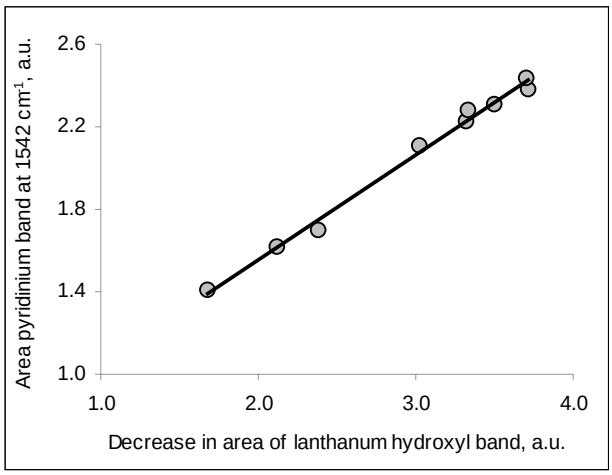

Figure 3.4: Area of the pyridinium IR band (1542 cm^{-1}) versus the decrease in area of the IR band corresponding to lanthanum hydroxyl groups (3522 cm^{-1}) after adsorption of pyridine on La-Y zeolite.

3.3.3. IR spectroscopy of H-Y zeolite

In Fig. 3.5 the IR spectra of the NH_4-Y zeolite activated *in situ*, i.e. in the vacuum IR cell, with and without a previous *ex situ* calcination step at 723K in flowing air are compared. When the sample was not calcined *ex situ* before activation and, thus, not exposed to atmospheric moisture in the activated state, very intense hydroxyl bands

were observed at 3640 and 3550 cm^{-1}, while the silanol band at ca. 3740 cm^{-1} was hardly observed. The band at 3640 cm^{-1} was narrower than the band at 3550 cm^{-1}.

However, when the sample was also calcined *ex situ* before *in situ* activation, the IR spectrum changed dramatically. The intensity of the bands at 3550 and 3640 cm^{-1} decreased strongly, while the silanol band was more intense, broader and located at ca. 3725 cm^{-1}. Additionally, a very broad band appeared in the 3500-3100 cm^{-1} region.

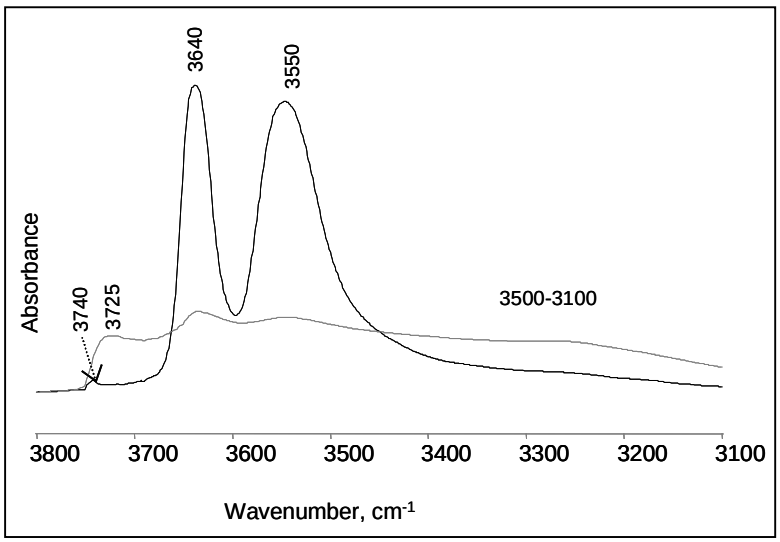

Figure 3.5: IR spectra of the H-Y zeolite recorded after *in situ* activation at 723K in vacuum IR cell of the NH_4-Y zeolite, with (gray line) and without (black line) a previous *ex situ* calcination step at 723K in flowing air.

The concentration of Brønsted acid sites, as determined by pyridine adsorption, was four times higher for the sample without *ex situ* calcination (0.94 mmol py/g compared with 0.22 mmol py/g). Moreover, as shown in Fig. 3.6, the extent of interaction between the different hydroxyl groups and pyridine was markedly different, i.e., pyridine mainly interacted with the hydroxyl groups corresponding to the IR band at 3640 cm^{-1} on the sample without *ex situ* calcination, while for the sample calcined also *ex situ* the interaction with silanol groups (band at 3732 cm^{-1}) was more important.

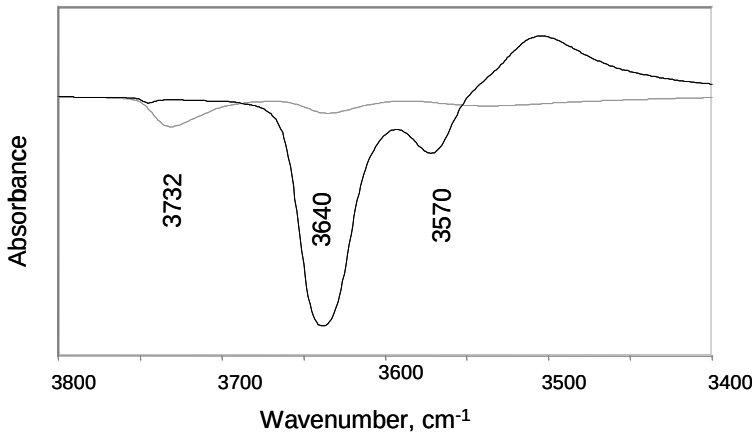

Figure 3.6: Profiles obtained by subtraction of the IR spectra recorded after and before pyridine adsorption on H-Y zeolite obtained by activated *in situ* of NH_4-Y, with (gray line) and without (black line) a previous *ex situ* calcination step.

The broad hydroxyl band observed at ca. 3550 cm^{-1} for the sample without *ex situ* calcination step did not react significantly with pyridine, when its pressure was about 5 Pa (normal adsorption pressures used in most of the experiments). Adsorption pressures higher than 100 Pa (from 100 to 500 Pa) were necessary to observe a decrease in the intensity of this band. However, the interaction with pyridine was very weak, because the initial intensity of this band was restored after evacuation (Fig. 3.7).

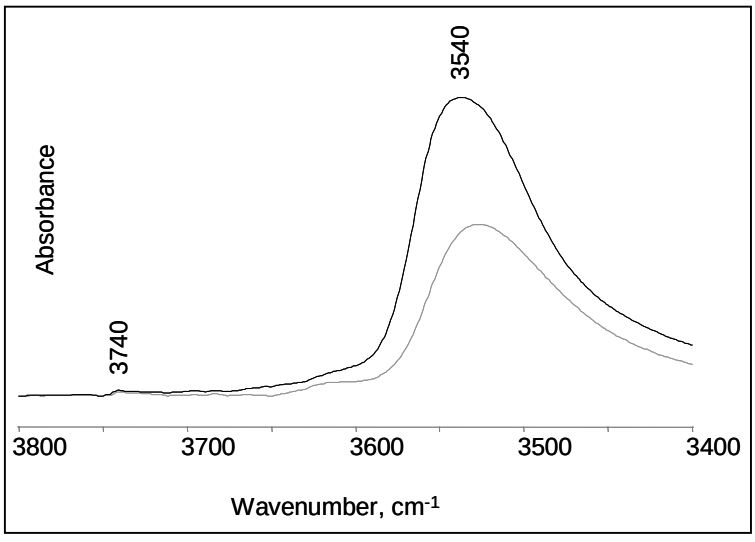

Figure 3.7: IR spectra of the *in situ* activated H-Y zeolite, recorded after adsorption of pyridine (100 Pa; gray line) and after evacuation (black line).

In order to understand why the *ex situ* calcination step before the *in situ* activation causes such marked differences in the IR spectra and acidity of H-Y zeolite, the effect of adsorption of water was investigated. After activation of the sample in the flow IR cell under 100 mL/min flowing air at 603K for 16 h, the IR spectrum (recorded at 303K) was very similar to of the sample activated in vacuum without previous *ex situ* calcination step (compare black lines of Fig. 3.5 and 3.8). Then, water was adsorbed at 303K and the sample was heated again to 603K. After this treatment, the IR spectrum showed the characteristics observed also for the sample that was undergone to *ex situ* calcination before *in situ* activation. The intense hydroxyl groups at ca. 3640 and 3550 cm^{-1} decreased appreciably, while the silanol band at 3725 cm^{-1} increased (compare gray lines of Fig. 3.5 and 3.8). These results show clearly that it is not the calcination step that determines the observed differences in IR spectra and acidity, but the effect of the atmospheric moisture to which the zeolite was exposed after *ex situ* calcination. It should be noted that at no time during these procedures the zeolite sample was exposed to significant water partial pressures at elevated temperatures.

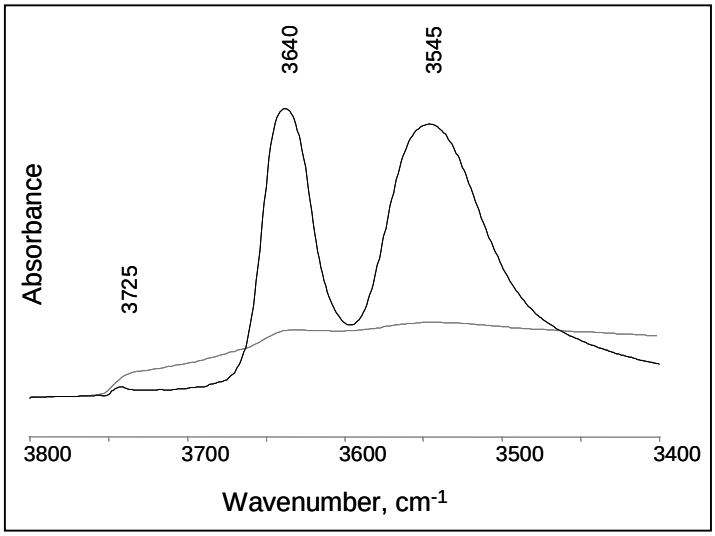

Figure 3.8: IR spectra recorded after (gray line) and before (black line) water adsorption on NH_4-Y zeolite activated *in situ* in a flow IR cell.

3.3.4. IR spectroscopy of H-La-Y zeolite

The IR band at 3633 cm^{-1} was more intense for H-La-Y than for H-Y and La-Y. Furthermore this band was more stable towards water compared to H-Y zeolite. The

enhanced stability of the H-La-Y sample led also to a less intense silanol band as compared to H-Y.

The IR spectra of the activated La-H-Y zeolite before and after pyridine adsorption are shown in Fig. 3.9. The IR spectra of adsorbed pyridine indicate that the hydroxyl groups corresponding to the band at 3633 cm^{-1} interact completely with pyridine contributing to the total Brønsted acidity. As for the pure La-Y zeolite, a fraction of the lanthanum hydroxyl groups at ca. 3520 cm^{-1} interacted with pyridine.

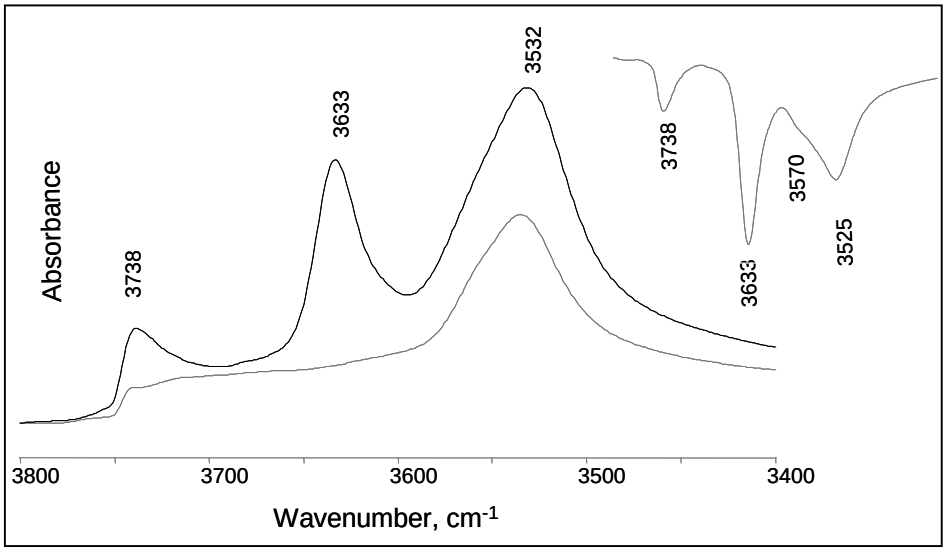

Figure 3.9: IR spectra of H-La-Y zeolite recorded after activation (black line) and after adsorption of pyridine (gray line). On the right the profile obtained by subtraction of the IR spectra recorded after and before pyridine adsorption.

3.3.5. IR spectroscopy of H-La-USY zeolite

The IR spectrum of the activated H-La-USY zeolite presented several OH bands in the region between 3750 and 3500 cm^{-1}. As shown in Fig. 3.10, six discrete bands could be distinguished, i.e., 3734 cm^{-1} (silanol groups), which is asymmetric toward low wavenumbers, 3670 cm^{-1} related to OH groups of EFAL species, 3620, 3600 and 3560 cm^{-1} (bridging hydroxyl groups), and ca. 3530 cm^{-1} related to OH groups of charge compensating polyvalent cations. All these groups reacted with pyridine to different extents. The profiles obtained by subtraction of the IR spectra recorded after and before pyridine adsorption showed bands at 3732 3667, 3627, 3598, 3550 and 3530 cm^{-1}. In the IR spectrum recorded after pyridine adsorption OH bands were

observed at ca. 3742, 3695, 3605 and 3532 cm^{-1}. We speculate that these groups are either located on positions not accessible to pyridine or that their acid strength is to low to allow stable interactions. Note in this context that the hydroxyl groups at 3670, 3630 and 3550 cm^{-1} reacted more extensively with pyridine than silanol and bridging hydroxyl groups at 3600 cm^{-1}. These results are in good qualitative agreement with an earlier report of the group of Lavalley on pyridine adsorption on USY materials [16].

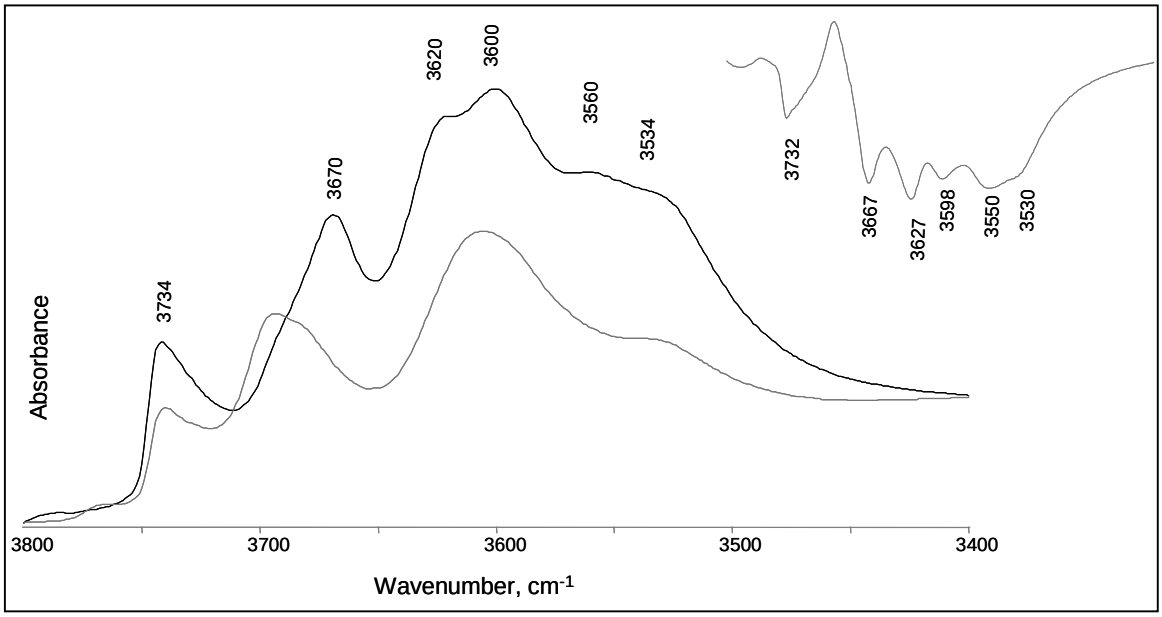

Figure 3.10: IR spectra of H-La-USY zeolite recorded after activation (black line) and after pyridine adsorption (gray line). On the right the profile obtained by subtraction of the IR spectra recorded after and before pyridine adsorption.

3.3.6. SEM images and IR spectroscopy of H-EMT zeolite

Although the framework structure of the zeolite Na-EMT is closely related to that of FAU type zeolites, its morphology is different. While X and Y zeolites are cubic, EMT zeolite has a hexagonal symmetry leading to different window and supercage structures. SEM micrographs of cubic and hexagonal synthesized zeolites are shown in Fig. 3.11.

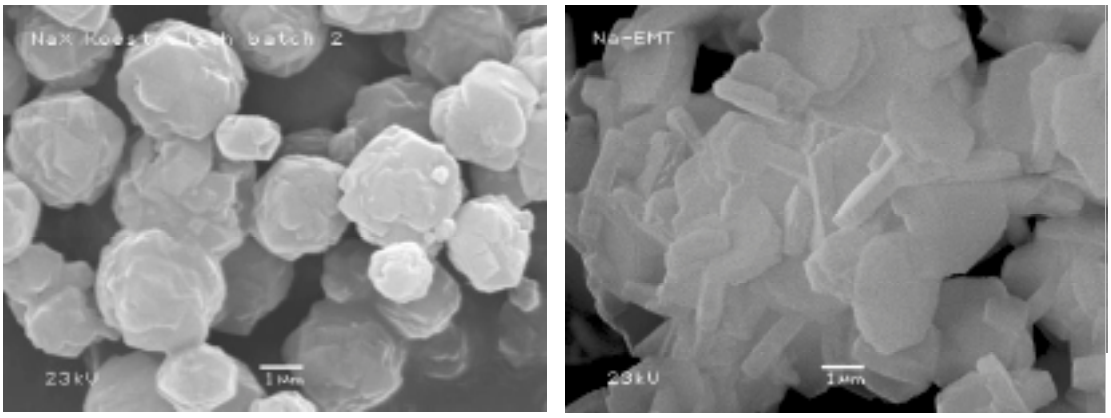

Figure 3.11: SEM micrographs of Na-X zeolite (left) and Na-EMT (right).

As shown in Fig. 3.12, the IR spectrum of the activated H-EMT material is similar to that obtained for the NH_4-Y zeolite activated without exposure to atmospheric moisture (very intense bridging hydroxyl bands at 3630 and 3550 cm^{-1}). However, while in the H-Y sample silanol groups at 3740 cm^{-1} were practically not observed, this band was intense in the spectrum of H-EMT. Additionally, this sample showed OH groups attached to extra-framework alumina species (band at ca. 3670 cm^{-1}). Pyridine mainly interacted with bridging hydroxyl groups. It is also important to remark that the bridging hydroxyl groups at 3550 cm^{-1} reacted extensively with pyridine at normal adsorption pressure of about 5 Pa in the H-EMT sample as compared to the *in situ* activated NH_4-Y zeolite, indicating either a more accessible location of these acidic sites or a higher strength.

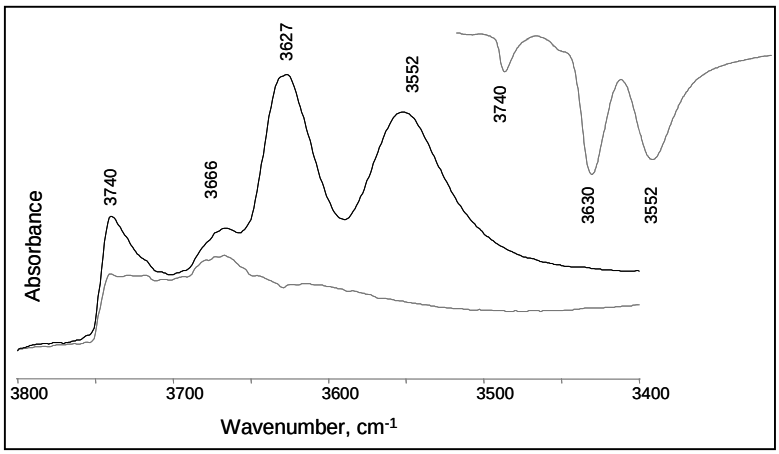

Figure 3.12: IR spectra of H-EMT zeolite recorded before (black line) and after (gray line) pyridine adsorption. On the right the profile obtained by subtraction of the spectra recorded after and before pyridine adsorption.

3.3.7. IR spectroscopy of H-BEA zeolite

As shown in Fig. 3.13, the IR spectrum of the H-BEA zeolite showed bands corresponding to silanol groups (3744 cm^{-1}) and to bridging hydroxyl groups (3608 cm^{-1}). The most important contribution to the total Brønsted acidity was due to the bridging hydroxyl groups that were quantitatively neutralized with pyridine.

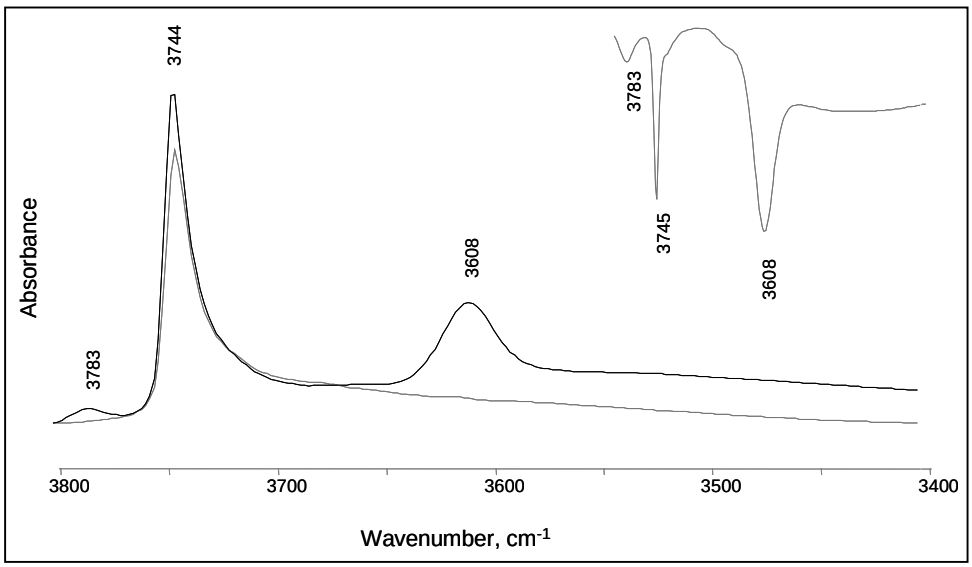

Figure 3.13: IR spectra of H-BEA zeolite recorded before (black line) and after (gray line) pyridine adsorption. On the right the profile obtained by subtraction of the spectra recorded after and before pyridine adsorption

3.3.8 Isobutane/cis-2-butene adsorption monitored by IR spectroscopy

Adsorption of the isobutane/cis-2-butene mixture on the zeolites always resulted in bands in the ranges 3040-2770 cm^{-1}, 1700-1600 and 1500-1350 cm^{-1}, and in the concomitant decrease of the bands corresponding to the acidic hydroxyl groups. The bands between 3040 and 2770 cm^{-1} were assigned to the asymmetric and symmetric stretching vibrations of the CH_3 and CH_2 groups (νCH_3, νCH_2). The bands between 1700 and 1600 cm^{-1} correspond to the C=C stretching vibration ($\nu C=C$). This

vibration, originally IR inactive, becomes active due to the interaction with the acidic hydroxyl groups [17]. Finally, in the range 1500-1350 cm^{-1} the CH bending modes (δ_{CH}) were observed. In Fig. 3.14 the IR spectra of adsorbed isobutane/cis-2-butene on La-X and La-Y zeolites are compared.

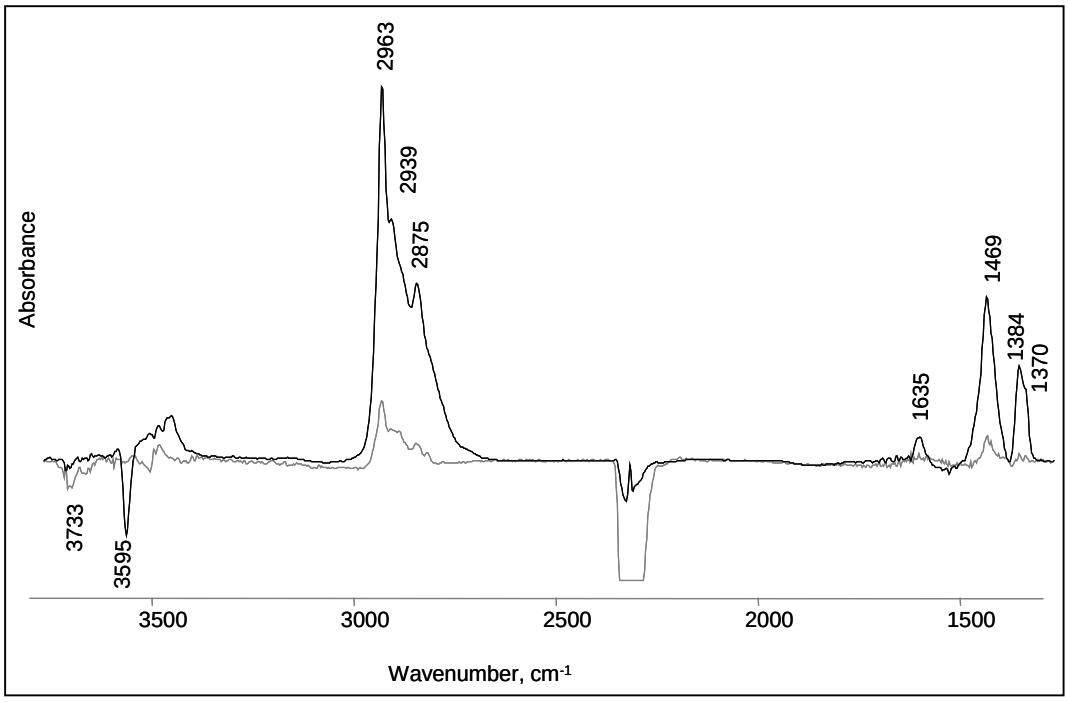

Figure 3.14: Profile obtained by subtraction of the IR spectra recorded after and before isobutane/cis-2-butene adsorption on La-X 1.1 (black line) and La-Y (gray line) zeolites.

The hydroxyl groups in the La-X 1.1 zeolite involved in the reaction with the mixture were mainly the bridging hydroxyl groups at ca. 3600 cm^{-1} and, in a minor extent, the bridging hydroxyl groups and the silanol groups at ca. 3640 and 3740 cm^{-1}, respectively. This indicates that the predominantly interacting acid sites at this coverage (ca. 0.3) are the bridging hydroxyl groups at 3600 cm^{-1}. On the other hand, the adsorption on La-Y was significantly weaker than on La-X. As discussed for the adsorption of pyridine on La-Y the predominant groups involved in the interaction are the $[La\text{-}OH]^{2+}$ groups. With weak bases such as isobutane and cis-2 butene these acid sites are not sufficiently strong to react extensively with these molecules.

In Fig. 3.15 the IR spectra after adsorption of the mixture isobutane/cis-2-butene on the *in situ* activated NH_4-Y zeolite, with and without a previous *ex situ* calcination step are shown. On both samples the ν C=C vibration at ca. 1640 cm^{-1} was very weak

suggesting a high degree of butene oligomerization or protonation. The hydroxyl groups involved in the isobutane/cis-2-butene adsorption were mainly those at ca. 3635 cm^{-1} for the directly *in situ* activated sample and those at 3736 and 3635 cm^{-1} for the *ex situ* calcined zeolite. For the latter sample the interaction with the silanol groups at 3736 cm^{-1} predominated.

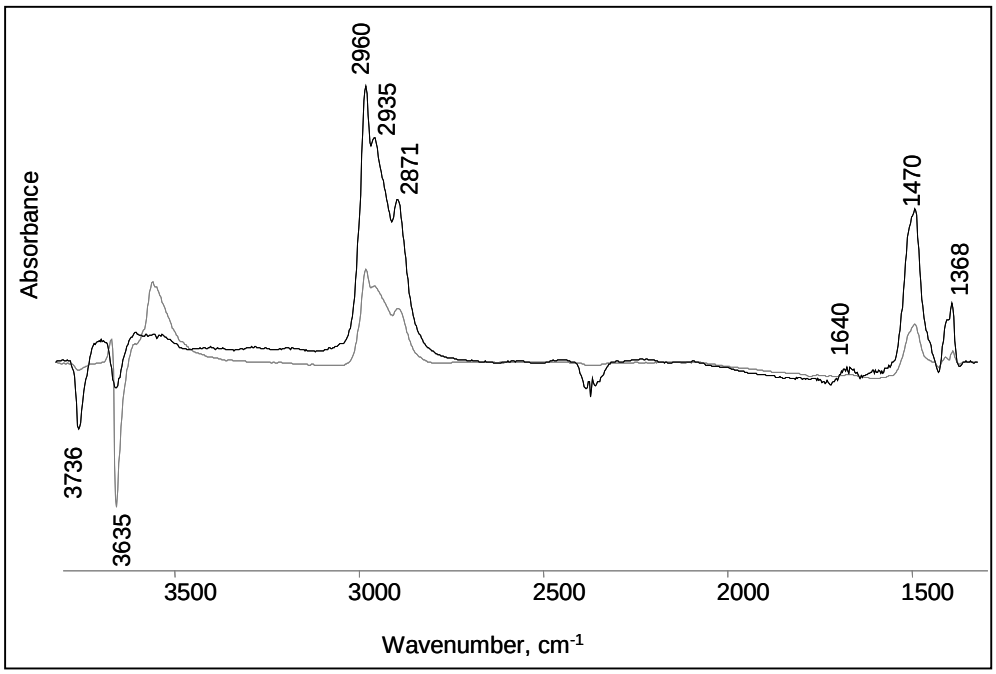

Figure 3.15: Profile obtained by subtraction of the IR spectra recorded after and before isobutane/cis-2-butene adsorption on *in situ* activated NH_4-Y zeolite, with (black line) and without (gray line) previous ex situ calcination step.

La-H-Y and H-EMT zeolites showed similar spectra than NH_4-Y when isobutane/cis-2-butene was adsorbed (Fig. 3.16). In both cases the predominant hydroxyl groups involved in the reaction with the mixture were those at ca. 3634 cm^{-1} and the silanol groups at 3736 cm^{-1}. Although with H-EMT OH-groups attached to extra-framework species (OH-EFAL) were present, they did not react with the molecules at the applied adsorption pressure. At this point it is important to note that both samples showed very similar concentration of total Lewis acid sites as measured by IR spectra of adsorbed pyridine IR. In the spectrum of the La-H-Y the OH-EFAL groups were not observed suggesting that the Lewis acid sites on these samples are of different nature. Finally, in both samples the olefinic ν C=C vibration at ca. 1640 cm^{-1} was practically absent.

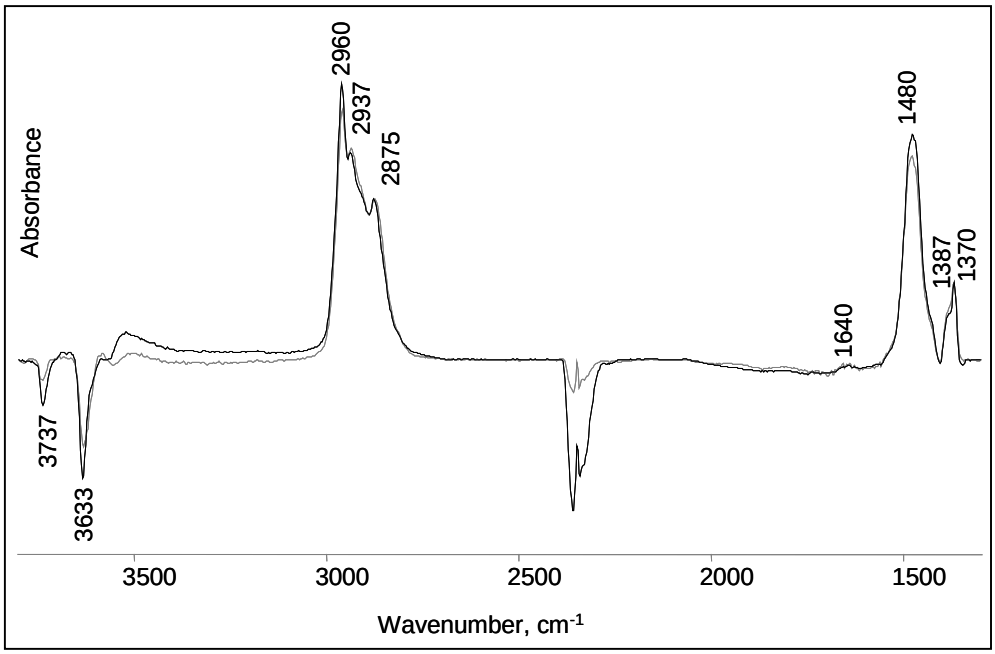

Figure 3.16: Profile obtained by subtraction of the IR spectra recorded after and before isobutane/cis-2-butene adsorption on La-H-Y (black line) and H-EMT (gray line) zeolites.

The spectrum obtained after isobutane/cis-2-butene adsorption on H-BEA zeolites showed important differences compared to those for the other samples studied (Fig. 3.17). On the one hand, it had more intense bands at 2929 cm^{-1} (asymmetric stretching vibration of the CH_2 group), at 2855 cm^{-1} (symmetric stretching vibration of CH_2), and at 1531 and 1505 cm^{-1} (to alkenyl cations $(C\text{-}C{=}C)^+$). On the other hand, it showed less intense bands at 1636 and 1370 cm^{-1} corresponding to the olefinic vibration ν C=C and to umbrella bending in $C(CH_3)_2$ groups, respectively. In comparison to La-X, the contribution to the adsorption of the silanol groups at 3746 cm^{-1} in the H-BEA was markedly higher.

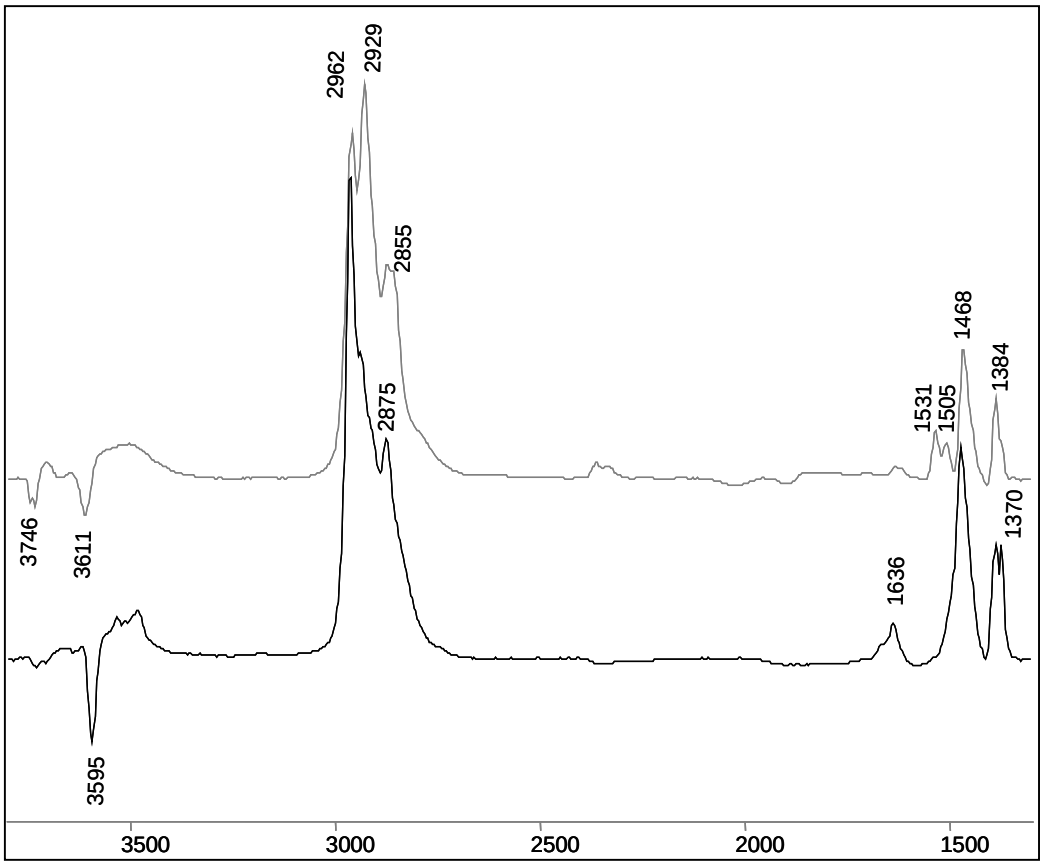

Figure 3.17: Profile obtained by subtraction of the IR spectra recorded after and before isobutane/cis-2-butene adsorption on La-X (black line) and H-BEA (gray line) zeolites.

3.3.9. Physicochemical characterization and alkylation activity of the different materials

A summary of the unit cell size, acid site concentration and catalyst lifetime in the isobutane/cis-2-butene alkylation of the investigated materials is compiled in Table 3.1.

Lifetimes from 1 to 13 h were measured. The sample with the shortest lifetime (only 1 h) was the H-Y zeolite obtained by activation of NH_4-Y in the reactor (H-Y *in situ*). At the same time it was the sample with the highest concentration of total Brønsted acid site (BAS_{423}) and the lowest total concentration of Lewis acid sites (LAS_{423}). Note that most of the Brønsted acid sites on this sample are, however, weak as seen by the concentration of strong Brønsted acid sites (BAS_{723}).

From the Table 3.1 is also remarkable that the sample with the highest concentration of Lewis acid sites was H-Y obtained by calcination *ex situ* of NH_4-Y (H-Y *ex situ*; LAS_{423} = 0.31 mmol/g). The cause of this dealumination was shown to be related to the adsorption of water as monitored by IR spectroscopy. This led to the decrease in total Brønsted acidity from 0.94 to 0.22 mmol/g.

The sample H-BEA with the highest Si/Al ratio showed the lowest total Brønsted acid site concentration. However, its lifetime was superior to samples like La-Y and H-Y with higher concentration of Brønsted acid sites.

Among the samples with an intermediate lifetime, H-EMT zeolite was the catalyst with a fraction of strong Brønsted acid sites comparable to La-X 1.4. However, for H-EMT, the Lewis acid site concentration was twice as high in comparison to La-X samples.

Sample	Si/Al	UCS	Lifetime	BAS_{423}	BAS_{723}	LAS_{423}	LAS_{723}
	mol/mol	Å	h	mmolpy/g			
La-X 1.1	1.1	25.01	12.5	0.46	0.34	0.11	0.07
La-X 1.4	1.4	24.90	13.3	0.41	0.15	0.09	0.05
La-Y	2.6	24.73	2.0	0.40	0.12	0.03	0.03
H-Y *in situ* (a)	2.4	24.74	0.8	0.94	0.13	0.02	0.02
H-Y *ex situ* (b)	2.4	24.56	1.6	0.22	0.04	0.31	0.24
H-La-Y	2.6	24.69	6.6	0.47	0.06	0.19	0.12
H-La-USY	2.6	24.52	8.3	0.51	0.17	0.18	0.11
H-EMT	3.5		5.8	0.38	0.15	0.22	0.11
H-BEA	11.6		7.2	0.18	0.04	0.14	0.12

Table 3.1: Selected physicochemical properties and lifetimes in isobutane/cis-2-butene alkylation of the studied samples.

(a) H-Y obtained by activation of NH_4-Y in the reactor for the catalyst lifetime determination and in the IR cell (without previous *ex situ* calcination) for acidity measurements.

(b) H-Y obtained by calcination *ex situ* of NH_4-Y before catalytic test or before IR acidity measurements.

Fig. 3.18 shows the changes in integral selectivities to the different groups of products with the catalyst lifetime. In all samples, the C_8 fraction dominated. The samples with the shortest catalyst lifetime had the lowest selectivity to C_8 alkanes and highest to C_9^+, compounds. The C_5-C_7 fraction remained approximately constant with catalyst lifetime.

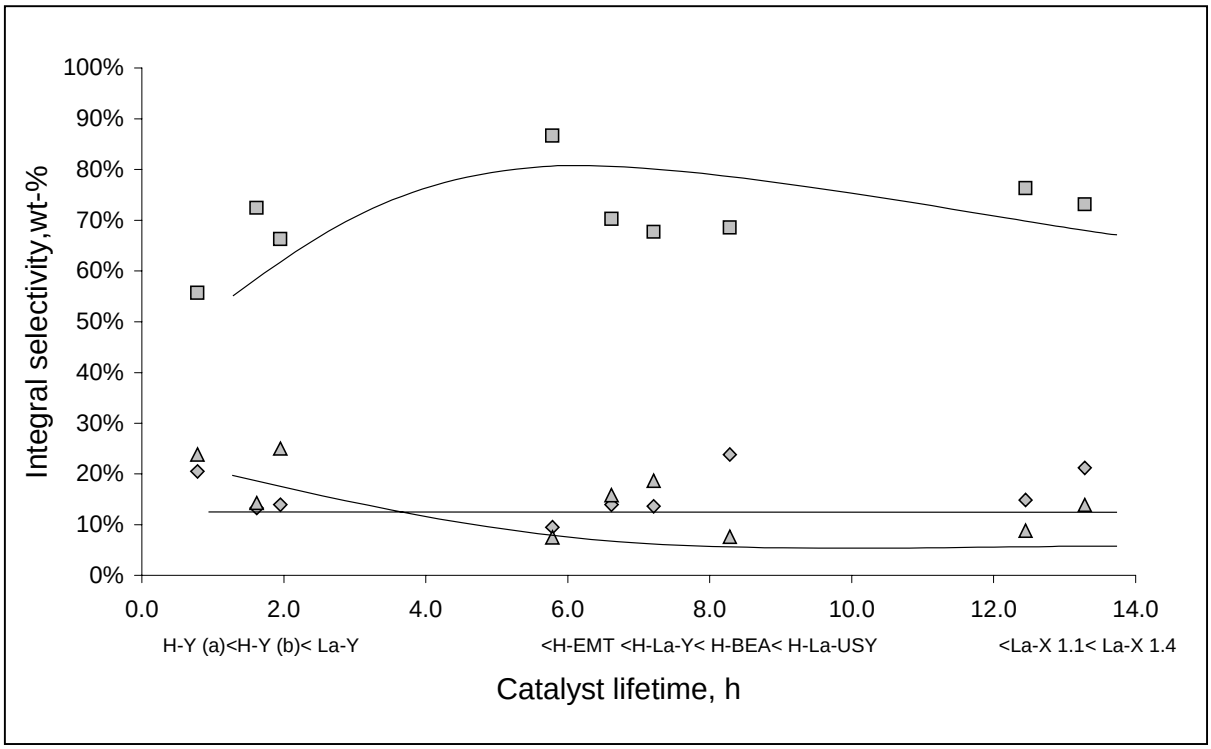

Figure 3.18: Integral selectivities to the different product groups as a function of catalyst lifetime (◻ C_8 products, ◇ C_5-C_7 products, △ C_9^+ products).

In the fraction C_8 (Fig. 3.19) the production of 2,2,4-TMP and 2,2,3-TMP + 2,5-DMH increased with longer catalyst lifetime. The selectivities to the other products in this fraction did not change significantly. The selectivity to 2,2,4-TMP for the samples H-BEA and H-La-USY were 49,3 and 39,2 wt-%, respectively, values markedly higher than in the other samples.

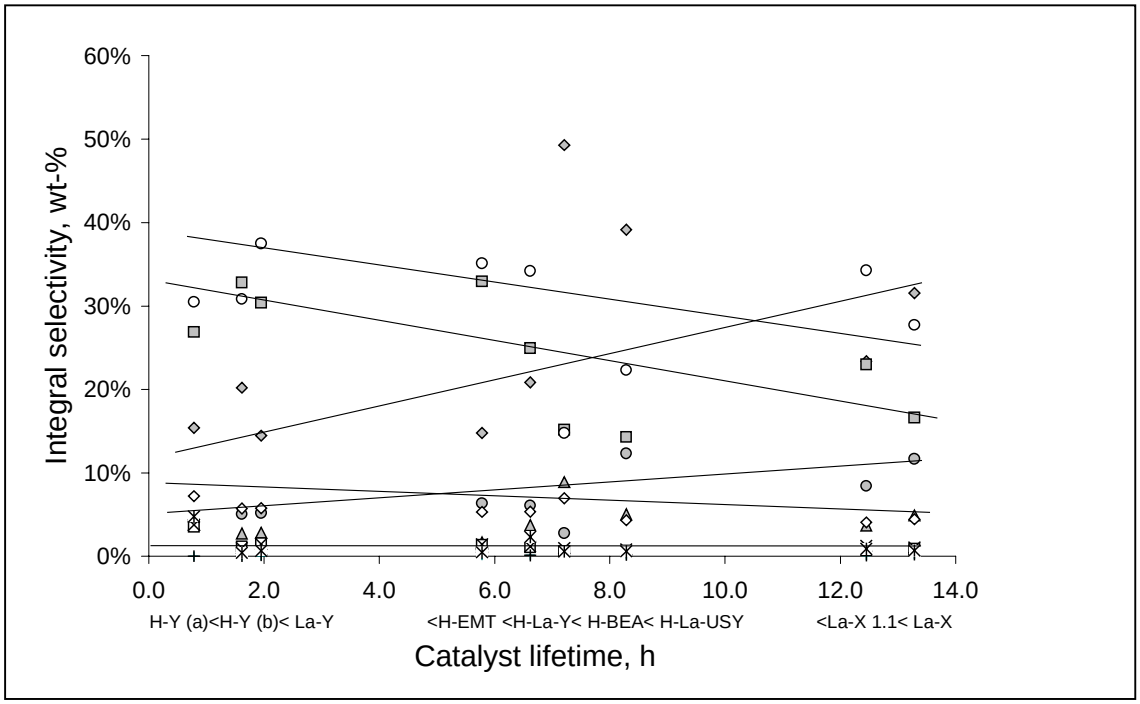

Figure 3.19: Variation in integral selectivities to the individual C_8 products with catalyst lifetime. ◇ 2,2,4-TMP, ○ 2,3,3-TMP, □ 2,3,4-TMP, ◇ 2,3-DMH, ○ 2,2,3-TMP + 2,5-DMH, * C8=, △ 2,4-DMH.

3.4. Discussion

3.4.1. Acidity of La-X zeolites with different Si/Al ratios

The concentration of Brønsted acid sites in zeolites is related to the concentration of aluminum atoms in the framework, which can be determined by NMR measurements [15]. Knowing the framework Si/Al ratio, it is possible to determine, how many aluminum atoms are present per unit cell (UC) assuming that the sum of Si and Al atoms is always 192 (in FAU-type zeolites). 89 and 79 Al atoms per UC were calculated for La-X 1.1 and 1.4, respectively. These results are in qualitative agreement with the relative intensity of the bridging hydroxyl groups in the IR spectra, i.e., the sample with 89 Al per UC had a more intense acidic band at approximately 3600 cm^{-1}.

3.4.2. Acidity of La-Y and comparison with La-X

As shown in Fig. 3.2 and 3.3, the acidic OH groups of La-Y differ significantly from those of La-X, i.e., in La-X the hydroxyl groups corresponding to the IR band at 3600 cm^{-1} are the most abundant and the most acidic (a large amount of adsorbed pyridine remains on these hydroxyl groups even after outgassing at 723K (Table 3.1)), while for La-Y the lanthanum hydroxyl groups ($[La\text{-}OH]^{2+}$) at ca. 3529 cm^{-1} predominate. When pyridine was adsorbed on La-Y, this latter band and the band at 3632 cm^{-1} were those the most affected by adsorbed pyridine. It is important to note that the band due to $[La\text{-}OH]^{2+}$ groups, generally considered as non-acidic [18], reacted to a great extent with pyridine. Furthermore the linear correlation between the decrease in intensity of this band and the increase of the pyridinium band at ca. 1542 cm^{-1} clearly indicates that these groups are Brønsted acid sites in La-Y. In fully exchanged lanthanum X-zeolites, the majority of the lanthanum hydroxyl groups is located in the small cavities of the framework and is not accessible to pyridine. In the case of La-Y a larger fraction of $[La\text{-}OH]^{2+}$ groups was accessible to pyridine indicating that they occupy exchange locations in the supercages. ^{139}La NMR measurements on Y-zeolites at different ion exchange levels are in agreement with these findings [19].

It is also important to remark that the IR band at 3550 cm^{-1} could be distinguished in the spectrum of La-Y zeolite only after pyridine adsorption. In the spectrum recorded after activation only a very intense band at ca. 3529 cm^{-1} was observed. The band at 3550 cm^{-1} ("low frequency (LF) band") is generally assigned to bridging hydroxyl groups in the sodalite cages [19] on the basis of its behavior towards adsorbed molecules and more specific to a location in a six-ring unit. This band did not react with pyridine at normal adsorption pressures (ca. 5 Pa). Ward observed that these groups can react with pyridine when it is present in excess [20]. In the present case, pyridine adsorption pressures higher than 100 Pa were necessary to achieve a decrease in the intensity of this band with the concomitant increase of the pyridinium band. The results indicate, thus, that these acid sites are able to react with pyridine. Jacobs *et al.* [21] showed that the low frequency hydroxyl band at 3550 cm^{-1} is in fact the superposition of different components. The multiplicity of these components can be explained if all the cage oxygens O_2, O_3, and O_4 are considered as possible sites for proton location.

3.4.3 Acidity of H-Y

In situ calcination of NH_4-Y close to 623K led to the decomposition of the ammonium ions to ammonia and Brønsted acid sites. The IR spectrum of the *in situ* activated NH_4-Y showed two very intense bands at 3550 and 3638 cm^{-1} corresponding to the bridging hydroxyl groups. The band at 3638 cm^{-1}, the "high frequency (HF) band", has been assigned to the oscillation of O_1-H hydroxyl groups inside the large cages [22]. On the other hand, the "low frequency band (LF)" at 3546 cm^{-1}, corresponds to protons attached to oxygen in different crystallographic locations, i.e., O_2 and O_3 in the small cavities and O_4 in the supercages. The LF and HF bands reacted in a different manner with pyridine. The low frequency band remained essentially unmodified after pyridine adsorption at the standard pressure of 5 Pa, while the band at high frequency markedly decreased. The easy accessibility of the OH groups corresponding to the HF band for different types of molecules, such as pyridine, supports this assignment. Additionally, the high frequency band was narrower than the low frequency band. The larger width of the LF band is attributed to the perturbation by neighbor oxygen in the lattice [21].

The hydroxyl groups corresponding to the band at low frequency interacted with pyridine only when it was introduced at pressure of 100-500 Pa. Nevertheless pyridine was easily desorbed through evacuation and the band at 3550 cm^{-1} was completely restored. This indicates that these hydroxyl groups hardly react with a strong base such as pyridine. They probably do not play an important role in alkylation, because this reaction is favored by strong Brønsted acid sites [23, 24]. This aspect will be further discussed in paragraph 3.4.8 in the light of the adsorption/desorption experiments with isobutane/cis-2-butene monitored by IR spectroscopy.

The NH_4-Y zeolite calcined *ex situ*, i.e., outside the IR cell, showed a completely different IR spectrum compared to that of the *in situ* activated samples. The low and high frequency bands at 3550 and 3640 cm^{-1}, respectively, became much less intense and the silanol band at 3740 cm^{-1}, very weak in the *in situ* activated NH_4-Y, became more intense and even comparable to the bridging hydroxyl bands. Most of the silanol groups observed correspond to framework terminal Si-OH as evidenced by the presence of the IR bands at 3732 cm^{-1} and in the region 3500-3100 cm^{-1} [25]. The concentration of all Brønsted acid sites (total Brønsted acidity) determined by pyridine adsorption was much lower on the *ex situ* calcined sample (0.22 mmol/g

compared to 0.94 mmol/g for the *in situ* activated sample), with the highest contribution to the Brønsted acidity resulting from Si-OH groups. The concentration of Lewis acid sites in the *in situ* activated NH_4-Y was very small (0.02 mmol/g) compared to the *ex situ* calcined sample (0.31 mmol/g).

The IR spectrum recorded after adsorption of water on the *in situ* calcined sample strongly resembles the spectrum of the *ex situ* calcined zeolite. This suggests that the freshly prepared H-Y zeolite reacts with atmospheric moisture and that this reaction is responsible for the decrease of the bridging hydroxyl bands and for the corresponding increase of silanol groups. In other words the sample is partially dealuminated by reaction with water, this process leading to a decrease of the total Brønsted acidity and to an increase of the Lewis acidity [26]. These results are in agreement with the changes of UCS measured for these samples: 24.673 Å for the parent material Na-Y and 24.560 Å for H-Y obtained by calcination of NH_4-Y and following equilibration with water.

3.4.4. Acidity of H-La-Y

The preparation plays an important role in the final properties of the catalyst. As discussed in the previous sections, when only lanthanum is exchanged in Na-Y zeolites most of the Brønsted acidity arises from the lanthanum hydroxyl groups. On the other hand, when only ammonium is exchanged, the catalyst presents a higher concentration of Brønsted acid sites and they are almost exclusively bridging hydroxyl groups. However this catalyst (H-Y) is very unstable to atmospheric moisture and readily dealuminated even at room temperature. When the ion exchange procedure comprised ammonium and lanthanum exchanges, the catalyst was simultaneously more stable against dealumination and with a higher concentration of acidic bridging hydroxyl groups (IR band at 3633 cm^{-1}) and a relative lower concentration of Lewis acid sites. However, $[La\text{-}OH]^{2+}$ groups and framework silanol groups at 3525 and 3738 cm^{-1} contributed appreciably to the total Brønsted acidity measured to this sample.

3.4.5. Acidity of H-La-USY zeolite

The hydroxyl region of the IR spectrum of the H-La-USY zeolite contains six distinguishable bands at 3734, 3670, 3620, 3600, 3560 and 3534 cm^{-1}. The bands at 3734, 3670 and 3534 cm^{-1} correspond to terminal Si-OH groups attached to the framework [24], OH-groups attached to species containing extra-framework Al-atom [27] and lanthanum hydroxyl groups, respectively. The bands at 3620 and 3560 cm^{-1} were also observed in the spectra of La-Y and H-Y zeolites, but at slightly different wavenumbers. They represent the high and the low frequency bands that have been assigned to bridging hydroxyls formed between the oxygen in the zeolite lattice and a proton produced by decomposition of NH_4^+ or by hydrolysis of the rare earth hydrated cation [4]. The band at 3600 cm^{-1} has been attributed to interactions of the cationic EFAL species with the high frequency band that normally occurs at ca. 3640 cm^{-1} in the other forms of the X and Y zeolites [28]. All the bridging hydroxyl groups present on H-La-USY interacted with pyridine. However, the hydroxyl groups associated to the presence of cationic EFAL retained pyridine even after heating at 723K indicating high acid strength. EFAL species are also present on La-X zeolites as indicated by the presence of Lewis acid sites determined by pyridine adsorption, but with lower concentration (approximately 0.10 mmol/g instead of 0.18 mmol py/g for H-La-USY). Based on this difference, one would expect that the H-La-USY shows a higher fraction of strong Brønsted acid sites than the La-X. However, the percentage of strong Brønsted acid sites obtained for H-La-USY (33%) was lower than that for La-X zeolites (72% and 36% for La-X 1.1 and La-X 1.4, respectively). This is tentatively explained by considering that the enhanced strong Brønsted acidity in rare-exchanged FAU zeolites may result from the polarizing effect of the rare earth cations the zeolite structure [29] resulting in strong lateral bonds to pyridine and aromatic rings. Thus, although both zeolites contain La^{3+}, the number of La^{3+}cations per UC in a La-X is higher than in H-La-USY. Therefore, the effect of the polyvalent cations on the strength of the acidic hydroxyl groups at 3600 cm^{-1} seems to be more important than the effect of EFAL species.

3.4.6. Acidity of H-EMT

The IR spectrum of the calcined ammonium exchanged EMT shows the terminal silanol band at 3740 cm^{-1}, the low and high frequency bands at 3552 and 3627 cm^{-1}, respectively, and the band at 3670 cm^{-1} assigned to OH groups related to extra-framework species. After pyridine adsorption at 423K only the bands at 3740, 3552 and 3627 cm^{-1} decreased. The last two bands showed the main contribution to the total Brønsted acidity (about 0.38 mmol/g). Compared to the H-Y zeolite prepared under similar conditions, H-EMT showed highly stable concentrations of the acidic groups at 3627 cm^{-1} and 3550 cm^{-1}. The difference in stability of the calcined H-EMT in the rehydration experiment is attributed to a higher Si/Al ratio (Si/Al = 3.5) that in the Y zeolite (Si/Al = 2.4). As already discussed in paragraph 3.4.3 the LF band in H-Y zeolites hardly reacted with pyridine. Higher adsorption pressures were required to observe an interaction between these groups and pyridine and after evacuation the band was completely restored. On the other hand, the LF band of H-EMT reacted extensively with pyridine at lower adsorption pressures (5 Pa) and after evacuation pyridine was still retained by these groups. This observation indicates that in the hexagonal EMT zeolite the Brønsted acidic OH groups in hexagonal rings are more accessible than in FAU type materials. Note that the most accessible protons of the three possible locations are those bonded to the O_4 framework oxygens.

3.4.7. Acidity of H-BEA

Most of the Brønsted acidity on the H-BEA zeolite is due to silanol hydroxyl groups (IR band at 3744 cm^{-1}) and bridging hydroxyl groups (IR band at 3608 cm^{-1}). Both hydroxyl groups extensively reacted with pyridine. Silanol groups present in H-BEA zeolites are similar to those found in amorphous silica-alumina (ASA) [25]. In ASA silanol groups at 3748 and 3746 cm^{-1} have been observed. The former are perturbed indirectly by pyridine coordination on Lewis acid centers and as consequence a decrease of the intensity of this band is observed. The H-BEA zeolite used in this study presented Lewis acid sites as evidenced by the presence of the corresponding band at 1454 cm^{-1}. Therefore the observed reactivity toward pyridine of the silanol groups in this sample was extensive and similar to that observed in ASA.

3.4.8 Isobutane/cis-2-butene adsorption on zeolites and correlation with acidic properties

Adsorption experiments with a 7/1 mixture of isobutane and cis-2-butene similar to that used for the alkylation reaction were carried out in the IR vacuum cell. The main objective of these experiments was to identify, which hydroxyl groups are involved in the reaction with the feed molecules and to compare these results with those obtained from adsorption of a much stronger base, such as pyridine.

In the case of the La-X samples, the most important OH groups that react either with pyridine or with isobutane/cis-2-butene correspond to the IR band at 3600 cm^{-1}. These bridging hydroxyl groups are responsible for the high activity of the La-X samples in isobutane/cis-2-butene alkylation. These OH groups, which occupy positions in the supercages and are speculated to be affiliated with O_1-type oxygens in the zeolite framework accessible to the reactants. The significant strength of these groups as evidenced by pyridine adsorption at higher temperatures has been tentatively attributed to the strong polarizing effect of the lanthanum cations on adsorbed molecules [29].

The hydroxyl groups accessible to pyridine in the La-Y zeolite are the $[La\text{-}OH]^{2+}$ groups and bridging hydroxyl groups at 3529 and 3630 cm^{-1}, respectively. When the isobutane/cis-2-butene mixture was adsorbed on this sample, only a small fraction of these hydroxyl groups reacted. Therefore, although a high fraction of the lanthanum hydroxyl groups are able to react with a strong base like pyridine, their strength is not sufficient to chemisorb butene. In line with these results, the lifetime of this catalyst in alkylation reaction was only 2h. Additionally, while in the spectrum (see Fig. 3.14) of the La-Y zeolite after isobutane/cis-2-butene adsorption a very weak ν(C=C) absorption at ca. 1635 cm^{-1} is observed, in the corresponding spectrum for the La-X zeolite this band was the highest between all the tested samples. This is interpreted as follows: on weak acid sites (La-Y) will predominate the formation of oligomers which makes that the olefin character of the formed compounds be scarcely observed while on stronger sites that have a higher selectivity to hydride transfer respect to oligomerization dimers are observed. Probably these dimeric species correspond to a stable tetra-substituted ethene based on the absence of the olefin CH stretching band above 3000 cm^{-1} [30].

On zeolite H-Y obtained by *in situ* activation of NH_4-Y, only the bridging hydroxyl groups with IR band at 3636 cm^{-1} were easily neutralized by pyridine. In order to neutralize the hydroxyl groups with IR band at 3550 cm^{-1} a higher pyridine pressure was required, thus, indicating that these are weak acid sites. In fact, among the investigated samples, this zeolite (H-Y *in situ* activated) showed the highest concentration of total Brønsted acid sites. A similar behavior was observed when the feed mixture was adsorbed on this sample. At low pressures (coverage 0.3) the mixture isobutane/cis-2-butene could be adsorbed only on the bridging hydroxyl groups corresponding to the band at 3636 cm^{-1}. Additionally, it is important to note that after isobutane/cis-2-butene the band at ca. 1640 cm^{-1}, attributed to the νC=C band olefinic properties of butene [17], was hardly detectable. This leads us to the conclusion that the majority of the weak Brønsted acid sites on this sample catalyze the oligomerization of butene leading to shorter lifetimes.

On the other hand, when the NH_4-Y was calcined *ex situ*, the silanol groups at ca. 3732 cm^{-1} generated after water adsorption also contributed to the Brønsted acidity. This component of silanol groups has been assigned to terminal Si-OH groups attached to the framework [16]. Therefore, they are not observed in amorphous materials as ASA or silica with the same Si/Al ratio. Additionally, the dealumination observed after water adsorption on calcined NH_4-Y led to the formation of a very broad band in the 3500-3100 cm^{-1} region. This band has been attributed to Si-OH pairs in dealuminated H-Y zeolites that interact mutually through hydrogen bonds [16]. Thus, dealumination creates complex structural defects in the zeolite in addition to silica-alumina or alumina debris. The silanol component at 3732 cm^{-1} also reacted with the paraffin/olefin mixture. Nevertheless, the low strength of these acid sites and their location, external and at structural defects makes this catalyst inadequate for alkylation reaction.

When lanthanum was introduced in combination with ammonium, the Y zeolite had improved stability to dealumination caused by rehydration of the calcined material. The material had a higher density of hydroxyl groups at 3633 cm^{-1} than the NH_4-Y sample calcined *ex situ*. Additionally, the number of silanol groups able to react with isobutane/cis-2-butene mixture was smaller in the sample stabilized with lanthanum. These characteristics (higher fraction of strong Brønsted acid sites and

smaller fraction of weak Brønsted acid sites) enhanced the liftetime of the H-La-Y zeolite for the alkylation reaction.

The H-La-USY zeolite is a much more complex system than the other forms of X and Y zeolites. Practically, all types of hydroxyl groups observed in the other zeolites studied are present in this material and they are able to react with the isobutane/cis-2-butene mixture. It presented two components of silanol groups at 3743 and 3734 cm^{-1} corresponding to extraframework silicon-rich amorphous debris and to framework terminal silanol, respectively. It was also observed that the IR band at 3670 cm^{-1} typical for extraframework aluminum species reacted with pyridine indicating that the sites are located in accessible positions. This suggests that these groups not only play a role as adsorption sites by coordination to the aluminum atoms (Lewis acidity) which increases the olefin concentration in the zeolite pores, but also interact with lateral hydrogen bonding. Brønsted acidity represented by the bridging hydroxyl groups at 3630 and 3600 cm^{-1} was also observed in this sample. However, not all the acidic groups at 3600 cm^{-1} reacted with pyridine, as it is observed in the La-X samples. Therefore, it is concluded that the strength of these sites is not uniform and probably the strongest sites are those in the vicinity of the lanthanum cations. Finally, another important difference observed in the H-La-USY sample, when it is compared to the La-X samples was the higher reactivity of the $[La\text{-}OH]^{2+}$ groups. While in La-X samples they are mostly located in the small cavities of the zeolites and consequently not accessible to molecules larger than 0.28 nm, in the H-La-USY they are reactive either to pyridine or to n-butenes and therefore it is concluded that they occupy locations in the zeolite supercavities. Considering these facts, the H-La-USY zeolite combines markedly different types of acid sites and, therefore, it is difficult to predict its catalytic behavior in the alkylation based on the Brønsted and Lewis acidity obtained from IR spectra of adsorbed pyridine.

The hydroxyl groups on the H-EMT zeolite are comparable to those observed on the investigated H-La-Y. Due to its higher Si/Al ratio, this material is, however, much more stable than the homologue form H-FAU even without the presence of lanthanum. When the mixture isobutane/cis-2-butene was adsorbed, the IR spectra of these two catalysts (H-EMT and H-La-Y) were very similar: the band corresponding to the hydroxyl groups at 3630 cm^{-1} strongly decreased in intensity. Slightly less silanol groups in the H-EMT zeolite were involved in the interaction with the isobutane/cis-2-mixture when compared to the H-La-Y. However, as it can be seen in

Fig. 3.16 only a small band at ca. 3520 cm^{-1} was observed that has been attributed to hydrogen-bonded OH groups [30]. This is a direct consequence of the adsorption temperature used in these experiments (348K), the long adsorption time (40 min) and evacuation after adsorption (30 min). These three parameters led to that almost exclusively strong interactions like protonation or oligomerization were detected [31].

The degree of branching of the hydrocarbons present on H-BEA after isobutane/cis-2-butene adsorption was lower in comparison to the other samples studied as evidenced by more intense bands at 2929 and 2855 cm^{-1} due to asymmetric and symmetric stretching vibration of the group $–CH_2$-, respectively and less intense band at 1370 cm^{-1} due to umbrella bending in $C(CH_3)_2$ groups. Additionally the band characteristic of the olefinic vibration ν C=C was much less intense. It is concluded therefore that the hydrocarbons deposits on H-BEA zeolite are the product of oligomerization of the cis-2-butene and probably is the result of the relative high concentration of silanol groups attached to amorphous silica-alumina debris that contributed to the total acidy observed in this sample.

3.4.9. Alkylation activity of the different zeolites

The lifetime achieved with the investigated samples varied from 1 to 13 hours. The longest catalyst lifetime was obtained with the La-X materials. In both materials (La-X 1.1 and La-X 1.4) the most important hydroxyl groups responsible for their high alkylation activity were those corresponding to the IR band at ca. 3600 cm^{-1}. Among the investigated samples, the La-X catalysts are the materials with the highest concentration of these bridging hydroxyl groups. All these groups are accessible to the alkylation reactants or probe molecules like pyridine. Furthermore, the strength of these Brønsted acid sites is high allowing retaining more than 36% of the pyridine after heating up to 723K. This last characteristic has been shown to be essential to produce a good alkylation catalyst [32]. Although the two La-X materials have a different distribution of Si(nAl) signals, their catalytic activity was the same. This indicates that the reaction is relatively robust in terms of subtle differences of Brønsted acid sites, but sensitive in the relative concentration of these strong Brønsted acid sites.

While the La-X catalyst showed an enhanced activity for alkylation, the homologous La-Y zeolite showed a very short lifetime (2 hours). This large difference in activity is explained on the basis that an important fraction of the accessible Brønsted acid sites on this material (La-Y) corresponds to the lanthanum hydroxyl groups, silanol groups. The difference spectra after isobutane/cis-2-butene adsorption showed that the silanol and lanthanum hydroxyl groups were the largest fraction of accessible and interacting sites. However, due to their low acid strength, the concentration of hydrocarbons adsorbed on La-Y was approximately 12 lower than on La-X zeolites. Thus, the sample acts like a La-X sample with only a 1/12 of the acid sites. Such a situation has been shown to be equivalent to much higher overall space velocity, i.e., the high abundance of available olefin leads to oligomerization reactions [32].

The lifetime of the *in situ* activated NH_4-Y zeolite was only 1 hour. Upon isobutane/cis-2-butene adsorption, only the high frequency band at 3640 cm^{-1} was reactive to the feed molecules. As for La-Y, only a low concentration of hydrocarbons was adsorbed on the catalyst as concluded from the integrated intensity of the CH_3-, -CH_2- stretching bands between 3000 and 2800 cm^{-1}. The majority of the Brønsted acid sites associated with the bridging hydroxyl groups at 3640 cm^{-1} are weak and do not retain pyridine at 723K. Additionally, for this sample the IR band corresponding to the characteristic olefinic vibration at about 1640 cm^{-1} was very weak indicating a high olefin oligomerization activity of these sites. It should be noted here that is not so much a result of a particular acid strength of sites catalyzing oligomerization, but is a direct result of the weak sorption of butene, which allows addition to carbenium ions. This leads in consequence to higher selectivity to C_{9+} products and therefore to a low activity in alkylation.

When this sample was activated *ex situ*, the active Brønsted acid sites were mainly associated with silanol groups of ASA phases and the HF hydroxyl groups at 3732 cm^{-1} and 3640 cm^{-1}, respectively. This sample was readily dealuminated after water adsorption, which resulted in an increase of Si-OH groups and a considerably decrease in the high frequency band at 3640 cm^{-1}. Even with these structural differences both samples showed very short lifetime. It should be noted however, that subtle differences were observed between the integral selectivities to the different groups of products (Fig. 3.18), i.e., 20% of C_5-C_7 and 4.8% of octenes for the *in situ* activated NH_4-Y zeolite compared to 13.3% and 0.4%, respectively, for the *ex situ*

calcined sample. Thus, we conclude that more oligomerization took place on the *in situ* activated NH_4-Y sample.

A simultaneous exchange of a Na-Y zeolite with NH_4^+ and La^{3+} before calcination stabilized the catalyst towards dealumination. This leads to a catalyst with enhanced acidity. The relative intensity of the high frequency band at 3640 cm^{-1} was more pronounced in this material compared to the pure NH_4^+-Y zeolite. During isobutane/cis-2-butene adsorption these acidic groups dominated compared to Si-OH groups. The contrary was observed with *ex situ* calcined NH_4^+-Y. This difference in acidic properties led to a 4 times longer lifetime for H-La-Y compared to NH_4^+-Y.

The performance of the H-EMT catalyst was similar to that obtained with the H-La-Y catalyst. In both samples the adsorption on the bridging hydroxyl groups (3640 cm^{-1}) predominated leading to comparable lifetimes. The Lewis acid sites in the H-EMT sample, most of them present as OH-EFAL species (IR band at 3670 cm^{-1}), are probably located in the sodalite cages, and therefore they are not accessible to pyridine as evidenced by the absence of interaction of these groups with pyridine. Thus, it is concluded that these groups do not influence appreciably the activity in alkylation.

In H-BEA the high contribution to the Brønsted acidity of the silanol groups present as amorphous silica-alumna debris are probably responsible for the lower activity in alkylation compared to La-X. With deactivated H-BEA [33] a fraction of the acidic hydroxyl band at 3608 cm^{-1} is visible and, hence, not completely covered by hydrocarbons. The ASA debris, a fraction of them probably at the external surface of the catalyst and of weak acidity, catalyzes oligomerization of n-olefin leading to pore blocking. As a consequence not all potential acidic bridging hydroxyl groups are used.

3.5. **Conclusions**

The alkylation activity is closely related to the density, location and strength of the hydroxyl groups in the investigated zeolites. La-X zeolite with the highest concentration of strong Brønsted acid sites in the supercages shows the longest lifetime (13 h) in isobutane/cis-2-butene alkylation. Although the two La-X catalysts from different parent materials showed a different distribution of groups Si (nAl), the density of bridging hydroxyl groups at 3600 cm^{-1} in both materials was the highest.

All these groups are located in the large cavities of the X zeolite and they are accessible to the reactants.

In the homologous La-Y zeolite bridging hydroxyl groups at 3600 cm^{-1} are not found. Only bridging hydroxyl groups at 3640 cm^{-1} are observed. Their concentration is very low, which leads to a much lower catalytic activity. A fraction of the lanthanum hydroxyl groups at 3520 cm^{-1} were observed in the large cavities. They contributed appreciably to the total Brønsted acidity measured.

The H-Y zeolite activated *in situ* showed the highest concentration of weak Brønsted acid sites the majority of them related to the HF band at 3640 cm^{-1}. The high concentration of weak Brønsted acid sites is an undesirable property in isobutane/cis-2-butene alkylation catalysts. When the freshly calcined H-Y adsorbed water, it was dealuminated, which resulted in a dramatic decrease of the HF and LF bands and the formation of framework terminal Si-OH groups (IR band at 3732 cm^{-1}). The latter band contributed surprisingly in an appreciable manner to the Brønsted acidity of this sample. This in turn leads to weak Brønsted acidity and therefore to low catalytic activity. Enhanced stability and activity could be reached by a combination of La^{3+} and NH_4^+ ion exchange on the Na-Y zeolite. The resulting material showed much higher catalytic activity, when compared to NH_4-Y as evidenced by the marked increase of the concentration of bridging hydroxyl groups (band at ca. 3640 cm^{-1}). The similar adsorption and catalytic properties of H-EMT zeolite are also explained by the high concentration of those hydroxyl groups.

OH-EFAL species at 3670 cm^{-1} were observed with H-EMT and H-La-USY zeolites. However, in H-EMT these species appear to be located in the small cavities of the zeolite as evidenced by their inaccessibility to pyridine and, hence, they do not play a direct role in the catalytic activity of this sample. On the contrary, the OH-EFAL observed in H-La-USY were able interact with pyridine by hydrogen bonding.

The distribution of the three possibly oxygen crystallographic position that give rise to the LF band at 3550 cm^{-1} was markedly different in the H-Y and H-EMT zeolites. While in H-Y zeolite, in situ activated, the majority of the hydroxyl groups are attached to O_2 and O_3 type oxygens in the small cavities of the zeolite, in the H-EMT the contribution of the component corresponding to O_4 in the large cavities was higher (see next drawing).

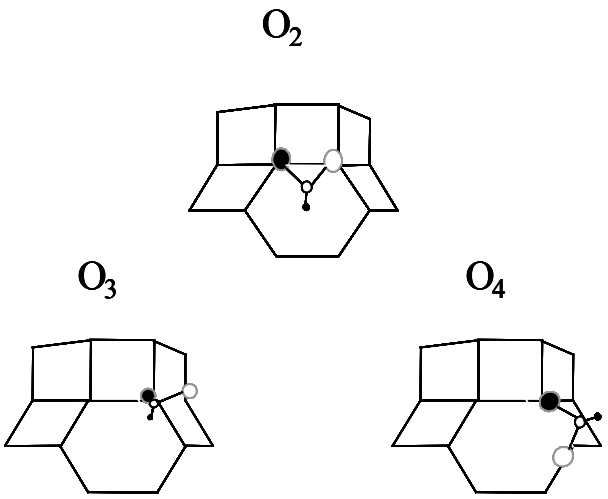

Schematic representation of the possible oxygen crystallographic positions that give rise to the LF band.

In H-BEA zeolites the high contribution of the silanol groups in the form of amorphous silica-alumina debris (IR band at 3746 cm^{-1}) leads to pore blocking. As a consequence not all acidic acid sites represented by the IR band at 3608 cm^{-1} are used when this sample was tested in isobutane/cis-2-butene alkylation.

3.6. Acknowledgments

Financial support from Süd-Chemie AG is gratefully acknowledged.

The authors wish also to thank Dr. Jan Kornatowski for the synthesis and characterization of some of the zeolites used in this study.

3.7. References

[1] A. Corma, A. Martínez, P.A. Arroyo, J.L.F. Monteiro, E.F. Sousa-Aguiar, Appl. Catal. A: General 142 (1996) 139.

[2] G.S. Nirvarthy, A. Feller, K. Seshan, J.A. Lercher, Micropor. Mesopor. Mat. 75 (2000) 35-36.

[3] T. Rørvik, H.B. Mostad, A. Karlsson, O.H. Ellestad, Appl. Catal. A: General 156 (1997) 267.

[4] J. Weitkamp, Y. Traa, Solid State Ionics 131 (2000) 175.

[5] M. Hunger, D. Freude, H. Pfeiffer, D. Prager, W. Reschetilowski, Chem. Phys. Lett. 163 (1989) 221.

[6] J. Weitkamp, Y. Traa, in: G. Ertl, H. Knözinger, J. Weitkamp (Eds), Handbook of Heterogeneous Catalysis, Vol. 4, 1997, p. 2039.

[7] L.A. Pine, P.J. Maher, W.A.Wachter, J. Catal. 85 (1984) 466.

[8] D. Fărcaşiu, Catal. Lett. 71 (2001) 95.

[9] H.G. Karge, in: G. Öhlmann, H. Pfeiffer, R. Fricke (Eds), Studies in Surface Science and Catalysis: Catalysis and Adsorption by Zeolites, Vol. 65, Elsevier, Netherlands, 1991, p. 133.

[10] N. Katada, Y. Kageyama, M. Niwa, J. Phys. Chem. B. 104 (2000) 7561.

[11] F. Delprato, L. Delmotte, L. Guth, L. Huve, Zeolites 10 (1990) 546.

[12] M. Stöcker, H. Mostad, A. Karlsson, H. Junggreen, B. Hustad, Catal. Lett. 40 (1996) 51.

[13] G.S. Nirvarthy, H. Yingjie, K. Seshan, J.A. Lercher, J. Catal. 176 (1998) 192.

[14] C.A. Emeis, J. Catal. 141 (1993) 347.

[15] J. Klinowski, Prog. Nucl. Mag. Res. Sp. 16 (1984) 237.

[16] A. Janin, M. Maache, J.C. Lavalley, J.F. Joly, F. Raatz, N. Szydlowski, Zeolites 11 (1991) 391.

[17] S. Yang, J.N. Kondo, K. Domen, Catal. Surv. Jpn. 5 (2002) 139.

[18] J. W. Ward, J. Catal. 13 (1969) 321.

[19] M. Weihe, M. Hunger, M. Breuninger, H.G. Karge, J. Weitkamp, J. Catal. 198 (2001) 256.

[20] J.W. Ward, J. Catal. 9 (1967) 225.

[21] P.A. Jacobs, J.B. Uytterhoeven, J. Chem. Soc., Faraday Trans. I. 69 (1973) 359.

[22] R.A. Van Santen, G.J. Kramer, Chem. Rev. 95 (1995) 637.

[23] A. Feller, I. Zuazo, A. Guzman, J-O. Barth, J.A. Lercher, J. Catal. 216 (2003) 313.

[24] A. Corma, A. Martinez, Catal. Rev.-Sci. Eng. 35 (1993) 483.

[25] J. A. Lercher, V. Veefkind and K. Fajerwerg, Vib. Spectrosc. 19 (1999) 107.

[26] N. Katada, Y. Kageyama, M. Niwa, J. Phys. Chem. B. 104 (2000) 7561.

[27] H.G. Karge, in: Verified Synthesis of Zeolitic Materials. 2nd Revised Edition, Elsevier, Amsterdam, (2001).

[28] A. Corma, A. Martinez, C. Martinez, Appl. Catal. A: General 134 (1996) 169.

[29] J.A. van Bokhoven, A.L. Roest, D.C. Konnigsberger, J. Phys. Chem. B. 104 (2000) 6743.

[30] N.J. Kondo, S. Liqun, F. Wakabayashi, K. Domen, Catal. Lett. 47 (1997) 129.

[31] G. Spoto, S. Bordiga, G. Ricchiardi, D. Scarano, A. Zecchina, E. Borello, J. Chem. Soc. Faraday Trans. 90 (1994) 2827.

[32] A. Feller, A. Guzman, I. Zuazo, J.A. Lercher, J. Catal. 224 (2004) 80.

[33] A. Feller, J-O. Barth, A. Guzman, I. Zuazo, J.A. Lercher, J. Catal. 220 (2003) 192.

Chapter 4

Influence of the activation temperature on the physicochemical properties and catalytic activity of La-X zeolites for isobutane/cis-2-butene alkylation

Abstract

The influence of the activation temperature on the physicochemical properties and catalytic activity of La-X zeolites for isobutane/cis-2-butene alkylation was investigated. The presence of molecularly adsorbed water under optimal activation conditions was shown by *in situ* IR and ^{1}H MAS NMR spectroscopy as well as temperature programmed desorption. Its presence affected mainly the overtones of the T-O-T lattice vibration of the zeolite. Bridging hydroxyl groups are not involved in hydrogen bonding. Significant variations in the Brønsted acid site concentration were not induced by the presence of water. Isobutane/cis-2-butene adsorption together with alkylation activity tests showed that the presence of water influenced mainly the selectivity to C_5-C_7 products. On catalyst with lower concentrations of water oligomerization, a side reaction, is favored. As a consequence the catalyst lifetime in alkylation was shorter (8 h) for the samples activated at higher temperatures (553K) than for samples having molecular water adsorbed in the zeolite pores.

Keywords: IR spectroscopy, molecularly adsorbed water, zeolitic hydroxyl groups and lattice vibration, hydrogen bonding, alkylation

4.1. Introduction

Alkylation is a very important refinery process in which part of the light hydrocarbons formed as by-products in the fluid catalytic cracking unit, mainly isobutane and n-butenes, are converted into a group of highly branched alkanes, the "alkylate" [1]. Liquid acids, especially anhydrous hydrofluoric and concentrated sulfuric acids, are widely used as catalysts in industrial alkylation processes.

The existing alkylation technology, while producing high-quality and environmental benign gasoline components, suffers from a number of disadvantages and drawbacks. In particular, the consumption of catalyst in the sulfuric acid process is relatively high reaching 70 to 100 kg per t of alkylate produced. The recovery of the spent catalyst has been estimated to be two or three times more expensive than sulfuric acid available on the market. In the hydrofluoric process the catalyst consumption is rather lower (below 1 kg/t), but its toxicity combined with its volatility and corrosiveness makes this process hazardous and expensive. Consequently, the search for alternative processes with environmentally benign catalysts has received special attention in the last decade [2].

Zeolites were the first solid acids tested as alternatives to sulfuric and hydrofluoric acids in isobutane/alkene alkylation, but only in the last decade they have been found to be suitable, when combined with the appropriate reactor technology [3]. Among the zeolites explored so far, materials based on faujasitic structure and zeolite BEA showed the best performance [4].

The acidity of the zeolites is the most important property with respect to their use as catalyst. Commonly, Brønsted acid sites are produced by ion exchange of the charge-compensating cations such as Na^+ by ammonium or polyvalent metal cations and subsequent thermal treatment. Calcination of the ammonium-exchanged zeolites at temperatures of about 623K results in the removal of ammonia and the formation of the bridging hydroxyl groups in the zeolite framework [5]. In polyvalent cation-exchanged zeolites the dissociation of water molecules associated with the metal cations results in the formation of OH groups bound to the metal and bridging hydroxyl groups. Regardless of the method used for their generation, the chemical nature of the Brønsted acid sites is the same, i.e., they are bridging hydroxyl groups formed by the proton and framework oxygen in an AlO_4 tetrahedron [6]. Additionally to the Brønsted acid sites generated, Lewis acid sites are also observed in the activated

zeolite. During heat treatment some of the bridging hydroxyl groups can be converted into Lewis acid sites by dehydroxylation. This process can be reversible if the temperature used is moderate. However, upon severe heat treatment (≥ 773K) structural aluminum tetrahedral atoms are irreversible removed from the framework. This process is referred as dealumination. The extent of the dehydroxylation or dealumination depends strongly on the activation mode and zeolite type. Generally, zeolites with higher Si/Al ratio have higher thermal and hydrothermal stability [7]. In consequence, a unique activation temperature for zeolite activation does not exist.

Under mild conditions dehydroxylation can be reversible, if the dehydroxylated zeolite is contacted with water. In this process Lewis acid sites are reconverted to Brønsted acid sites. In that sense acidity on the activated or rehydrated zeolite could differ significantly. However, during the rehydration water will be not only chemisorbed to restore the Brønsted acidity of the zeolite, but also physically adsorbed on the zeolite surface blocking or modifying acid and base sites. However, during the activation procedures, normally carried out prior to reaction tests or characterization, molecular water is mostly removed.

In our recent work, the optimum activation temperature for zeolitic alkylation catalysts was found to be around 443K [4]. However, the activation temperature used prior to characterization of acid sites via adsorption of pyridine (by IR spectroscopy) and NH_3-TPD was significantly higher (723K). Therefore, the potential differences between these two states need to be explored in order to rationalize property-performance relationships in a quantitative way.

Since many catalytic processes are operated in the presence of at least some water, its influence on the acidity of zeolites has been investigated by several authors. Ward [8] studied the influence of water on ammonium-, alkali-, and alkali earth- exchanged X and Y zeolites by observing changes in the IR spectrum of chemisorbed pyridine. In this study, after activation at 673K for 6 h, the samples were cooled to room temperature and an excess of pyridine was adsorbed. After equilibration for 2 h the samples were evacuated at 523K for 2 h and again cooled down to room temperature. Water was then adsorbed on the zeolite and the spectra were recorded after evacuation at room temperature, 423K and 523K. In a second set of experiments, the zeolites were evacuated at 873-903K instead of 673K. Based on these experiments it was concluded that addition of water on magnesium and calcium X zeolites leads to the

formation of Brønsted acid sites that could, however, be eliminated by subsequent evacuation.

Rare earth exchanged Y zeolites were also studied by Ward [9]. Dehydration under vacuum at increasing temperatures (498-723K) was carried out. After dehydration at 723K IR bands at 3740, 3640 and 3522 cm^{-1} were observed. Addition of water gave rise to a band at 3610 cm^{-1} and one near 3550-3560 cm^{-1}. Subsequent dehydration removed the water, and no new hydroxyl groups were formed.

Recently Corma *et al.* [10] studied the interaction of water with the surface of USY zeolites during catalytic cracking by IR spectroscopy and kinetic studies. Under cracking conditions (T > 673K) neither interaction of water with the acidic OH groups nor formation of new hydroxyl groups was observed.

In this chapter, the influence of water on the catalytic properties of a lanthanum exchanged X zeolite is investigated. For this purpose IR spectroscopy of pyridine and a mixture of isobutane/cis-2-butene, along with catalytic experiments after activation at temperatures between 120 and 723K, are used.

4.2. Experimental

4.2.1. Material preparation

Na-X zeolite used in this study was supplied by Chemische Werke Bad Köstritz (Si/Al = 1.14). The Na-X parent material was brought into the acidic form by two ion exchange steps with 0.2 M lanthanum nitrate solution, using a liquid-to-solid ratio of about 10 mL/g. The ion exchange was carried out at 353K for 2 h. After washing and drying, the resulting material was calcined at 723K for 1 h in 100 mL/min flowing air, with a slow temperature ramp up to 723K. After re-hydration by exposition to atmospheric moisture, the calcined material was further exchanged three times with lanthanum nitrate under the same conditions above described. The resulting material, identified as La-X, was stored at atmospheric conditions.

4.2.2. Material characterization

The specific surface area and the micropore volume of La-X samples activated at temperatures between 393 and 723K were estimated by N_2 adsorption (BET and t-plot methods [11]). The chemical composition was determined by AAS.

The effect of the activation temperature on the release of water and on the nature of water remaining on the catalyst was studied by means of IR and ^{1}H MAS NMR spectroscopy as well as with temperature programmed desorption (TPD).

For TPD experiments approximately 25 mg of sample were activated in a six ports parallel vacuum system (0.1 Pa) for 2 h at 453, 503, 553 and 723K. After activation the samples were heated up to 1053K with a rate of 10K/min. Water desorption was monitored by a mass spectrometer (Pfeiffer QMS 200 Prisma). The amount of water desorbed during TPD experiments was determined by thermogravimetric analysis (TGA).

The acidity was studied by adsorption/desorption of pyridine monitored by IR spectroscopy. For this purpose the sample was pressed into a self-supporting wafer (with a density between 5 and 10 mg/cm^2). After activation in vacuum for 2 h at 423, 453, 503, 553 and 723K, the sample was cooled down to 423K and pyridine at a partial pressure between 1-5 Pa was introduced into the cell. IR spectra were recorded at 423K before adsorption of pyridine, and after adsorption of pyridine and outgassing at 423K. The spectra were measured with a Perkin-Elmer System 2000 spectrometer with a resolution of 4 cm^{-1}. The concentration of Brønsted and Lewis acid sites was estimated from the bands at 1540 and 1454 cm^{-1}, respectively. The extinction coefficients were taken from Emeis [12]. The Brønsted and Lewis acid site concentrations measured after outgassing at 423K are referred as BAS_{423} ("*total Brønsted acidity*") and LAS_{423} ("*total Lewis acidity*"), respectively.

Isobutane/cis-2-butene adsorption/desorption experiments monitored by IR spectroscopy were also carried out. Self-supporting wafers (5-10 mg/cm^2) were activated in a sorption cell in vacuum for 2 h at 423, 453, 503, 553 and 723K. After cooling down to 348K, a mixture isobutane/cis-2-butene (with molar ratio 7/1) was introduced into the cell. This mixture was dosed by using a loop of 250 μL maintained at 299K. Spectra were recorded with a resolution of 4 cm^{-1} on a Bruker IFS88 spectrometer during adsorption until equilibrium conditions were reached (approximately 40 minutes).

4.2.3. Catalytic experiments

The alkylation of isobutane with cis-2-butene was performed in a stirred tank reactor operated in continuous mode. The liquefied gases were received from Messer with a purity of 99.95% (isobutane) and 99.5% (cis-2-butene). The La-X zeolite (typically 2.6 g) was activated *in situ* at temperatures of 393, 423, 453, 503 and 553K for 16 h in 100 mL/min flowing hydrogen. After cooling down to the reaction temperature, typically 348K, the reactor was filled with liquid isobutane at a pressure of $2x10^3$ KPa and stirred at 1600 rpm. The reaction was started by admitting an isobutane/cis-2-butene mixture with a paraffin-to-olefin (P/O) ratio of 10 and an olefin space velocity (OSV) of 0.2 (g butene)$*$(g catalyst)$^{-1}*$ h^{-1}. Both reactants were fed through syringe pumps (ISCO 100D and 500D) and mixed in a non-return valve before reaching the reactor. After expansion, the product from the reactor passed through a six-port-valve with a sample loop, the content of which was injected automatically into a HP 6890 gas chromatograph equipped with a FID-detector and a 35 m DB-1 column. The reactions were stopped when the conversion of butene started to be not complete (<99%). The corresponding time on stream was named "*catalyst lifetime*". During the whole catalyst lifetime the product was condensed after the six-port-valve and weighted. Its integral composition was determined by GC analysis. The results obtained were compared with the mathematical integration of the differential data points gathered during the test, the difference being less than 10%.

4.3. Results

4.3.1. Influence of the activation temperature on the physicochemical properties of La-X samples

4.3.1.1. Specific surface area and pore volume

The specific surface area and micropore volume of the La-X zeolite activated at 723, 553, 503, 453, 423 and 393K were measured. As the activation temperature increased, both specific surface area and micropore volume, increased. For the two extreme temperatures, 393 and 723K, the area increased from 368 to 544 m^2/g, while

the micropore volume increased from 0.14 to 0.20 cm^3/g, respectively (Fig. 4.1). Both properties increased as a result of water removal with activation temperature.

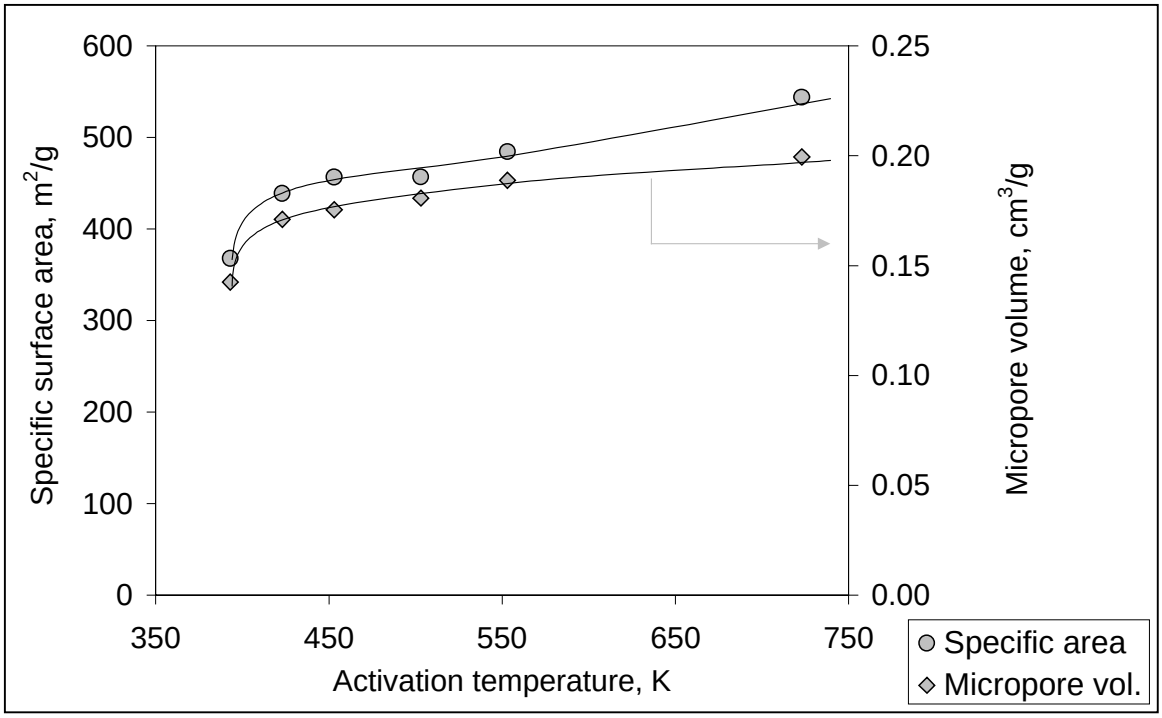

Figure 4.1: Variation of the specific surface area and micropore volume with activation temperature of La-X zeolite.

4.3.1.2. IR spectra of samples at various stages of activation

The activation of the La-X zeolite in vacuum was monitored by IR spectroscopy during increasing of the temperature up to 723K. Hydroxyl bands between 3750 and 3500 cm^{-1} were distinguishable only above 393K outgassing temperature (Fig. 4.2). Molecularly adsorbed water was concluded to be present from the observation of the band at 1630 cm^{-1} (δas [HOH]) [9]. As shown in Fig. 4.3, this band decreased monotonically with temperature and disappeared at ca. 573K.

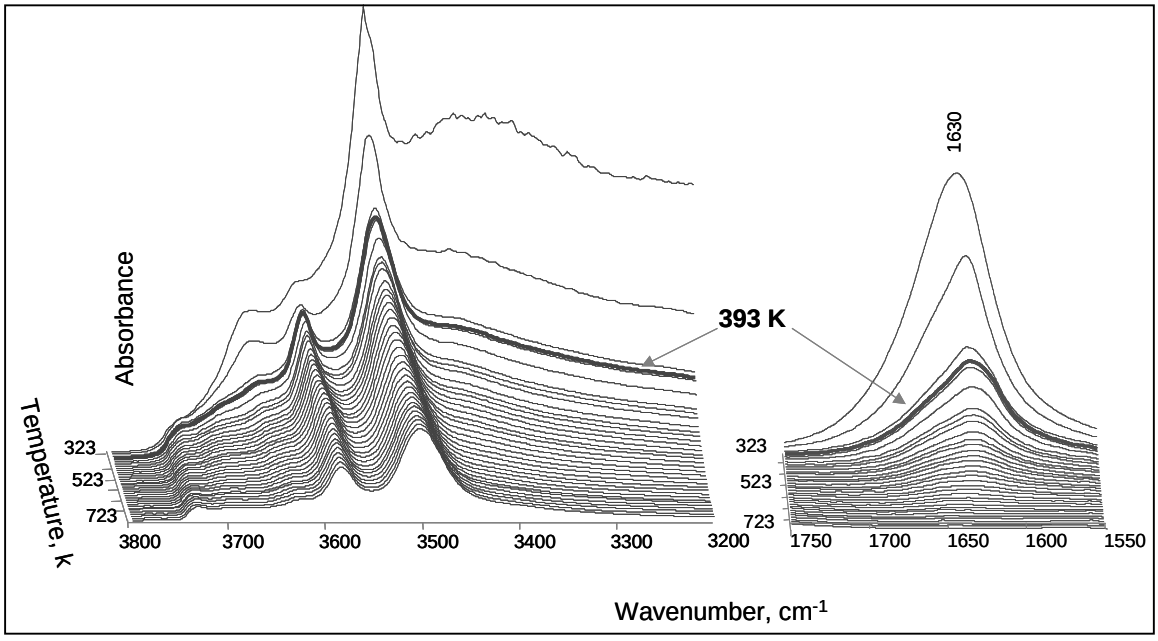

Figure 4.2: IR spectra recorded during activation of La-X up to 723K.

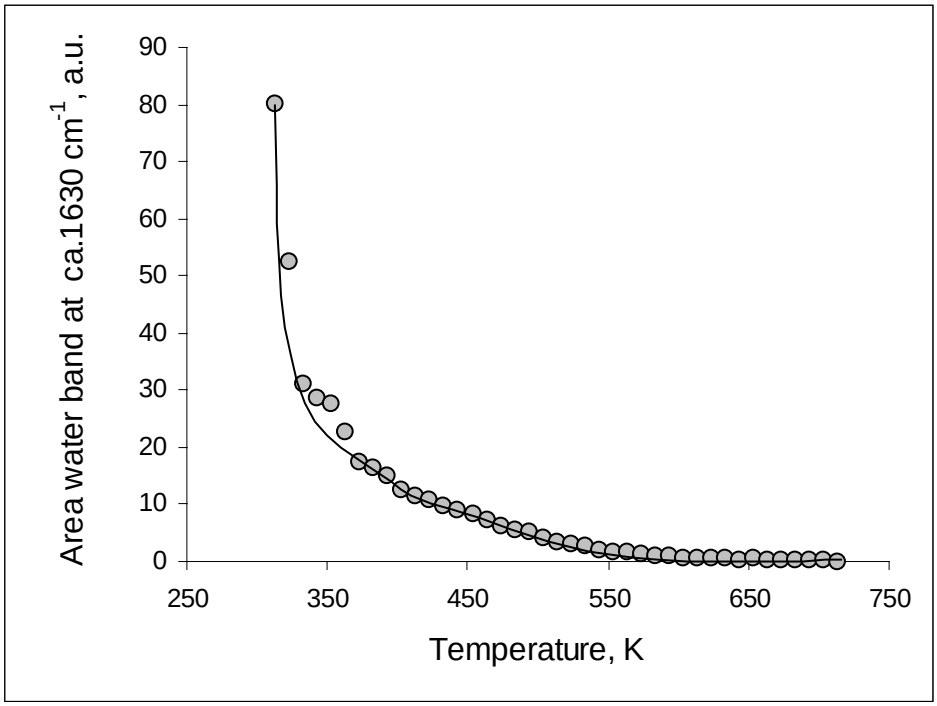

Figure 4.3: Integral intensity of the IR band corresponding to the water deformation vibration (1630 cm^{-1}) *vs.* activation temperature of La-X zeolite.

4.3.1.3. TPD profiles

The effect of the activation temperature on the release of water from La-X samples was studied by means of TPD experiments. As shown in Fig. 4.4 (left site), after activation at 453 and 503K the TPD profiles presented two peaks at ca. 603 and 723K, while only one peak was observed after activation at 553K. After activation at 723K, water desorbed only at temperatures higher than 773K. Even with the activation at 723K a significant and constant rate of desorption was observed at the final temperature of our TPD experiments (1053K). Fig. 4.4 (right site) compiles the curves obtained by subtraction of the TPD profile recorded after activation at 723K to the TPD profiles obtained after activation at 453, 503 and 553K. The corresponding amounts of water desorbed were estimated by TGA and expressed as weight percentage with respect to the weight of the sample before activation (Table 1). The total amount of water remaining after activation at 453K was 1.73%.

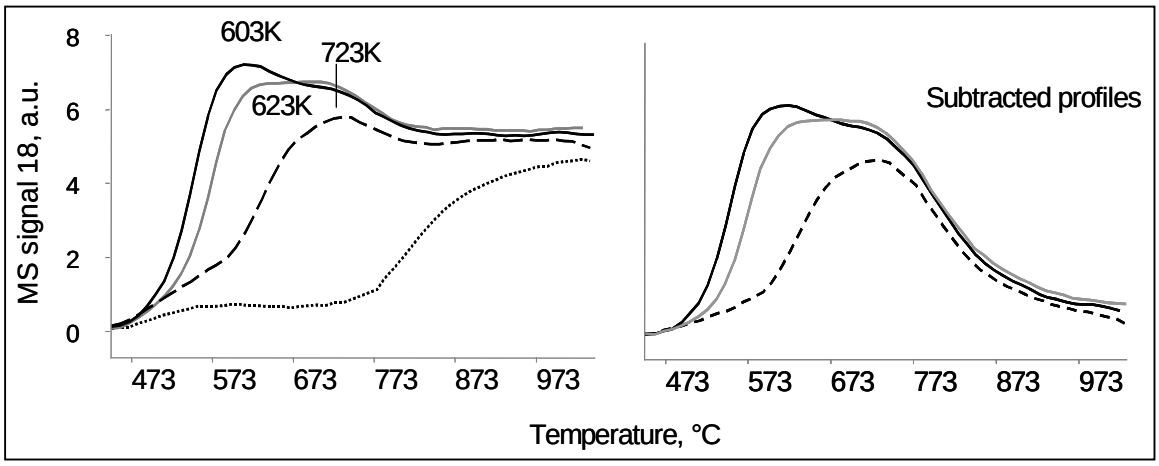

Figure 4.4: Left site: TPD profiles of La-X after activation at

(——) 453K, (——) 503K, (- - -) 553K and (·····) 723K. Right side: curves obtained by subtraction of the TPD profile reordered after activation at 723K to the TPD profiles after activation at 453, 503 and 553K.

Activation Temperature, K	Remaining water, wt-%
453	1.73
503	1.55
553	1.13

Table 4.1: Water removed from the La-X zeolite during heating up to 1053K as function of the activation temperature. The quantity of water removed is expressed as percentage of the weight of the catalysts before activation.

4.3.1.4. ^{1}H NMR spectra

The effect of water remaining adsorbed on La-X samples as function of the activation temperature was also investigated by ^{1}H MAS NMR spectroscopy. The NMR spectra recorded after activation at 453 and 723K showed four distinguishable peaks at ca. 6.3, 4.0, 2.9 and 1.8 ppm (Fig. 4.5). These correspond to OH groups bound to lanthanum cations $[La(OH)]^{2+}$, bridging hydroxyl groups SiOHAl in large cavities of the zeolite, OH bounded to extra-framework aluminium species AlOH and silanol groups at the external surface or at lattice defects, respectively [13]. The total OH concentration was 3.71 mmol/g for the sample activated at 453K and 1.06 mmol/g for that activated at 723K. The concentration of Brønsted acid sites, obtained by integration of the peaks corresponding to bridging hydroxyl groups (4.0 ppm) and silanol groups (1.8 ppm), was 1.11 and 0.22 mmol/g for activation temperatures of 453 and 723K, respectively.

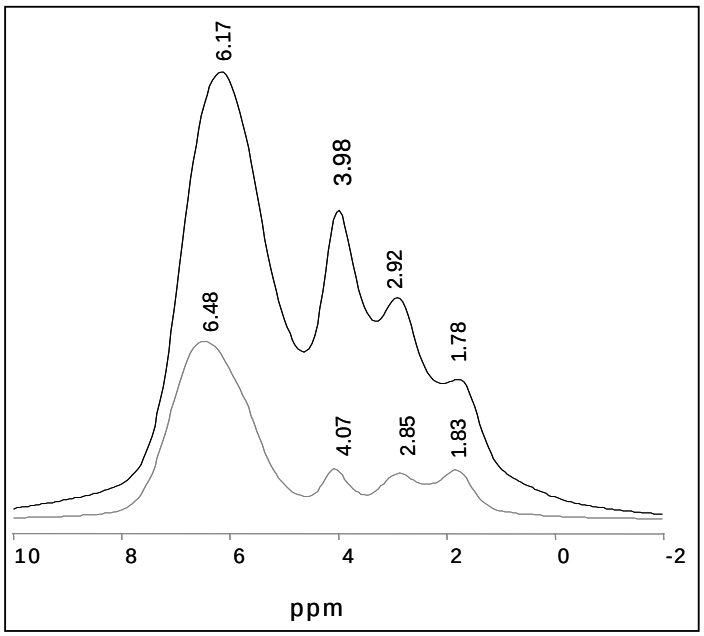

Figure 4.5: ^{1}H NMR spectra of La-X activated at 723K (gray line) and at 453K (black line).

4.3.1.5. Acid site characterization by IR spectra of adsorbed pyridine

The IR spectra recorded before pyridine adsorption on the La-X samples activated at temperatures between 423 and 723 are shown in Fig. 4.6 (all the spectra were recorded at 423K). In the hydroxyl region bands at ca. 3520, 3600, 3640, 3700, 3733 and 3743 cm^{-1} were observed. These bands were assigned to lanthanum hydroxyl groups $[La(OH)]^{2+}$, bridging hydroxyl groups (3600 and 3640 cm^{-1}), $\nu_{as}(H_2O)$ in molecularly adsorbed water, silanol groups at lattice defects and terminal silanol groups [8, 9]. Significant differences in the intensity were not observed in the hydroxyl region of spectra, when water was present in the sample. The bands corresponding to lanthanum hydroxyl groups and bridging hydroxyl groups (at ca. 3600 cm^{-1}) were slightly shifted to higher wavenumbers with increasing activation temperatures. The intensity of the band assigned to the silanol groups at lattice defects (3733 cm^{-1}) decreased with activation temperature.

It should be also noted that the lattice combination vibration at 1850 cm^{-1} is affected by the presence of water. A linear correlation was observed between the area of the lattice combination vibration of the zeolite and the water deformation band at 1630 cm^{-1} (Fig. 4.7).

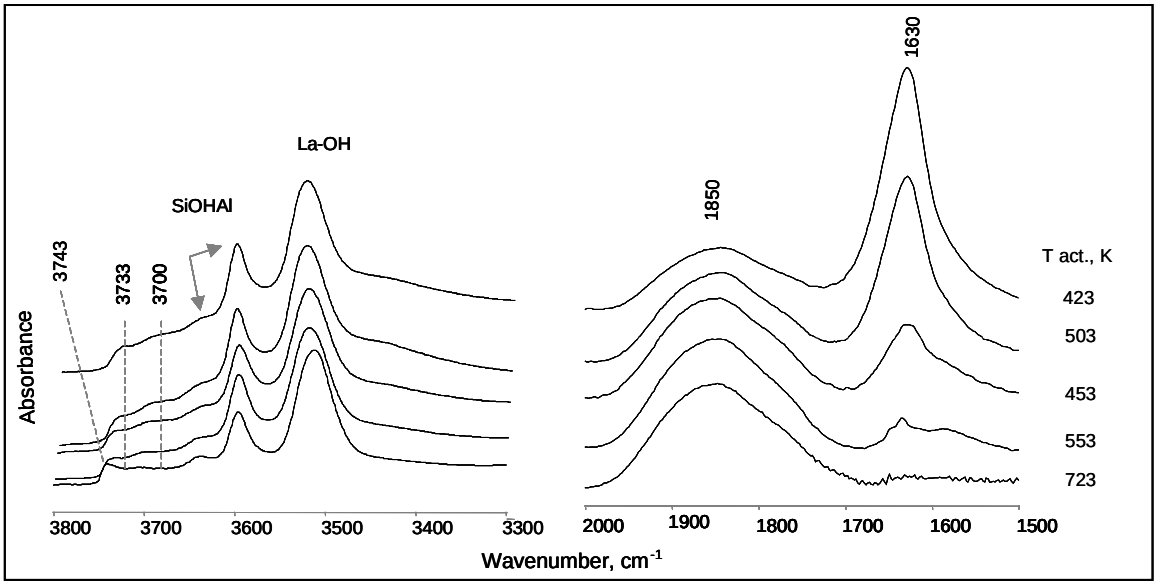

Figure 4.6: Left side: hydroxyl region in the IR spectra of La-X activated at different temperatures. Right side: IR lattice combination vibration (1850 cm^{-1}) and water deformation band (1630 cm^{-1}).

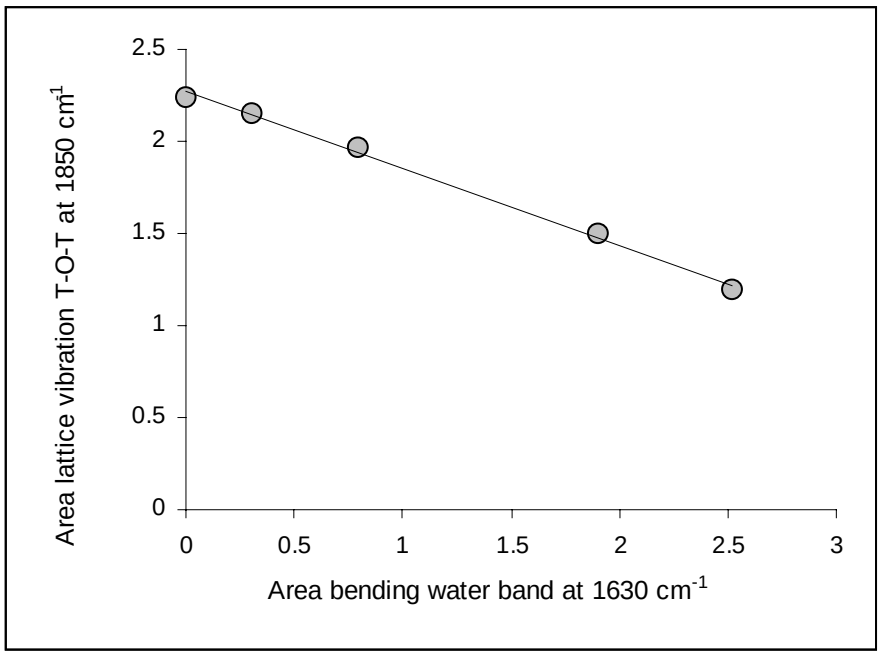

Figure 4.7: Variation of the area of the lattice vibration combination band at 1850 cm^{-1} with the area of the water deformation band at 1630 cm^{-1}.

The concentrations of Brønsted and Lewis acid sites were measured by pyridine adsorption. Significant differences in total Brønsted acid site concentration (BAS_{423}) for samples activated at temperatures between 423 and 553K (Table 2) were not

observed. Only after activation at 723K the Brønsted acid site concentration decreased slightly. The total concentration of Lewis acid sites (LAS_{423}) did not change with activation temperature. After activation at 723K the concentration of Brønsted acid sites determined by IR of adsorbed pyridine (0.29 mmol/g) was comparable to that obtained by ^1H MAS NMR (0.22 mmol/g of bridging hydroxyl groups at ca. 4 ppm and silanol groups at 1.8 ppm). However, when the sample was activated at 453K the concentration of Brønsted acid sites determined by ^1H MAS NMR (1.11 mmol/g) was markedly higher than the value obtained by IR of adsorbed pyridine (0.38 mmol/g).

Activation temperature, K	423	453	503	553	723
BAS_{423} mmolpy/g	0.38	0.40	0.34	0.34	0.29
LAS_{423} mmolpy/g	0.10	0.11	0.10	0.10	0.12

Table 4.2: Total concentration of Brønsted (BAS_{423}) and Lewis (LAS_{423}) acid sites, measured by pyridine adsorption, as function of the activation temperature.

4.3.2. Effect of the activation temperature on isobutane/cis-2-butene adsorption on La-X samples

The adsorption of isobutane/cis-2-butene on La-X zeolite resulted in distinguishable hydrocarbon IR bands at 2964, 2939, 2874, 1670 (shoulder), 1634, 1469, 1383 and 1370 cm^{-1} (Fig. 4.8). These bands have been assigned to asymmetric stretching of the CH_3 group, asymmetric stretching of the CH_2, symmetric stretching of the group CH_3, stretching of C=C in trans, tri- and tetra-substituted olefins, C=C stretching in cis olefins, asymmetric bending of the CH_3, doublet umbrella bending in $C(CH_3)_2$ groups (IR bands at 1383 and 1370 cm^{-1}) [14]. The hydroxyl groups involved in the adsorption of isobutane/cis-2-butene were the external silanol groups (IR band at 3743 cm^{-1}), silanol groups at defect sites (IR band at 3733 cm^{-1}), and the bridging hydroxyl groups (IR bands at 3640 and 3600 cm^{-1}). Profiles obtained from subtraction of IR spectra taken before and after adsorption with the paraffin/olefin mixture

revealed that from the zeolitic hydroxyl groups, the acidic bridging hydroxyl groups at 3600 cm^{-1} were more active and partially consumed upon adsorption (Fig. 4.8). Integration of this band together with the CH_3/CH_2 symmetric and asymmetric stretching bands showed that in the sample activated at 723K less acidic groups were involved in the adsorption, but at the same time apparently more hydrocarbons were adsorbed (Fig. 4.9).

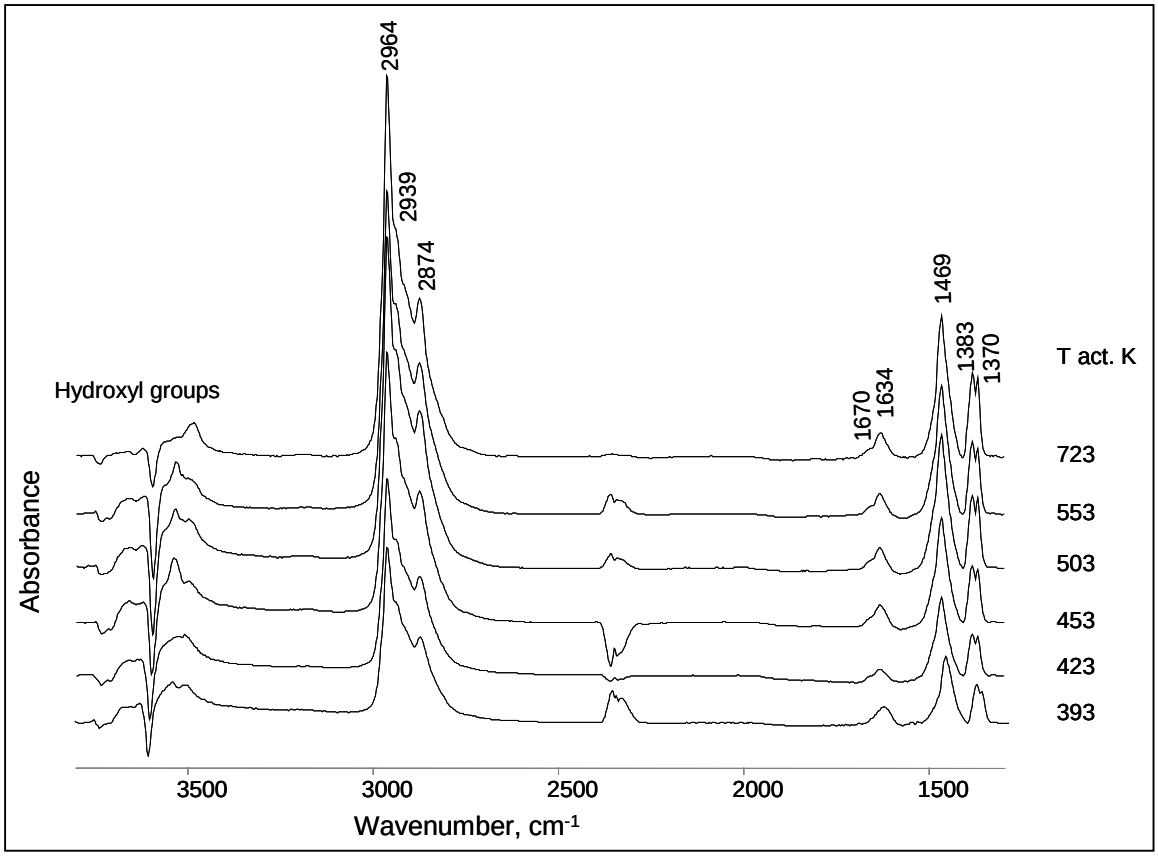

Figure 8: Profiles obtained by subtraction of the IR spectra recorded before and after isobutane/cis-2-butene adsorption on La-X samples activated at different temperatures.

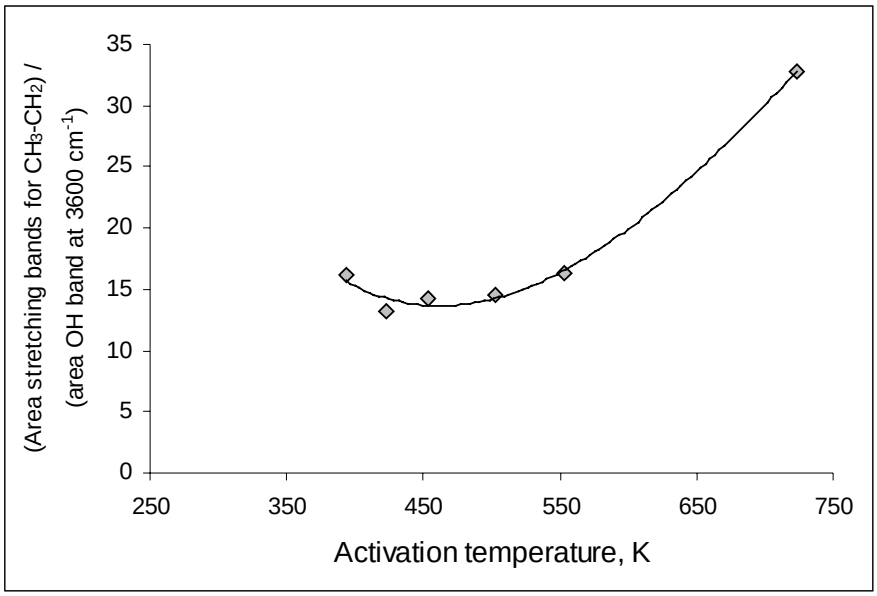

Figure 4.9: Effect of the activation temperature on the ratio between the area of the IR bands corresponding to the asymmetric and symmetric stretching of CH_3/CH_2 groups and the area of the IR band corresponding to hydroxyl group observed after adsorption of isobutane/cis-2-butene at 348K.

Isobutane was adsorbed on the sample activated at 723K (Fig. 4.10). The IR spectrum obtained was used for comparison with the isobutane/cis-2-butene adsorption.

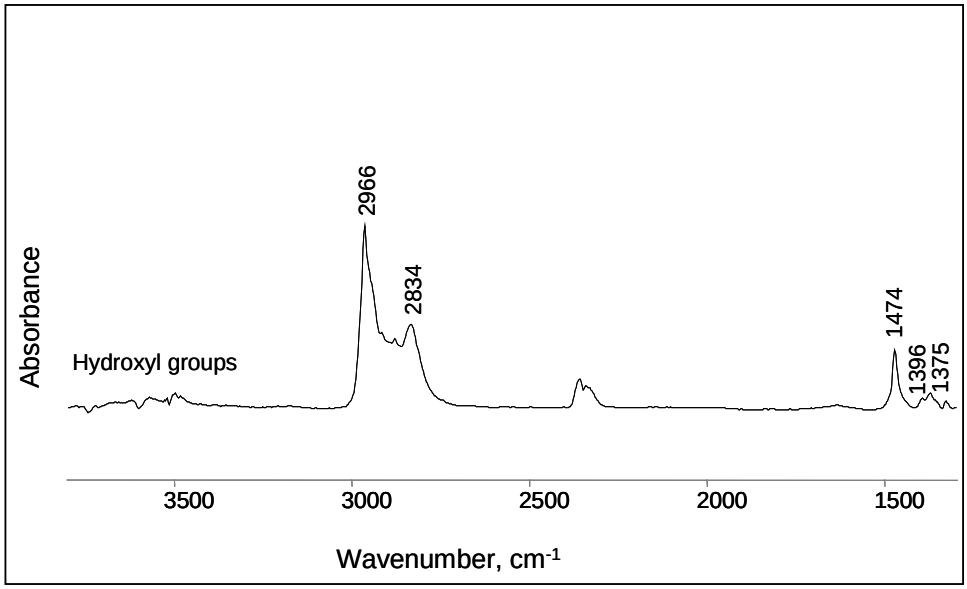

Figure 4.10: Profile obtained by subtraction of the IR spectra recorded before and after isobutane adsorption on La-X samples activated at 723K.

4.3.3. Effect of activation temperature on catalytic activity of La-X samples in isobutane/cis-2-butene alkylation

The catalyst lifetime *vs.* activation temperature shows a trend with a maximum corresponding to ca. 13 h for activation temperature of about 423-453K (Fig. 4.11). When the sample was activated at the maximum temperature investigated (553K), the catalyst lifetime decreased to 8.2 h.

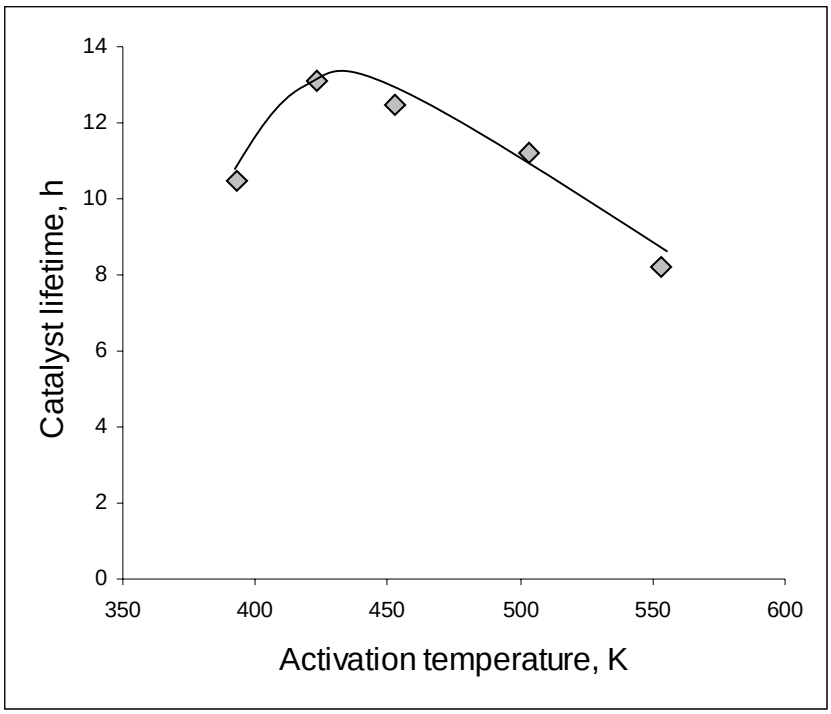

Figure 4.11: Variation of the catalyst lifetime with the activation temperature.

In Fig. 4.12, the dependence of the integral selectivities of the different groups of products on the activation temperature is shown. Remarkable differences in the integral selectivities to the groups of products C_8 and C_{9+} were not observed. Only a slightly increase in the C_5-C_7 fraction with activation temperature was seen. For all the activation temperatures, the C_8 fraction dominated, representing approximately 80% of the alkylate.

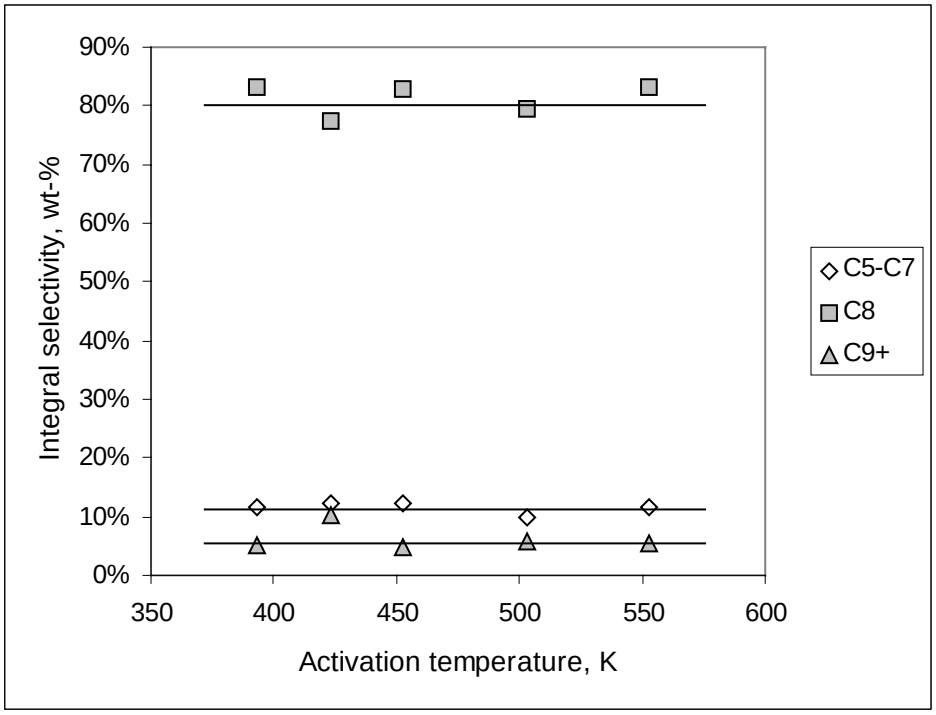

Figure 4.12: Influence of the activation temperature on the integral selectivities to the different groups of products in isobutane/cis-2-butene alkylation.

The integral selectivities in the C_8-fraction, based on the total product, are shown in Fig. 4.13. The most prominent changes in selectivities were observed for 2,2,4-TMP and 2,5-DMH + 2,2,3-TMP. They increased from 17 and 6%, for low activation temperatures (393 and 423K) to 20.5 and 9.3% for higher activation temperatures, respectively. It should also be noted that for the tested samples with the activation temperatures of 423 and 453K the selectivity to octenes ($C_8^=$) was the lowest.

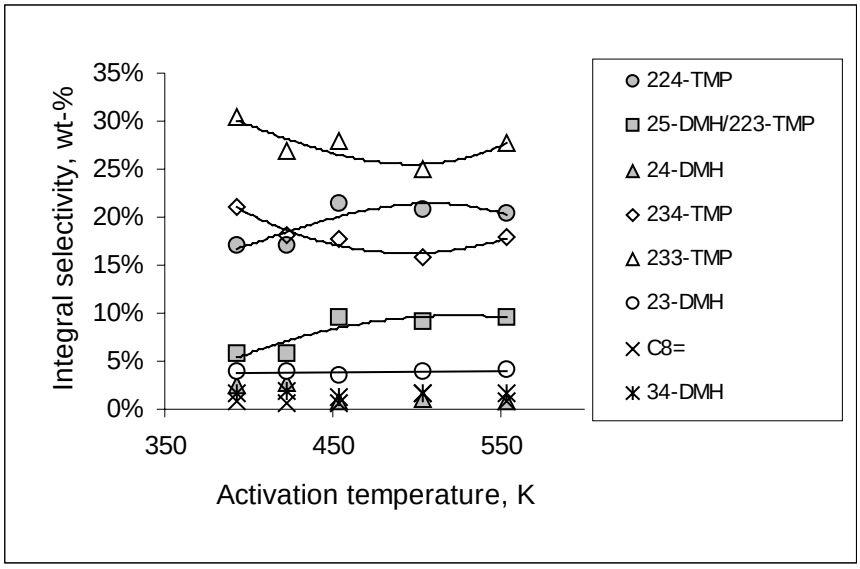

Figure 4.13: Changes in integral selectivities to the individual C_8 products with activation temperature in isobutane/cis-2-butene alkylation.

4.4. Discussion

4.4.1. Effect of the activation temperature on the physicochemical properties of La-X zeolite

As evidenced by IR spectroscopy, La-X samples calcined at 723K adsorb water when subsequently exposed to atmospheric conditions. Molecularly adsorbed water can be progressively removed by vacuum activation and finally completely desorbed for temperature above 573K (as indicated by the disappearance of the IR band at ca. 1630 cm^{-1}). A similar temperature of complete desorption of molecular water was obtained from TPD experiments. The TPD profile of the sample activated for 2 h at 553K did not show the peak at approximately 603K, typical for the desorption maximum of molecular water observed with the samples activated at lower temperatures (453 and 503K). When the zeolite was activated at 723K, another release of water was observed in the TPD profile, corresponding to a broad band starting from approximately 773K. This water is attributed to the dehydroxylation of the zeolite [6]. It is likely that this procedure starts already at temperatures below 723-773K and, therefore, can be responsible also for the TPD-peak at about 723K observed for samples activated at 453, 503 and 553K. Bolton [15] showed that

dehydroxylation in rare earth exchanged Y zeolites starts at approximately 623K, occurs to a major extent between 673-873K, and is essentially completed at 973K. The La-X zeolite studied here appears to be more thermally stable. In fact we observed a very broad desorption peak and continuous desorption of water even at the final temperature of the TPD experiment (1053K). Additionally, during activation up to 723K, only a slight decrease of the hydroxyl bands in the IR spectra was observed and the total concentration of Brønsted acid sites, for the sample activated at 723K (determined by IR spectroscopy of adsorbed pyridine) decreased only slightly from approximately 0.36 mmol/g (for lower activation temperatures) to 0.29 mmol/g. This value was semi-quantitatively confirmed by ^{1}H MAS NMR (0.22 mmol/g).

As determined by TPD and TGA experiments the amount of water desorbed from 453 and 553K, the temperature at which all the molecular water has been removed, was 0.33 mmol H_2O/g of zeolite corresponding to 0.6 % of the weight of the zeolite before activation. The total Brønsted acid site concentration determined on the sample activated at 453K was 0.40 mmol/g. The molar ratio between adsorbed water and OH acidic groups is hence 0.8. Although the ratio is close to unity, the typical Fermi resonance spectroscopic infrared bands at 2880, 2460 and 1700 cm^{-1} [16, 17] generated by hydrogen-bonded water, were not observed. Moreover, the parallel decrease in intensity of the bridging hydroxyl bands that results from the presence of hydrogen-bonded water to those groups was not observed.

Thus, adsorbed water is not localized on Brønsted acid sites on these materials. As shown by IR spectroscopy water adsorbed on the sample interacted mainly with the lattice of the zeolite. The decrease in intensity of the lattice vibration at 1850 cm^{-1} with water suggests that most of the water is involved in hydrogen-bonded molecular interactions with the T-O-T groups.

Based on the ^{1}H MAS NMR experiments molecularly adsorbed water was also observed. In fact the enhanced signal at ca. 4.0 ppm for the sample activated at 453K compared to the sample activated at 723K confirmed the presence of physisorbed water [18]. This signal was also observed in the Na-X parent material. As a consequence, the obtained hydroxyl concentration corresponding to the bridging hydroxyl groups at also 4.0 ppm was considerably higher compared to that obtained by IR of adsorbed pyridine.

4.4.2. Effect of the activation temperature on isobutane/cis-2-butene adsorption on La-X samples

Qualitative differences were not observed in the IR spectra obtained after adsorption of isobutane/cis-2-butene on the La-X zeolite activated at the studied temperatures. In all spectra the doublet umbrella bending vibration in $C(CH_3)_2$ groups (IR bands at 1383 and 1370 cm^{-1}) was more intense than when only isobutane was adsorbed on the sample (Fig. 4.10). This suggests that the formed products on the catalyst are highly branched.

The correlation found between the ratio of the integrated areas of the CH_3 and CH_2 symmetric and asymmetric stretching bands to the hydroxyl groups band and the catalyst activation temperature indicates that less Brønsted acid sites are able to react with more hydrocarbon molecules in the mixture, when the catalyst activation temperature is increased. Especially when the sample was activated at 723K the ratio was 2 times higher compared to the value obtained with the sample activated at lower temperatures. Note that the total concentration of Brønsted acid sites measured by IR of adsorbed pyridine on this sample was only 0.07 mmol/g lower, when compared to the concentration obtained at lower activation temperatures. Thus, this difference cannot explain, why the sample activated at 723K adsorbed more hydrocarbons. However, the intensity of CH_3/CH_2 band can also be more intense if the adsorbed compounds, with similar nature, have a higher molecular weight. This can be only possible if oligomerization of the olefin is favored. Thus, the presence of water interacting mainly with the zeolite lattice and not with the acidic and catalytic active sites seems to retard the oligomerization rate of the olefin. It should be emphasized, however, that an optimum activation temperature exists around 393K based on the ratio of the CH_3/CH_2 to hydroxyl groups band.

4.4.3. Catalytic activity of La-X zeolite activated at temperatures between 393 and 553K in isobutane/cis-2-butene alkylation

The catalyst lifetime varied with the activation temperature. A maximum was observed at catalyst activation temperatures between 423 and 453K. This is in agreement with the results obtained by IR spectroscopy of isobutane/cis-2-butene

adsorption. The optimum observed is related to the amount of water adsorbed on the catalyst.

Of the three main groups of products only the C_5-C_7 fraction, which consists of cracking products of C_{12}-carbenium ions [4], increased with activation temperature. In the C_8 fraction, higher concentrations of C_8 olefins were detected in the sample activated at 503 and 553K. Thus, as observed in the IR experiments with a mixture isobutane/cis-2-butene, the presence of water affected mainly the formation of oligomers in the isobutane/cis-2-butene alkylation. As a consequence the catalyst lifetime was shorter in samples with decreasing content of water.

4.5. Conclusions

Molecularly adsorbed water is present on La-X until activation temperatures of approximately 573K. Its presence does not significantly affect the total concentration of Brønsted acid sites as determined by IR spectroscopy of adsorbed pyridine. At higher activation temperatures the zeolite is slightly dehydroxylated. This is evidenced by the decrease in the total Brønsted acid site concentration and by the corresponding decrease in the intensity of hydroxyl groups.

Water interacts mainly with the lattice of the zeolite. As evidenced by IR spectroscopy, the overtones and combination vibrations of the lattice are affected by the presence of molecularly adsorbed water. Bridging hydroxyl groups are (surprisingly) hardly involved in hydrogen bonding.

Water adsorbed on the catalyst affected mainly the fraction C_5-C_7 in the alkylate. The integral selectivity to this fraction was higher at higher activation temperatures. Therefore, with zeolite catalysts having less water oligomerization is favored.

The optimal catalyst activation temperature lies between 423 and 453K, leading to longer catalyst lifetime and less oligomerization. In that respect catalytic experiments and adsorption of isobutane/cis-2-butene monitored by IR spectroscopy were in perfect agreement.

4.6. Acknowledgments

Financial support from Süd-Chemie AG is gratefully acknowledged.

4.7. References

[1] J. Weitkamp, Y. Traa, in: G. Ertl, H. Knözinger, and J. Weitkamp (Eds), Handbook of Heterogeneous Catalysis Vol. 4, 1997, p. 2039.

[2] A. Corma, A. Martinez, Catal. Rev.-Sci. Eng. 35 (1993) 483.

[3] A. Feller, I. Zuazo, A. Guzman, J-O. Barth, J.A. Lercher, J. Catal. 216 (2003) 313.

[4] A. Feller, A. Guzman, I. Zuazo, J.A. Lercher, J. Catal. 224 (2004) 80.

[5] M. Hunger, Catal. Rev.-Sci. Eng. 39 (1997) 345.

[6] J. Weitkamp, Y. Traa, Solid State Ionics 131 (2000) 175.

[7] J. Klinowski, Prog. Nucl. Mag. Res. Sp. 16 (1984) 237.

[8] J.W. Ward, J. Catal. 11 (1968) 238.

[9] J.W. Ward, Phys. Chem. 72 (1968) 4211.

[10] A. Corma, O. Marie, F.J. Ortega, J. Catal. 222 (2204) 338.

[11] S. Lowell, J.E. Shields, in: Chapman and Hall, Powder and Surface Area and Porosity, Cornwall, 1991, p. 241.

[12] C.A. Emeis, J. Catal. 141 (1993) 347.

[13] M. Hunger, Solid State Nucl. Mag. 6 (1996) 1.

[14] S. Yang, J.N. Kondo, K. Domen, Catal. Surv. Jpn. 5 (2002) 139.

[15] A.P. Bolton, J. Catal. 22 (1971) 9.

[16] K. Hadjiivanov, J. Saussey, J.L. Freysz, J.C. Lavalley, Catal. Lett. 52 (1998) 103.

[17] R.A. Van Santen, G.J. Kramer, Chem. Rev. 95 (1995) 637.

[18] M. Hunger, D. Freude, H.J. Pfeiffer, J. Chem. Soc., Faraday Trans. 87 (1991) 657.

Chapter 5

5. 1 Summary

Control of emissions of olefins, sulfur and aromatic compounds, especially benzene, from automotive gasoline engines becomes every day more strict due to new environmental standards. That implies that, in the refineries, the pool gasoline components have to be adjusted to meet the required specifications. Branched alkanes with high octane number are the more suitable component of environmental friendly gasoline. They are industrially produced by alkylation of isobutane with C_3-C_5 alkenes. Therefore, it is expected, that the demand for alkylation catalysts will increase in the coming years.

While the products from alkylation are perfect gasoline components, the catalysts used currently, sulfuric and anhydrous hydrofluoric acids, are toxic and corrosive. That has stimulated the effort of many research groups to the development of more environmental friendly and safer alternative process, the majority focused on zeolite-base catalysts.

Although most of the investigations have shown that the product distribution in the alkylate obtained with zeolites as catalysts is comparable to that from industrial liquid acid technology, the rapid deactivation of zeolite has impeded their implementation on large-scale.

As a consequence, and due to the relatively high cost of zeolitic catalysts (compared specially to those of sulfuric acid), an efficient and economic regeneration method of the deactivated zeolite must be designed.

Moreover, in order to develop a competitive process based on zeolites, a deep knowledge of the physicochemical properties of these catalysts, especially their acidity, associated with the understanding of the effect of reaction parameters, have to be reached.

In this thesis special attention was paid to understand the nature of the acid sites in FAU- and BEA-type zeolites. In *Chapter 2* the acidic properties of La-X zeolite at different preparation steps were thoroughly characterized by *in situ* IR spectroscopy, under vacuum and flow conditions. It was found that the rehydration of the materials calcined only one time affects the distribution of different hydroxyl groups.

Rehydration leads to dealumination and, as consequence, the concentration of silanol groups (IR band at 3740 cm^{-1}) and of Lewis acid sites increases. This in turn results in an enhanced thermal stability of the rare earth zeolite for the next steps of catalyst preparation.

Chapter 3 dealt with the comparison between La-X based catalysts and different forms of Y zeolite, H-EMT and H-BEA based catalysts. IR characterization of the acid sites present in these zeolites has shown that the kind of hydroxyl groups responsible for Brønsted acidity is highly dependent on the zeolite investigated. The differences in density, location and strength of the Brønsted acid sites led to catalyst lifetimes in isobutane/cis-2-butene alkylation varying from 1 to 13 hours.

Chapter 4 was focused on the influence of the activation temperature on the catalytic performance of La-X based catalysts. IR spectroscopy, ^{1}H NMR and TPD experiments have evidenced the presence of physisorbed water, its amount being dependent on the activation temperature. IR spectroscopy of adsorbed pyridine has showed that water on the catalyst does not modify appreciably the concentration of Brønsted acid sites. Adsorption of isobutane/cis-2-butene monitored by IR spectroscopy, along with the activity tests carried out with the sample activated at different temperatures, has shown that the presence of water influences mainly the formation of oligomers. More C_5-C_7 products were observed on samples activated at higher temperatures.

5.2 Zusammenfassung

Neue Umweltgesetze erfordern eine zunehmend strenge Kontrolle der Olefin-, Schwefel- und Aromatengehalte in Automobilabgasen. Folglich müssen Raffinerien die Benzinpool-Zusammensetzung anpassen, um die geforderten Spezifikationen zu erfüllen. Verzweigte Alkane mit hohen Oktanzahlen sind die idealen Komponenten für ein umweltfreundliches Benzin. Sie werden industriell durch die Alkylierung von Isobutan mit C_3-C_5-Alkenen hergestellt. Aus diesem Grund wird in den nächsten Jahren eine zunehmende Nachfrage nach Alkylierungskatalysatoren erwartet.

Obwohl die Alkylierungsprodukte perfekte Benzinkomponenten darstellen, sind die derzeit verwendeten Verfahren problematisch, weil sie entweder Schwefelsäure oder wasserfreie Flußsäure verwenden. Beide Katalysatoren sind giftig und korrosiv. Dies ist der Antrieb für eine Vielzahl von Gruppen, umweltfreundlichere Katalysatoren und sicherere alternative Prozesse zu entwickeln. Dabei konzentriert sich die Mehrzahl auf Katalysatoren auf Zeolitbasis.

Die meisten Untersuchungen haben gezeigt, dass die Produktzusammensetzung des Alkylats mit Zeolitkatalysatoren vergleichbar mit derjenigen aus industriellen Prozessen mit flüssigen Säuren ist. Allerdings verhinderte bis jetzt die schnelle der Deaktivierung eine Umsetzung im großen Maßstab.

Aus diesem Grund und wegen der relativ hohen Kosten von Zeolitkatalysatoren (besonders im Vergleich zu Schwefelsäure) muß eine effiziente und wirtschaftliche Methode zur Regenerierung von deaktivierten Zeoliten gefunden werden.

Ein umfassendes Verständnis der physikochemischen Eigenschaften, insbesondere der Azidität, von Zeolitkatalysatoren ist notwendig, um einen wettbewerbsfähigen Prozess zu entwickeln. Ebenfalls wichtig sind die Auswirkungen der Reaktionsbedingungen auf den Prozess.

Ein besonderer Schwerpunkt dieser Arbeit war das Verständnis der Beschaffenheit der Säurezentren in FAU- und BEA-Zeoliten. In Kapitel 2 wurden die Säureeigenschaften von Zeolit La-X nach verschiedenen Präparationen mit *in situ* IR-Spektroskopie im Vakuum sowie unter Durchflußbedingungen sorgfältig charakterisiert. Es wurde gezeigt, dass die Verteilung verschiedener Hydroxylgruppen durch Rehydrierung eines nur einfach kalzinierten Materials beeinflußt wird. Rehydrierung führt zu einer Dealuminierung und damit zu einer Zunahme der Konzentration von Silanolgruppen (IR-Bande bei 3740 cm^{-1}) und Lewissäurezentren.

Dies wiederum führt zu einer gesteigerten thermischen Stabilität der selten Erden Zeolite im nächsten Präparationsschritt.

Kapitel 3 befasste sich mit dem Vergleich zwischen La-X und verschiedenen Katalysatoren auf Basis von Zeolit Y, H-EMT und H-BEA. IR-Untersuchungen der Säurezentren haben gezeigt, dass die Art der Hydroxylgruppen, welche mit Brønsted-Azidität in Verbindung gebracht werden, stark vom untersuchten Zeolit abhängt. Die Unterschiede in der Dichte, Position und Stärke der Brønstedsäurezentren führte zu Lebenszeiten des Katalysator zwischen 1 und 13 Stunden.

In Kapitel 4 wurde der Einfluss der Aktivierungstemperatur auf die Leistung von La-X-Katalysatoren untersucht. Die Anwesenheit von physisorbiertem Wasser konnte mit IR-Spektroskopie, ^{1}H-MAS-NMR und TPD-Experimenten gezeigt werden. Die beobachtete Wassermenge hing dabei von der Aktivierungstemperatur ab. Mit IR-Spektroskopie von adsorbiertem Pyridin wurde gezeigt, das Wasser auf dem Katalysator keinen wesentlichen Einfluß auf die Konzentration der Brønstedsäurezentren hat. Durch die IR-spektroskopische Beobachtung der Adsorption eines Isobutan/2-Buten-Gemisches und Aktivitätstest von Proben mit verschiedenen Aktivierungstemperaturen wurde gezeigt, dass die Gegenwart von Wasser vor Allem die Bildung von Olefinen beeinflußt. Ein größere Menge von C_5-C_7-Produkten wurde für Proben beobachtet, welche bei höheren Temperaturen aktiviert worden waren.

Curriculum Vitae

Alexander Guzmán-Monsalve is a Colombian citizen who was born on the 11th January 1966. He has a degree in Chemistry from the National University of Colombia (Bogotá, Colombia) in 1996.

He started primary studies in 1973 in the Quiroga district school in Bogotá.
He was to the high school in 1978 in the Restrepo Millán National school in Bogotá.
He finished the six year of high school in the Manuela Beltrán district school in 1983.
In the next year, 1984, he was at the army.

From 1985 to 1988 he worked in several jobs and studied English at the Colombian-American center in Bogotá during a year.

He started to study in 1988 at the National University of Colombia in Bogotá, where he graduated as chemist in 1996.

He is married with Martha Molina who is chemist from the National University of Colombia, too. They have two children: Natalia 9 and Santiago 11 years old.

Before he had graduated as chemist he worked at Fundiciones (foundries) Vulcano in Bogotá during 3 months, October-December 1993, as laboratory analyst and at the National University as auxiliary teacher during 5 months . He worked also in analytical chemistry on the determination of lead and mercury in blood from July 1994 to September 1995 at Andreas Rothstein clinic laboratory in Bogotá. From September 1995 to march 2001 he worked at Empresa Colombiana de Petróleos-Instituto Colombiano del Petróleo (ECOPETROL-ICP) in catalysis field as chemist (contractor) holding various assignments in evaluating and characterizing FCC catalysts.

He studied german at Goethe Institute in Bogotá from 1993 to 1995, where he made basic level (Grundstufe I, II and III) and Mittelstufe I.

After working by the ICP in April 2001 he started to work as PhD student in the group of Prof. Dr. J.A. Lercher. The work on solid acid Alkylation of isobutane with 2-butenes was embedded in an international research project with two academic and two industrial project partners from Germany.

The main results on the study of the acid sites in zeolite catalyzed isobutane/2-butenes alkylation are described in this thesis.